

**Identification and Characterization of mycovirus in  
Botrytis species**

---



**By**

**Aqeel Ahmed**

**NUST201590333PASAB8015F**

**Thesis supervisor: Dr. Muhammad Faraz Bhatti**

---

**Atta-ur-Rahman School of Applied  
Biosciences (ASAB) National University of  
Sciences & Technology (NUST) Islamabad,  
Pakistan**

**2023**

# **Identification and Characterization of mycovirus in Botrytis species**

---



**By**

**Aqeel Ahmed**

**NUST201590333PASAB8015F**

A thesis submitted to the National University of Sciences and Technology,  
Islamabad, in partial fulfillment of the requirement for the degree of  
Doctor of Philosophy

**In**

**Applied Biosciences**

**Supervisor: Dr. Muhammad Faraz Bhatti**

**Atta-ur-Rahman School of Applied  
Biosciences (ASAB) National University of  
Sciences & Technology (NUST) Islamabad,  
Pakistan**

**2023**

THESIS ACCEPTANCE CERTIFICATE

Certified that final copy of PhD Thesis written by Mr. Aqeel Ahmed (Registration No. NUST201590333PASAB8015F), of (School/College/Institute) Atta-ur-Rahman School of Applied Biosciences has been vetted by undersigned, found complete in all respects as per NUST Statutes/Regulations/PhD Policy, is free of plagiarism, errors, and mistakes and is accepted as partial fulfillment for award of PhD degree. It is further certified that necessary amendments as pointed out by GEC members and foreign/local evaluators of the scholar have also been incorporated in the said thesis.

Signature: \_\_\_\_\_

Name of Supervisor Dr. Muhammad Faraz Bhatti

Date: \_\_\_\_\_

Signature (HOD): \_\_\_\_\_

Date: \_\_\_\_\_

Signature (Dean/Principal) Dr. Muhammad Asghar

Date: \_\_\_\_\_

Dr. Muhammad Faraz Bhatti  
Tenured Professor  
Head of Department (HoD)  
Dept of Plant Biotechnology  
Atta-ur-Rahman School of Applied  
Biosciences (ASAB), NUST Islamabad

Dr. Muhammad Faraz Bhatti  
Head of Department (HoD)  
Dept of Plant Biotechnology  
Atta-ur-Rahman School of Applied  
Biosciences (ASAB), NUST Islamabad

Prof. Dr. Muhammad Asghar  
Principal  
Atta-ur-Rahman School of Applied  
Biosciences (ASAB), NUST Islamabad

## Certificate of Approval

This is to certify that the research work presented in this thesis, entitled Identification and Characterization of mycovirus in Botrytis species was conducted by Mr. Aqeel Ahmed under the supervision of Dr. Muhammad Faraz Bhatti. No part of this thesis has been submitted anywhere else for any other degree. This thesis is submitted to the Atta-ur-Rahman School of Applied Biosciences in partial fulfillment of the requirements for the degree of Doctor of Philosophy in field of Applied Biosciences Department of Atta-ur-Rahman School of Applied Biosciences, University of National University of Sciences & Technology (NUST).

Student Name Aqeel Ahmed

Signature \_\_\_\_\_

Examination committee:

a) External examiner 1: Dr. M. Farooq Hussain Munis Signature \_\_\_\_\_

(Associate Professor)

Department of Plant Sciences,

Quaid-i-Azam University, Islamabad.

b) External Examiner 2: Dr. M. Imran Shabbir Signature \_\_\_\_\_

(Assistant Professor)

Department of Biological Sciences

International University Islamabad, Pakistan

c) Internal Examiner: Dr. Muhammad Qasim Hayat Signature \_\_\_\_\_

(Professor)

ASAB (NUST), H-1 2 Campus, Islamabad, Pakistan

**Dr. Muhammad Faraz Bhatti**  
Tenured Professor  
Head of Department (HOD)  
Dept of Plant Biotechnology  
Atta-ur-Rahman School of Applied  
Biosciences (ASAB), NUST Islamabad

Supervisor Name: Dr. Muhammad Faraz Bhatti

Signature \_\_\_\_\_

Name of Dean / HOD: Dr. Muhammad Asghar

Signature \_\_\_\_\_

64/09/2023  
Atta-ur-Rahman School of  
Applied Biosciences (ASAB)  
NUST Islamabad



## National University of Sciences & Technology REPORT OF DOCTORAL THESIS DEFENCE

Name: Aqeel Ahmed NUST Regn No: NUST201590333PASAB8015F

School/College/Centre: Atta-ur-Rehman School of Applied Biosciences (ASAB)

Title: Identification and Characterization of mycovirus in Botrytis species

### DOCTORAL DEFENCE COMMITTEE

Doctoral Defence held on 4<sup>th</sup> September 2023

	QUALIFIED	NOT QUALIFIED	SIGNATURE
GEC Member-1: <u>Dr. Muhammad Qasim Hayat</u>	<input checked="" type="checkbox"/>	<input type="checkbox"/>	
GEC Member-2: <u>Dr. Hussain Ahmed Janjua</u>	<input checked="" type="checkbox"/>	<input type="checkbox"/>	
GEC Member (External): <u>Dr. Atif Jamal</u>	<input checked="" type="checkbox"/>	<input type="checkbox"/>	
Supervisor: <u>Dr. Muhammad Faraz Bhatti</u> <small>Tenured Professor Head of Department (HOD) Dept of Plant Biotechnology Atta-ur-Rahman School of Applied Biosciences (ASAB), NUST Islamabad</small>	<input checked="" type="checkbox"/>	<input type="checkbox"/>	
Co Supervisor (if appointed): <u>Dr. Nasar-um-Minullah Mirzobad</u>	<input checked="" type="checkbox"/>	<input type="checkbox"/>	
External Evaluator-1: <u>Dr. M. Farooq Hussain Munis</u> (Local Expert)	<input checked="" type="checkbox"/>	<input type="checkbox"/>	
External Evaluator-2: <u>Dr. M. Imran Shabbir</u> (Local Expert)	<input checked="" type="checkbox"/>	<input type="checkbox"/>	
External Evaluator-3: <u>Dr. Lying Sun</u> (Foreign Expert)	<input type="checkbox"/>	<input type="checkbox"/>	
External Evaluator-4: <u>Dr. Selin Ozkan</u> (Foreign Expert)	<input type="checkbox"/>	<input type="checkbox"/>	

### FINAL RESULT OF THE DOCTORAL DEFENCE

(Appropriate box to be signed by HOD)

**Dr. Muhammad Faraz Bhatti**  
Head of Department (HOD)  
Dept of Plant Biotechnology  
Atta-ur-Rahman School of Applied Biosciences (ASAB), NUST Islamabad

PASS

FAIL

The student Aqeel Ahmed Regn No NUST201590333PASAB8015F is / is NOT accepted for Doctor of Philosophy Degree.

Dated: 04/09/2023

**Principal**  
Atta ur Rahman School of Applied Biosciences (ASAB)  
NUST Islamabad  
Dean/Commandant/Principal/DG

**Distribution:**

01 x original copy each for PGP Dte, Exam Branch Main Office NUST and Student's dossier at the School 'College' Centre.  
01 x photocopy each for HoD, Supervisor, Co-Supervisor (if appointed), sponsoring agency (if any) and 05 copies for insertion in Dissertation.  
Note: \* Decision of External Evaluators (Foreign Experts) will be sought through video conference, if possible, on the same date and their decision will be intimated (on paper) to HQ NUST at a later date.

## **Author's Declaration**

I, **Aqeel Ahmed**, hereby state that my PhD thesis titled "**Identification and Characterization of mycovirus in Botrytis species**" is my own work and has not been submitted previously by me for taking any degree from this university **National University of Sciences and Technology (NUST), Islamabad, Pakistan** or anywhere else in the country/world.

At any time if my statement is found to be incorrect even after my graduation the university has the right to withdraw my PhD degree.

**Aqeel Ahmed**

Dated:

## **Plagiarism Undertaking**

I solemnly declare that the research work presented in the thesis titled “**Identification and Characterization of mycovirus in Botrytis species**” is solely my research work with no significant contribution from any other person. Small contribution/help wherever taken has been duly acknowledged and that complete thesis has been written by me.

I understand the zero-tolerance policy of the HEC and **National University of Sciences and Technology (NUST), Islamabad** towards plagiarism. Therefore, I as an author of the above-titled thesis declare that no portion of my thesis has been plagiarized and any material used as reference is properly referred to/cited.

I undertake that if I am found guilty of any formal plagiarism in the above-titled thesis even after award of PhD degree, the university reserves the right to withdraw/revoke my PhD degree and that HEC and the University website on which name of students are placed who submitted plagiarized thesis.

**Aqeel Ahmed**

# **DEDICATION**

**This thesis is a dedication of  
gratitude and love to  
my parents and other  
family members for their  
help and continuous  
support  
throughout this entire  
journey.**



## ACKNOWLEDGEMENT

Though words may never say what we want to, still there is the most appropriate way of expressing emotions. I am, though, never be able to offer my thanks to **Allah Almighty**, the propitious, the sole creator of the universe, the source of all knowledge and wisdom, the Most Merciful and the Most Beneficent, WHO bestow us with the mind to think, the ability to observe, the power to understand the things and to seek the knowledge. Trembling lips and wet eyes praise for **Holy Prophet Muhammad** (Peace Be Upon Him), who is a torch of guidance and knowledge for humanity forever, for His sacredness, due to whom I have been able to achieve this milestone of my academic career.

I would like to express my special appreciation and thanks to my helpful and enthusiastic supervisor **Dr. Muhammad Faraz Bhatti**, Professor, ASAB-NUST, for having been a tremendous mentor for me throughout the research phase, encouraging me to grow as a research scientist. His advice for both research as well as on my career has been precious. I am very thankful for his keen personal interest, dynamic supervision, immense cooperation, valuable suggestions, unfailing patience, sincerity, and selfless support. I would like to express my special appreciation and thanks to my co-supervisor advisor, **Prof. Dr. Nasar-um-Minullah Virk**. I consider it my privilege to have accomplished my research objectives under his right guidance and supervision.

I am also thankful to **Dr. Atif Jamal**, Principal scientific officer CDRI, NARC for his endless support, guidance, valuable advice suggestions and guidance during the whole research phase. His valuable suggestions, encouragement, support, and constructive criticism truly helped the progression and smoothness throughout my course of research.

Special thanks to my internal GEC members, **Dr. Muhammad Qasim Hayat and Dr. Hussnain Ahmed Janjua** , for their support, guidance, and cooperative recommendations and for providing and facilitating an encouraging environment for research at ASAB, NUST. I am highly thankful to the **Higher Education Commission, Pakistan** for providing me the opportunity to visit Prof. Dr. Eeva Vainio lab and for funding me with international fellowship for achieving my research objectives. I would also like to thank my family for their support, encouragement, and motivation. Last but not least, I would like to pay my heartiest thanks to all my friends who helped me in my tough times.

**Aqeel Ahmed**

# Table of Contents

1.	Introduction.....	22
	7	
1.2	Yield losses caused with Botrytis species.....	30
1.2.1	Management and cultural practices to control grey mold .....	31
	Mycoviruses – (viruses of fungi) .....	32
1.3	Mycovirus diversity and classification.....	37
1.6	Vertical and horizontal transmission in mycoviruses .....	47
	Geographic Distribution and Incidence of RNA Mycoviruses in Botrytis.....	48
1.8	Mycoviruses can alter host fitness (In case of Botrytis cinerea) .....	56
1.9	Techniques in mycoviral identification for molecular characterization.....	56
1.9.1	RT-PCR for detection of mycoviruses .....	57
1.9.2	Metagenomics and Next-generation sequencing.....	57
1.10	Objectives of the research Project .....	58
2.	Materials and Methods Used: .....	58
2.1	Isolation and culture conditions for B. cinerea isolates .....	64
2.2	DsRNA extraction and agarose gel electrophoresis.....	66
2.3	Identification of fungal strains using ITS region .....	67
2.7	Detection of mycoviruses from Botrytis isolates.....	69
2.8	DNase Treatment of Isolated RNA.....	69
2.9	S1 Nuclease Treatment of isolated Nucleic acid Prep. ....	70
2.10	Genomic Characterization of isolated mycoviruses .....	70
2.10.2	Raw data & Quality Control.....	71
2.10.3	Preprocessing .....	71
2.10.4	K-mer Analysis & De novo assembly .....	71
2.10.5	Assembly validation .....	71

2.10.6	Validation of NGS data .....	71
2.10.7	Sequence and phylogenetic analysis.....	72
2.10.8	RLM-RACE for viral terminal confirmation.....	72
Table 2.4. Recipe of RACE. ....		73
2.10.9	Ligation of PCR products.....	74
2.10.10	Transformation of ligated PCR products colony PCR and sequencing.....	74
2.7	Impact of botrytis mycovirus on the fitness of their host.....	75
Development of isogenic lines .....		76
2.11.2.	Method for Biological Impact Assessment on PDA Media .....	76
2.11.3	Fungal Pathogenicity Test on Apple Fruits .....	77
3.	Results: .....	77
3.1.2	Screening of mycoviruses from identified Botrytis strains .....	80
3.2	Characterization of novel mycovirus genomes identified during the screening process in order to understand the nature of mycoviruses (Objective 2) along with their phylogeny (Objective 3).....	82
3.2.1	.1 Characterization of Novel Endornavirus from Kst 31.....	86
(b) Identity matrix of viruses used in phylogenetic tree. The scale represents the level of identity. ....		91
3.2.2.1	Characterization of Novel Fusariviruses in Kst14a strain .....	91
3.2.2.2	Phylogenetic analysis of both fusariviruses from Kst14a .....	94
3.3	Genomic features of other new viruses identified in this study .....	96
3.3.1	Botrytis cinerea mymonavirus .....	96
3.3.2	Botrytis cinerea ourmiavirus .....	102
3.3.4	Botrytis cinerea negative stranded RNA virus .....	105
3.3.5	Plasmopara viticola lesion associated orfanplasmovirus 4.....	111
3.3.6	Botrytis cinerea hypovirus.....	114
3.3.6	Botrytis cinerea mycotymovirus.....	117
3.3.7	Botrytis cinerea birnavirus .....	121
3.3.8	Botrytis cinerea umbra-like virus.....	126

3.3.9 Botrytis cinerea Narnavirus .....	129
3.3.10 Botrytis cinerea Mitovirus.....	132
Figure 3.50 Genome organization of Botrytis cinerea mitovirus.....	133
3.4 Studying the infection and its effect on the fungal samples to identify the hypovirulentmycoviruses as a potential tool to control Botrytis infecting different crops (Objective 4).....	135
Growth Comparison of Kst5C .....	139
Growth Comparison of Kst10A.....	142
Growth Comparison of 14A.....	144
Growth Comparison of Kst31C .....	145
Growth Comparison of Kst32B .....	148
Growth Comparison of Kst33A .....	150
3.4.2 Pathogenicity Tests of virus infected and uninfected isolates (Apple Assay).....	151
3.5.0 Choosing the compatible strains for generation of isogenic line for virustransmission (Objective 5) ....	153
3.5.1.1 Bc-hch amplification for analysis of diversity and compatibility among fungal strains .....	154
3.5.1.2 Enzymatic digestion of PCR amplicons for pattern analysis .....	156
3.6.1 Horizontal transmission of mycovirus (Objective 6) .....	157
3.6.1.2 Confirmation of virus transmission though RT-PCR.....	157
3.7.1 Evaluation of potential hypovirulent strain for biocontrol (Objective 7; Final objective) .....	161
Apple Assay of Hypovirulence inducing Endornavirus.....	164
3.7.2 Comparison of Growth Rate and fungal pathogenicity .....	165
Graphical Representation .....	167
4. Discussion: .....	167
5. Conclusion:.....	172
6. Future Prospects:.....	174
7. References: .....	175

## LIST OF FIGURES

<b>Figure 1.1</b> Life cycle of <i>Botrytis cinerea</i> showing both sexual and asexual reproduction cycles (Billard et al., 2011).....	25
<b>Figure 1.1a</b> Life cycle of <i>B. cinerea</i> and associated symptoms.....	27
<b>Figure 1.2.</b> A pictorial demonstration of presence of mycoviruses in <i>Botrytis cinerea</i> isolates cultured in lab conditions.....	29
<b>Figure 1.3.</b> A representative organization of complete genome of a typical totivirus. Complete genome encodes for two ORFs i.e. CP and RdRP. A ribosomal frame shift events occurs between	

both ORFs together with a slippery sequence which helps in translation of Coat protein and RdRP protein (<https://viralzone.expasy.org/745>) ..... 34

**Figure 1.4.** A representative organization of complete genome of a typical partitivirus representing CP and RdRP ([https://talk.ictvonline.org/ictv-reports/ictv\\_online\\_report/dsrna-viruses/w/partitiviridae](https://talk.ictvonline.org/ictv-reports/ictv_online_report/dsrna-viruses/w/partitiviridae)). ..... 35

**Figure 1.5.** Genome organization of a typical megabirnavirus ([https://talk.ictvonline.org/ictv-reports/ictv\\_online\\_report/dsrna-viruses/w/megabirnaviridae](https://talk.ictvonline.org/ictv-reports/ictv_online_report/dsrna-viruses/w/megabirnaviridae)). ..... 36

**Figure 1.6.** Genomic organization of members of family quadriviridae. ([https://talk.ictvonline.org/ictv-reports/ictv\\_online\\_report/dsrna-viruses/w/quadriviridae](https://talk.ictvonline.org/ictv-reports/ictv_online_report/dsrna-viruses/w/quadriviridae)). ..... 37

**Figure 1.7.** Genome organization of viruses belonging to family Mycoreoviridae. (Tanaka et al., 2012) ..... 38

**Figure 1.8.** Genome organization of some representative members belonging to family Alfalexiviridae ([https://talk.ictvonline.org/ictv-reports/ictv\\_online\\_report/positive-sense-rna-viruses/w/alphalexiviridae](https://talk.ictvonline.org/ictv-reports/ictv_online_report/positive-sense-rna-viruses/w/alphalexiviridae)). ..... 39

**Figure 1.9.** Genome organization of typical Botourmiavirus ([https://talk.ictvonline.org/ictv-reports/ictv\\_online\\_report/positive-sense-rna-viruses/w/botourmiaviridae](https://talk.ictvonline.org/ictv-reports/ictv_online_report/positive-sense-rna-viruses/w/botourmiaviridae)). ..... 40

**Figure 2.1** Sample collection of infected strawberry fruits from strawberry fields which showed symptoms of grey mould infestation ..... 55

**Figure 2.2.** Map of Pakistan showing the collecting sites of understudied fungal samples. The samples were collected from Mardan, Muridke and Kamoke from different farms of strawberry ..... 56

**Figure 3.1** A pie graph showing the percentage of dsRNA positive fungal samples. A total of 102 fungal samples were collected from which only nine showed dsRNA positive profile which showed an incidence rate of 8.8% ..... 74

**Figure 3.2** ITS region amplification of different fungal isolates using two primers: ITS5F & ITS4. .... 76

<b>Figure 3.3</b> Colony morphology of <i>Botrytis</i> isolates, (A1; Kst5C, B2; Kst10A, C2; Kst14A & D1; Kst31C) on PDA medium over a period of 2-4 days .....	77
<b>Figure 3.4</b> Agarose gel electrophoresis indicating total nucleic acid extraction for the screening of mycoviral infection. Lane M indicate molecular weight marker DNA; PC indicate the Positive control and other lane include the sample screened for mycoviral infection .....	78
<b>Figure 3.5:</b> Lane M shows molecular marker, lane 1-6 show bands of DNA amplified by using Primerset End1F & End1R while 7 and 8 show bands which were amplified by using End1F and End2R. .....	82
<b>Figure 3.6</b> Genome organization of <i>Botrtis cinerea</i> endornavirus 4 showing conserved regionswith already reported endornaviruses .....	84
<b>Figure 3.7</b> No conserved cysteine regions were observed in BcEV4 when compared within already reported endornaviruses .....	84
<b>Figure 3.8</b> Conserved regions identified in RdRP region using multiple alignment.....	85
<b>Figure 3.9</b> conserved (5' and 3') terminals in <i>Botrytis cinerea</i> endornavirus 4.....	85
<b>Figure 3.10</b> (a) Phylogenetic analysis, based on the deduced amino acid sequences of RdRP, revealed that BcEV4 belongs to the family <i>Endornaviridae</i> . (b) Identity matrix of viruses used in phylogenetic tree. The scale represents the level of identity .....	86
<b>Figure 3.11</b> Genome organization of both fusariviruses identified from <i>Botrytis cinerea</i> isolate Kst-14a. Black regions shows the conserved RdRP and green regions shows the other conserved regionspresent in the genome.....	87
<b>Figure 3.12</b> Conserved regions predicted in the genome of both fusariviruses using multiple alignment.....	90
<b>Figure 3.13</b> Conserved poly A tail identified in both fusariviruses at 3' terminal .....	90
<b>Figure 3.14</b> Phylogenetic analysis of both fusariviruses identified from <i>Botrytis cinerea</i>	



isolateKst-14a .....	91
----------------------	----

<b>Figure 3.15</b> Identity matrix of all fusariviruses used in phylogenetic analysis. The red in the scale represents the maximum identity .....	92
<b>Figure 3.16</b> Genome organization of Botrytis cinerea mymonavirus showing three different ORFs. ORF1 encodes for RdRP and cap protein while other ORFs encode hypothetical proteins.....	96
<b>Figure 3.17</b> A). Phylogenetic analysis, based on the deduced amino acid sequences of RdRP, revealed that Contig 8 belongs to the family Mymonaviridae. B). Identity matrix of viruses used in phylogenetic tree. The scale represents the level of of identity .....	97
<b>Figure 3.18</b> Conserved regions identified in RdRP region using multiple alignment.....	97
<b>Figure 3.19</b> Conserved (5' and 3') terminals in Botrytis cinerea mymonavirus .....	97
<b>Figure 3.20</b> Genome organization of Botrytis cinerea ourmiavirus showing three different ORFs. ORF1 encodes for RdRP while ORF2 encode for hypothecial protein .....	98
<b>Figure 3.21</b> (A). Phylogenetic analysis, based on the deduced amino acid sequences of RdRP, revealed that Contig 20 (Botrytis cinerea ourmi-like virus) belongs to the ourmiaviruses which is genus of Botourmiaviridae. (B). Identity matrix of viruses used in phylogenetic tree. The scale representthelevelofofidentity.....	100
<b>Figure 3.22</b> Conserved regions identified in RdRP region using multiple alignment.....	101
<b>Figure 3.23</b> conserved (5' and 3') terminals in Botrytis cinerea ourmiavirus Contig 20.....	101
<b>Figure 3.24</b> Genome organization of Botrytis cinerea negative stranded RNA Virus ].....	103
<b>Figure 3.25</b> Phylogenetic analysis, based on the deduced amino acid sequences of RdRP, revealed that Contig 5 belongs to the family Negative stranded RNA viruses. identity matrix of viruses used in phylogenetic tree. The scale represents the level of of identity.....	105
<b>Figure 3.26</b> Conserved regions identified in RdRP region using multiple alignment.....	106
<b>Figure 3.27</b> conserved (5' and 3') terminals in Botrytis cinerea negative stranded RNA Virus Contig	

5.....106

**Figure 3.28** Genome organization of *Plasmopara viticola* lesion associated orfanplasmovirus 4...  
107

**Figure 3.29.** A). Phylogenetic analysis, based on the deduced amino acid sequences of RdRP, revealed that Contig 43 belongs Plasmopara viticola lesion associated orfanplasmoviruses. B). Identity matrix of viruses used in phylogenetic tree. The scale represents the level of of identity

**Figure 3.30** Conserved regions identified in RdRP region using multiple alignment..... 109

**Figure 3.31** conserved (5' and 3') terminals in Plasmopara viticola lesion associated orfanplasmovirus 4 Contig 43.....109

**Figure 3.32** Genome organization of Botrytis cinerea hypovirus ..... 110

**Figure 3.33** Phylogenetic analysis, based on the deduced amino acid sequences of RdRP, revealed that Contig 4 belongs to the family Hypoviridae. identity matrix of viruses used in phylogenetic tree. The scale represents the level of of identity.....111

**Figure 3.34** Conserved regions identified in RdRP region using multiple alignment..... 112

**Figure 3.35** conserved (5' and 3') terminals in Botrytis cinerea hypovirus..... 113

**Figure 3.36** Genome organization of Botrytis cinerea mycotymovirus ..... 113

**Figure 3.37 (A).** Phylogenetic analysis, based on the deduced amino acid sequences of RdRP, revealed that Contig 5 belongs to the mycotomyviruses. (B). Identity matrix of viruses used in phylogenetic tree. The scale represents the level of of identity.....116

**Figure 3.38** Conserved regions identified in RdRP region using multiple alignment..... 117

**Figure 3.39** conserved (5' and 3') terminals in Botrytis cinerea mycotymovirus..... 117

**Figure 3.40** Genome organization of Botrytis cinerea birnavirus ..... 119

**Figure 3.41 (A).** Phylogenetic analysis, based on the deduced amino acid sequences of RdRP, revealed that Contig 5 belongs to the family Birnaviridae. (B). Identity matrix of viruses used in phylogenetic tree. The scale represents the level of of

identity.....120

**Figure 3.42** Conserved regions identified in RdRP region using multiple alignment..... 121

**Figure 3.43** conserved (5' and 3') terminals in Botrytis cinerea birnavirus Contig 12..... 121

<b>Figure 3.44</b> Genome organization of <i>Botrytis cinerea</i> umbra-like virus .....	122
<b>Figure 3.45 (A).</b> Phylogenetic analysis, based on the deduced amino acid sequences of RdRP, revealed that Contig 5 belongs to the umbra-like viruses. <b>B).</b> Identity matrix of viruses used in phylogenetic tree. The scale represents the level of identity.....	123
<b>Figure 3.46</b> Conserved regions identified in RdRP region using multiple alignment.....	123
<b>Figure 3.47</b> Genome organization of <i>Botrytis cinerea</i> narnavirus .....	125
<b>Figure 3.48 A).</b> Phylogenetic analysis, based on the deduced amino acid sequences of RdRP, revealed that Contig 5 belongs to the family Narnaviridae. B). Identity matrix of viruses used in phylogenetic tree. The scale represents the level of identity.....	127
<b>Figure 3.49</b> Conserved regions identified in RdRP region using multiple alignment.....	128
<b>Figure 3.50 Genome organization of <i>Botrytis cinerea</i> mitovirus.....</b>	129
<b>Figure 3.51 A).</b> Phylogenetic analysis, based on the deduced amino acid sequences of RdRP, revealed that viral sequence belongs to the family Birnaviridae. B). Identity matrix of viruses used in phylogenetic tree. The scale represents the level of identity.....	130
<b>Figure 3.52</b> Conserved regions identified in RdRP region using multiple alignment.....	131
<b>Figure 3.53</b> show relative growth comparison test at 25 C for 4 days at regular 12 hour light and 12 hour dark period.....	133
<b>Figure 3.54</b> Relative growth comparison test on PDA at 25 C for 4 days at regular 12 hour light and 12 hour dark period. ....	134
<b>Figure 3.55 A.</b> Histogram showing a comparison of the growth rates of the virus-infected isolate (Kst5C) and virus-free isolate (Control, Kst51) on PDA plates. As the P value (0.02) calculated by T.test is less than $\alpha$ (0.05) so the data is significant.....	136

**Figure 3.55 B** Histogram showing a comparison of the growth rates of the virus-infected isolate (Kst10A) and virus-free isolate (Control, Kst51) on PDA plates. As the P value (0.17) calculated by

T.test is greater than (0.05) so the data was not significant .....	138
<b>Figure 3.55C</b> Histogram showing a comparison of the growth rates of the virus-infected isolate (Kst14A) and virus-free isolate (Control, Kst51) on PDA plates. As the P value (0.14) calculated was greater than (0.05) so the data was not-significant .....	138
<b>Figure 3.56A</b> Histogram showing a comparison of the growth rates of the virus-infected isolate (Kst31C) and virus-free isolate (Control, Kst51) on PDA plates. As the P value (0.05) was equal to (0.05) so the data was significant.....	140
<b>Figure 3.56 B</b> Histogram showing a comparison of the growth rates of the virus-infected isolate (Kst32B) and virus-free isolate (Control, Kst51) on PDA plates. As the P value (0.5) calculated greaterthan $\alpha$ (0.05) so the data was not-significant .....	144
<b>Figure 3.56 C</b> Histogram showing a comparison of the growth rates of the virus-infected isolate (Kst33A) and virus-free isolate (Control, Kst51) on PDA plates. As the P value (0.06) was greater than $\alpha$ (0.05) so the data was non-significant.....	146
<b>Figure 3.57</b> shows the pathogenicity test of 4 Botrytis isolates (Kst5C, Kst10A, Kst14A &Kst51) along with their fungal morphology at 4 <sup>th</sup> day.....	148
<b>Figure 3.58</b> Shows the pathogenicity test of 4 Botrytis isolates (Kst31C, Kst32B, Kst33A &Kst58) along with their fungal morphology at 4 <sup>th</sup> day.....	149
<b>Figure 3.59 PCR</b> amplicon of Bc-hch gene using gene specific primers from different isolates. The size of amplicon was almost 1.2 kb .....	151
<b>Figure 3.60</b> Digestion Bc-hch amplicon with Hha-I endonuclease resulted into two different banding patterns corresponding to their respective groups .....	153
<b>Figure 3.61</b> shows picture of hyphal anastomosis, in which Kst31C is donor and Kst51 is potential recipient of mycovirus. Location of three plugs is also shown and these plugs were used for the determination of transfer of mycovirus.....	155
<b>Figure 3.62</b> shows RTPCR results of Endornavirus after hyphal anastomosis. Lane M as molecular	



marker, PC; PCR negative control, 1; Receptient strain, 2; positive control, 3; Near plug, 4; middle plug and 5; far plug of the recipient isolate .....	156
<b>Figure.3.63</b> Growth comparsion test of virus free (VF) and virus infected isogenic lines to analyze the impact of virus on its host .....	158
<b>Figure.3.64</b> shows the front views of growth pattern of KST 51 Virus infected (VI) and KST51- Virus free (VF) isogenic line at 7 <sup>th</sup> day of post-inoculation.....	159
<b>Figure 3.65</b> Pathogenicity test of Endornavirus infected Kst51 with uninfected Kst51 shows the diameter of lesions caused by KST51 virus infected (I) and Virus Free (F) isolates.....	160
<b>Figure. 3.66</b> shows the growth comparison of Virus-free (VF) and Virus-infected (VI) isolateof Botrytis cinerea (Kst51). Growth measurements were taken for 7 days. As the P value (0.001) calculated was less than 0.05 so the difference observed were significant.....	113
<b>Figure 3.67</b> shows the comparison of lesions caused by Virus-Free (VF) and Virus- Infected (VI) isolates on the host apple. As the P value (0.007) calculated was less than 0.05 so the difference observed were significant.....	163

## LIST OF TABLES

<b>Table 1.1</b> List of reported mycoviral families with their molecular features .....	42
<b>Table 1.2.</b> Mycoviruses identified from Botrytis species so far .....	46
<b>Table 2.1.</b> Details of fungal isoates collected and screened during this study. Genetic diversity analysis showed almost all fungal samples belongs to group II .....	57
<b>Table 2.2.</b> Sequences of primers used for amplification of ITS region and Bc-hch Gene .....	63
<b>Table 2.3.</b> Recipe of PCR mixture used in this study.....	64
<b>Table 2.4.</b> Recipe of RACE.....	69
<b>Table 2.5</b> The purified PCR products of RACE were ligated into pGEM-T Easy vector (Promega, Madison, WI, USA). The ligation reaction was set as follows .....	70
<b>Table 3.1</b> List of viruses infected fungal isolates with their sampling location and Genbank accession numbers .....	48
<b>Table 3.2</b> List of Contigs and virus Names (Virus detected in six NGS processed Botrytis isolates) .....	52

## ABSTRACT

Mycoviruses are common and have been reported to infect nearly all significant fungal taxonomic groupings. Mycovirus neo-lifestyles have been revealed by the identification and characterization of huge number of mycoviruses. This study reports an extensive screening survey on Pakistani *Botrytis cinerea* (Fungal) strains for the identification of viral infections. A sum of 102 *Botrytis cinerea* samples were screened, 9 isolates were found positive for mycoviral elements when analyzed by a classical dsRNA isolation method with an infection frequency of 8.8%. Six isolates (Kst5c, Kst10a, Kst14a, Kst31c, Kst32b & Kst33c) were subjected to Next-generation sequencing for virome analysis. A total of 27 mycoviruses were identified in the infected isolates, belonging to the families *Endornaviridae*, *Fusariviridae*, *Botourmiaviridae*, *Narnaviridae* and *Mitoviridae*. Based on the International Committee on Taxonomy of Viruses (ICTV) demarcation criteria, 4 identified mycoviruses are considered novel. Viruses from three isolates (Kst5c, Kst14a & Kst31c) were completely characterized and sequences have been submitted in the NCBI database. Isolate Kst31c was found to harbor infection of hypovirulent mycovirus (BcEV4) which shows debilitating effects in host fungus. Following genomic characterization, the biological assessment was also conducted in which mycovirus was successfully transferred from virus-infected (VI) strain to virus-free (VF) strain. Both said strains were vegetatively compatible because both belong to same genetic group (Group II). Genetic grouping of all the *B. cinerea* isolates was analyzed based on *Bc-hch* gene amplification followed by restriction digestion method. Isogenic lines were compared later on, virus infected strain showed persistent infections due to presence of mycovirus (BcEV4). Afterwards, pathogenicity tests were also performed which showed promising results.

## Chapter 1:

# 1. Introduction

### ***Botrytis cinerea* as phytopathogenic fungus**

*Botrytis cinerea* is a phytopathogenic fungus and belongs to family *Sclerotiniaceae* in the Ascomycota group. This pathogen infects economically important crops and is responsible for huge losses including pre- and post-harvest each year worldwide ([Williamson et al., 2007](#)). Due to recent advances in molecular tools for studying the mechanisms associated with pathogenicity, availability of complete genomic sequences and considering its worldwide pathogenic importance, *Botrytis* is ranked as model necrotrophic fungi ([Hua et al., 2018](#)). Considering these observations *Botrytis cinerea* is considered as 2<sup>nd</sup> most important fungal pathogen throughout the world ([Dean et al., 2012](#)). It derives its nutrients from both dead and decaying organic matter and also from living tissues and can behave as saprophytes as well as parasite of different plants ([van Kan et al., 2014](#)). Host range of this pathogen is very wide and extends up to 1400 different plants (mainly dicotyledonous plants) ([Fillinger and Elad, 2016](#)). From these 1400 plants, most of them are economically important and have commercial value. Some are major food crops and others are used for oil and fiber extraction. Other cultivatable plants in nurseries are also susceptible to this fungus i.e. beans, lettuce and cabbage. *Botrytis* is a great threat to fruits including strawberry, black berry, grapes. Infection of this fungus causes fruit rotting ([El-Ramady et al., 2015](#)).

### **Disease Cycle of *Botrytis cinerea***

Mycelium of this fungus forms a compact structure which has the ability to survive the harsh conditions, i.e. harsh temperatures and nutrient and water availability. The specialized structure is called sclerotia (dormant mycelium) and remains predominantly in dead fruits of strawberry, black berries and straw mulch ([Jaspers et al., 2013](#)). As conditions becomes

suitable for growth in spring, sclerotia generates into new mycelium and large number of conidial spores are produced which can disperse and produce multiple infections of different flowers and can be enveloped in seeds, where they can continue to spread infection in new generation. Conidia are produced on special structures called conidiophores from where they can be dispersed by air vibrations, water splashes and rapid decrease in humidity ([Van der Heyden et al., 2021](#)). In spring season, there is a bloom of flowers on almost all plants which along with wounds are most susceptible structures for establishing a successful infection. Mycelium germinated from conidia tries to invade floral parts and continues to invade fruits and remains dormant until fruit development is completed. Spore production is again started when fruit is ripened and continues all over the season, which serves as subsidiary inoculum (Figure 1.1)([Holz et al., 2007](#)).

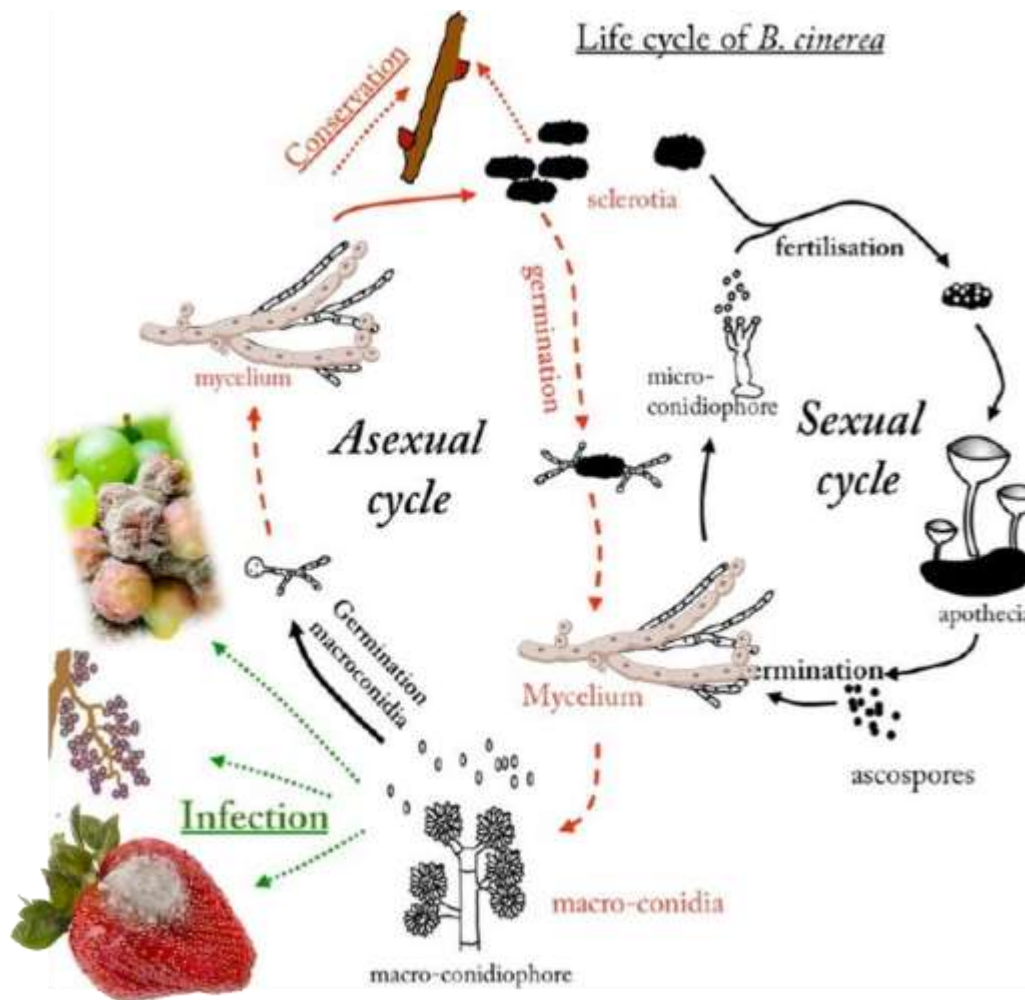


**Figure 1.1** Life cycle of *Botrytis cinerea* showing both sexual and asexual reproduction cycles (Billard et al., 2011).

The suitable temperatures for the growth of this fungus ranges between 15-25°C, but it can also have the ability to grow at lower temperatures i.e. 0°C. Due to this capability, it can easily infect samples at stored temperatures. Humidity is also required for establishing successful infection (Ciliberti et al., 2015). Thus, periodic rains and more availability of water due to irrigation increases the chances of infection establishment (González-Fernández et al., 2021). Reproduction occurs by both sexual and asexual means.

## 1.2 Yield losses caused with *Botrytis* species

*Botrytis* spp., including *B. cinerea*, can only infect when the growing conditions of their host are restricted, such as insufficient ventilation in tomato leaves, high humidity in a greenhouse, or physical harm to the plant, such as pruning ([Carisse et al., 2012](#)). The availability of resources such as carbohydrates and pollen greatly aid conidia germination on plant surfaces ([Dewey and Grant-Downton, 2016](#)). Even though *Botrytis* has become well-known around the world due to its infectivity, there is a considerable gap in the scientific literature about reliable estimates of crop losses caused by this pathogen. *Botrytis* bunch rot causes a \$2 billion loss in grapes each year ([Calvo-Garrido et al., 2019](#)). *Botrytis* spp. can cause direct losses by permanently destroying agriculture products such as berries, bulbs, fruits and flowers, rendering them unattractive and unmarketable ([Poveda et al., 2020](#)). In Florida, *botrytis* causes damage to strawberry fruit which varies between 0.5 - 13% in chemicals used plots, but losses in plots where no chemicals were used, can reach up to 35%, with substantial post-harvest losses ([Mertely et al., 2000](#)). *B. squamosa* caused onion production losses of 8 to 40% in untreated plots and yield losses were observed up to 26% in the Netherlands. *B. cinerea*, causes grey mold/*Botrytis* fruit rot (BFR) ([Beever et al., 2004](#)). Due to the infection, all type of pre and post-harvest losses are unavoidable. Its infection can lead to 100% yield reduction. It has a significant economic impact over the world, with annual losses ranges from \$11 billion to \$90 billion (Boddy, 2016). A thin coating of greyish white to dark grey mycelium appears on strawberry fruit, which thereafter becomes fuzzy and rots the entire fruit. The disease's predominance is followed by a rapid spread, resulting in direct losses due to decaying fruit.

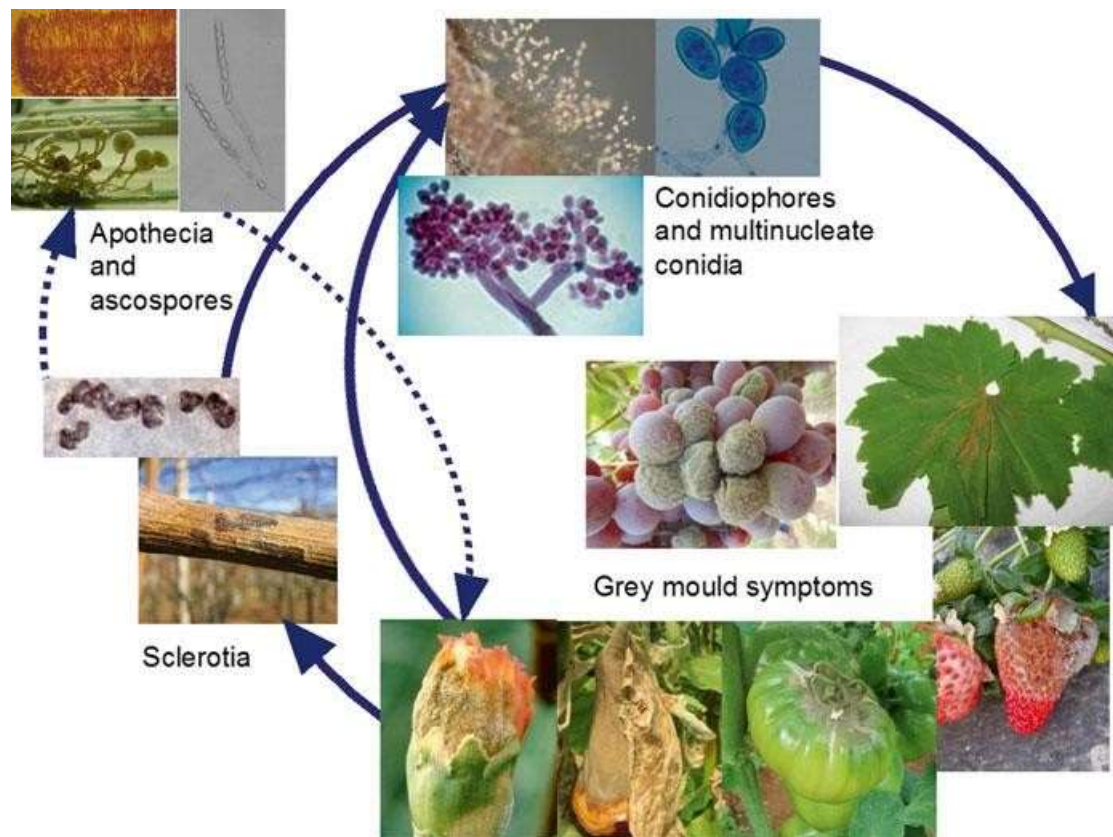


**Figure 1.1a** Life cycle of *B. cinerea* and associated symptoms

### 1.2.1 Management and cultural practices to control grey mold

Controlling botrytis infection is not easy as it has different modes to establish infection and a wide host range of this pathogen ([Cheung et al., 2020](#)). One of the best methods for controlling is integrating the most used cultural practices including chemicals / fungicides and biocontrol agents. Sanitation practices, shifting to drip irrigation instead of overhead-irrigation can help in reduce incidence of this disease ([Panno et al., 2021](#)). Using plastic tunnels, cleaning leaf wastes and avoiding excessive rainfall helps in minimizing grey mold. Providing a wide space between plants provide proper ventilation which can reduce the disease incidence but yield of plant decreases ([Rupp et al., 2017](#)). Manure and biofertilization should be used for growth purposes. The use of nitrogen fertilizers should be minimized as nitrogen aids in fungal vegetative growth which eventually leads to increase in disease severity (60-80 folds). Using insect and pest traps can also minimize fungal infection ([Abro, 2013](#)).



These commercially available chemicals / fungicides have harmful effects on other living organisms on this planet and also fungal species are becoming resistant against them. So, an environmentally friendly biocontrol is required. Nature has gifted us with mycoviruses which have the ability to diminish fungal growth. In other words we can say that mycoviruses are potential best alternatives against fungicides ([Köhl et al., 2019](#)).

### **Mycoviruses – (viruses of fungi)**

Our understanding of fungal viruses (mycoviruses) has considerably expanded since the discovery of the first virus from edible mushroom ([Hollings, 1962](#)). Mycoviruses can infect all major phyla of fungi, including yeasts, filamentous fungi and oomycetes ([Ghabrial and Suzuki, 2009](#); [Pearson et al., 2009](#)). Fungal viruses were responsible for causing La France disease in cultivated mushrooms in 1948. Three distinct virions were detected in the host fungi's diseased sporophores ([Hollings, 1962](#)).

Mycoviruses, in particular, might be used to control plant diseases in their natural environments ([Dawe and Nuss, 2001](#); [Xie and Jiang, 2014](#)). In their natural host, the majority of fungal viruses induce asymptomatic infections. They are typically transferred vertically (through spores) and intracellularly in nature (by hyphal anastomosis). Even though they lack extracellular means of transmission still they could be efficiently transmitted via hyphal contact between compatible isolates, since they are present in all major fungal species. Figure 1.2 shows the pictorial demonstration of presence of mycoviruses in a lab cultured isolate of *B. cinerea*.

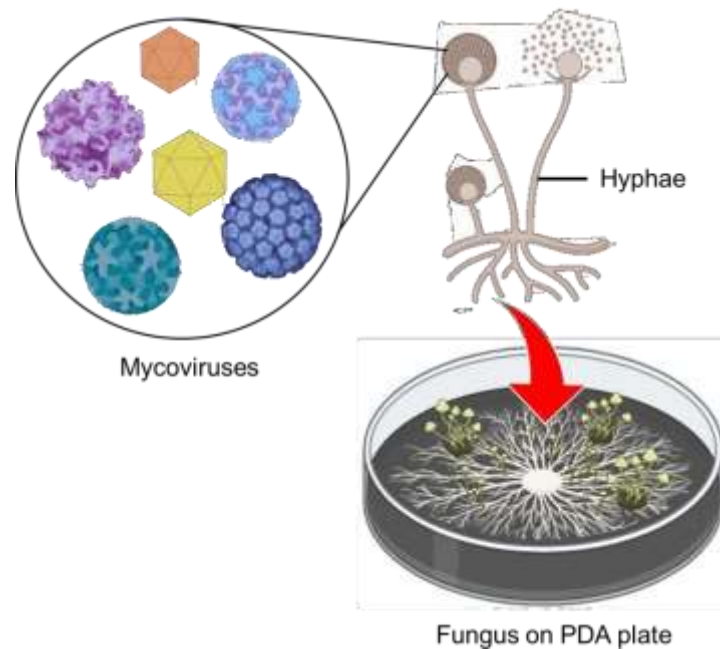


**Figure 1.2.** A pictorial demonstration of presence of mycoviruses in *Botrytis cinerea* isolates cultured in lab conditions.

### **General Properties of mycoviruses**

With improvements in Next generation sequencing (NGS) techniques, the number of fungal viruses (both dsRNA and ssRNA) is rising (Khan et al., 2021). Mycoviruses typically have an icosahedral form, and their diameter varies from family to family (Kondo et al., 2013). Mycoviruses from various families exhibit a considerable deal of variety (Jia et al., 2017; Luque et al., 2018; Nuss, 2014). According to Ghabrial et al. (2015), Jia et al. (2017), and Varga et al. (2003), mycoviruses can take the form of spherical, flexuous rods, stiff rods, club-shaped, or enveloped bacilliform particles. The genomes of the mycoviruses might be segmented. They could be encapsidated or not. Polymycoviridae, Narnaviridae, and Mitoviridae are a few more families of mycoviruses that lack capsids (Luque et al., 2018; Valverde et al., 2019). Although polymycoviruses lack a capsid, they do include a protein called PASrp that allows them to be pelleted by ultracentrifugation (Koonin and Dolja, 2014; Zhang and Nuss, 2016). Mycoviruses are distinct in that they lack an extracellular method of infection, in contrast to plant and animal viruses that fundamentally need a movement protein

for their life cycle (Son et al., 2015). Because of the intricate lifecycles of hosts and their horizontal transmission, it is exceedingly difficult to understand the function of mycoviruses in various fungal hosts. Mycoviruses can easily penetrate the septal partitions in septate fungus even though they often lack the extracellular route of transmission (van de Sande et al., 2010). There are some mycoviral infections that are an exception, such as *Sclerotinia sclerotiorum* hypovirulence-associated DNA virus 1 (SsHADV-1), which can infect intact fungal cells exogenously and decrease fungal virulence (Yu et al., 2013). This demonstrates the startling capacity of these viruses to be used as biological control. From a variety of fungi, including *C. parasitica*, *R. necatrix*, *S. sclerotium*, *Fusarium* spp., *Aspergillus* spp., fungal diseases, comprehensive data on the virome characterisation is available online (Li et al., 2019a; Telengech et al., 2020; van Diepeningen et al., 1998; Zhu et al., 2018).

### **Mycovirology's background and importance**

In Pennsylvania in 1948, a mushroom called *Agaricus bisporus*, a basidiomycete, was found to contain the first mycovirus. The disease was named La France disease (Sinden and Hauser, 1950). Low production, abnormal fruiting bodies, increased post-harvest degradation, and abnormal and delayed mycelial growth are symptoms. It was at this point that mycovirology was born. The Chestnut Blight Fungus (*Cryphonectria parasitica*) was successfully controlled using mycoviruses for the first time (Anagnostakis, 1982). New York, in America, provided the first report of the illness in 1945. In light of these factors, it is urgently necessary to control plant pathogenic fungal infection utilising hypovirulent mycoviruses, as fungicides are dangerous for both humans and animals, and fungal species are becoming resistant to them.

### **Aims of the study**

The aims of this study are presented below (chapter-wise).

- Screening phytopathogenic fungus (*Botrytis cinerea*) isolates for the presence of mycoviruses
- Molecular characterization of mycoviruses
- Molecular characterization of *Botrytis cinerea*
- Biological characterization of mycoviruses

## **REVIEW OF LITERATURE**

The hunt for potent hypovirulent mycoviruses has continued despite advances in our understanding of fungal viruses over the past few decades. According to Xie and Jiang (2014), these approaches will eventually help with the biological management of dangerous fungus and prevent yearly large economic losses.

### **Theories about the mycoviruses' existence, evolution, and origin**

The origin of mycoviruses is thought to be very ancient (Forterre, 2006), and there are currently two theories that have been proposed (Pearson et al., 2009; Varga et al., 2003), which are listed below;

#### **The coevolution hypothesis**

This theory states that the ancient illnesses evolved with their hosts (Ghabrial, 1998). Mycoviruses are thought to have evolved along the same lines as their hosts (Varga et al., 2003; Voth et al., 2006). This theory is supported by the fact that the capsid of the *Helminthosporium victoriae* virus 190S is produced via host-encoded machinery (Ghabrial et al., 2013). This hypothesis adds to the limited explanations for the diversity of mycoviruses (Varga et al., 2003).

The co-evolution theory is supported by the rare horizontal and natural vertical transmission of mycoviruses (Goker et al., 2011).

### **The plant virus hypothesis**

According to this theory, fungal viruses may have developed from plant viruses or may have transferred from plants to fungi as a result of fungal infections. It's possible that these viruses lost their mobility proteins throughout this process of evolution. This theory is supported by the sequence similarity and phylogenetic affiliation of a number of potyviruses with *Cryphonectria parasitica* viruses (*Cryphonectria hypovirus* 1, 2, and 4) (Linder-Basso et al., 2005; Xie et al., 2006). According to research by Hao et al. (2018) and You et al. (2016), several *Botrytis* mycoviruses, such as *Botrytis cinerea virus F* (BVF) and *Botrytis ourmia-like virus* (BOLV), also resemble plant viruses.

### **1.3 Mycovirus diversity and classification**

There are 23 established families of mycoviruses which are currently accepted by International Committee for the Taxonomy of Viruses (ICTV), mostly comprising of double-stranded RNA (dsRNA), and positive and negative sense single-stranded RNA ((+,-)ssRNA). Viruses with single-stranded DNA (circular) genomes have also been discovered. There will be an increasing number of taxa that accommodate mycoviruses year by year. The number and size of genome segments vary among mycoviral families. The electrophoretic profile with multiple dsRNA elements could be due to single infections by multipartite mycoviruses, multiple infections of mycoviruses or both, with or without subviral RNAs. Mixed infections of fungal isolates are commonly observed.

### 1.3.1 *Totiviridae* (dsRNA)

Members belonging to this family are single segmented with two overlapping ORFs encoding for both RNA dependent RNA polymerase (RdRP) and coat protein CP. The genomes range between 4 - 7 kbp. They family has five genera and members of only two genera infect fungi i.e. totivirus and victorivirus ([Ghabrial,2008](#); [Wickner et al., 2013](#)). Totiviruses are mostly associated with yeasts infections like *S. cerevisiae*, *Xanthophyllomyces dendrorhous* and *Scheffersomyces segobiensis*. ([Baeza et al., 2012](#)). Victoriviruses, which infect filamentous fungi, were only recently identified ([Ghabrialand Suzuki, 2009](#)) (Figure 1.3).

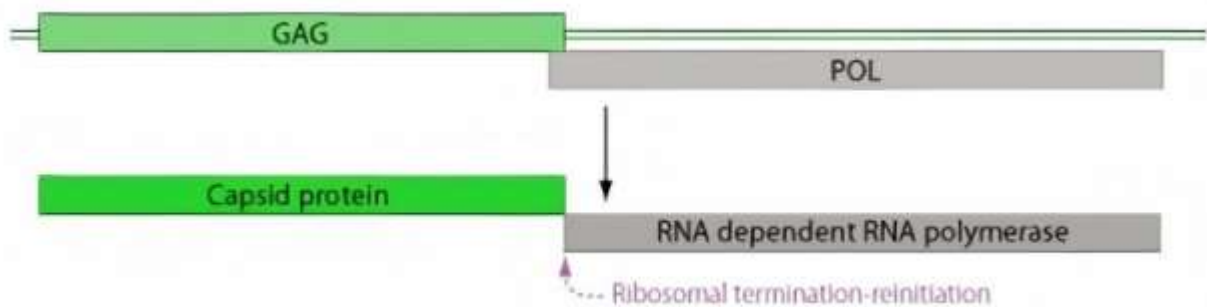


**Figure 1.3.** A representative organization of complete genome of a typical totivirus. Complete genome encodes for two ORFs i.e., CP and RdRP. A ribosomal frame shift events occurs between both ORFs together with a slippery sequence which helps in translation of Coat protein and RdRP protein (<https://viralzone.expasy.org/745>).

### 1.3.2 *Partitiviridae* (dsRNA)

This family of viruses has bisegmented genomes with a single large ORF in each segment, ranging in length from 1.4 to 2.5 kbp. dsRNA 1 (larger segment) usually produce RdRP while dsRNA 2 (smaller segment) produces CP. Some Partitiviruses can also encode for a third segment. Each of these two genomic regions is packed in its own viral particle. Alphapartitiviruses, Betapartitiviruses, and Gammapartitiviruses are the three genera of viruses that infect fungus (Nibert et al., 2014). Alpha and Betapartitiviruses have a wide host range since they infect both fungus and plants, whereas Gammapartitiviruses have only been found to infect filamentous fungi (Figure 1.4).

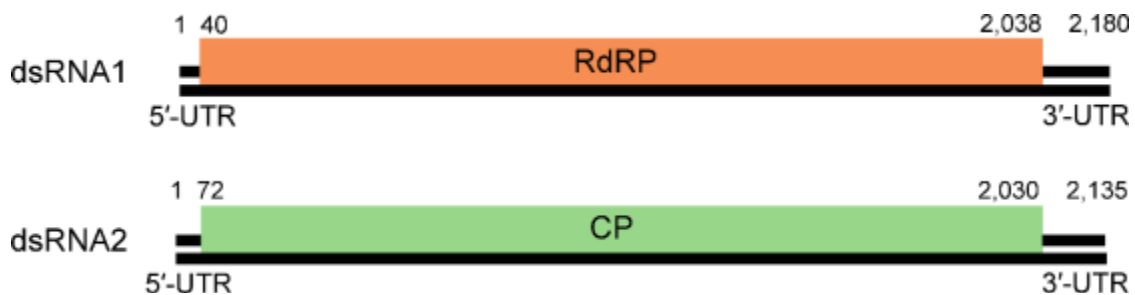


**Figure 1.4.** A representative organization of complete genome of a typical partitivirus representing CP and RdRP ([https://talk.ictvonline.org/ictv-reports/ictv\\_online\\_report/dsrna-viruses/w/partitiviridae](https://talk.ictvonline.org/ictv-reports/ictv_online_report/dsrna-viruses/w/partitiviridae))



### 1.3.3 Megabirnaviridae (dsRNA)

There are two genomic regions in this family, each of which is encapsidated separately. dsRNA1 genome is 9 kbp long, with two overlapping ORFs. ORF1 codes for CP, while ORF2 codes for RdRP (Chiba et al., 2009; Salaipeth et al., 2014). dsRNA2 has 7.4 kbp size and includes two ORFs in a single frame. The product of ORF3 seems to be sliced down into small pieces by the host infected mycelia, whereas the predicted result of ORF4 expression appears to be exposed (Kanematsu et al., 2014) (Figure 1.5).

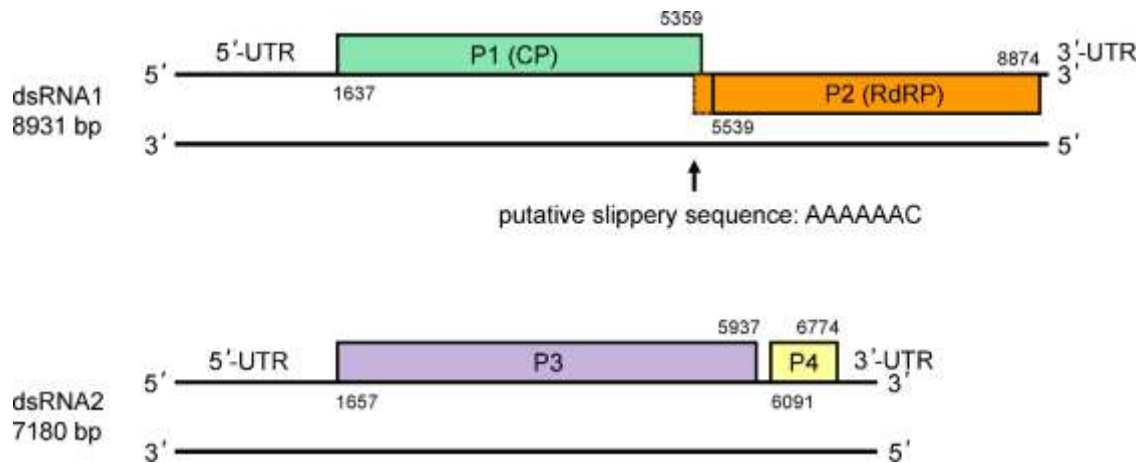


**Figure 1.5.** Genome organization of a typical megabirnavirus ([https://talk.ictvonline.org/ictv-reports/ictv\\_online\\_report/dsrna-viruses/w/megabirnaviridae](https://talk.ictvonline.org/ictv-reports/ictv_online_report/dsrna-viruses/w/megabirnaviridae)).

### 1.5.5 *Quadriviridae* (dsRNA)

To date, only one species of quadrivirus, *Rosellinia necatrix quadrivirus 1*, has been identified, and currently there are only two strains: W1075 and W1118, (Lin et al., 2012, 2013). Viruses belonging to this family contain four monocistronic genome segments, each having a length of 3.7 - 4.9 kbp. Translation product of dsRNA1 has unknown function, dsRNA3 encodes for RdRP whilst dsRNA2 and dsRNA4 translation products are involved in CPs (Figure 1.6).

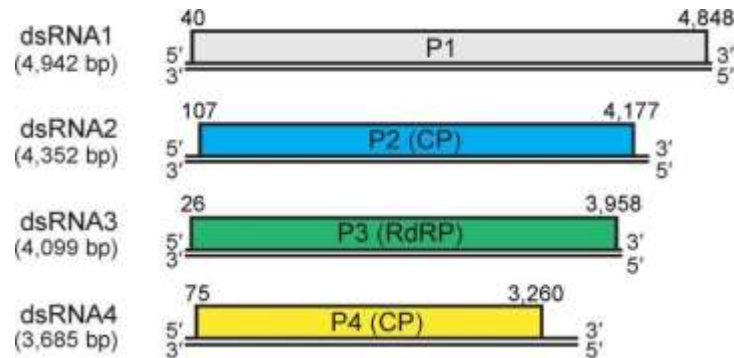


**Figure 1.6.** Genomic organization of members of family quadriviridae.

([https://talk.ictvonline.org/ictv-reports/ictv\\_online\\_report/dsrna-viruses/w/quadriviridae](https://talk.ictvonline.org/ictv-reports/ictv_online_report/dsrna-viruses/w/quadriviridae)).

### 1.5.6 *Reoviridae* (dsRNA)

First Reo-like-virus was reported in 1994. The genome segments of mycoreovirus encode for single protein. Mycoreoviruses vary in number of genome segments: MyRV1 and 2 harbor 11 segments, while MyRV3 has 12 segments ([Sotirovski et al., 2011](#)) (Figure 1.7).

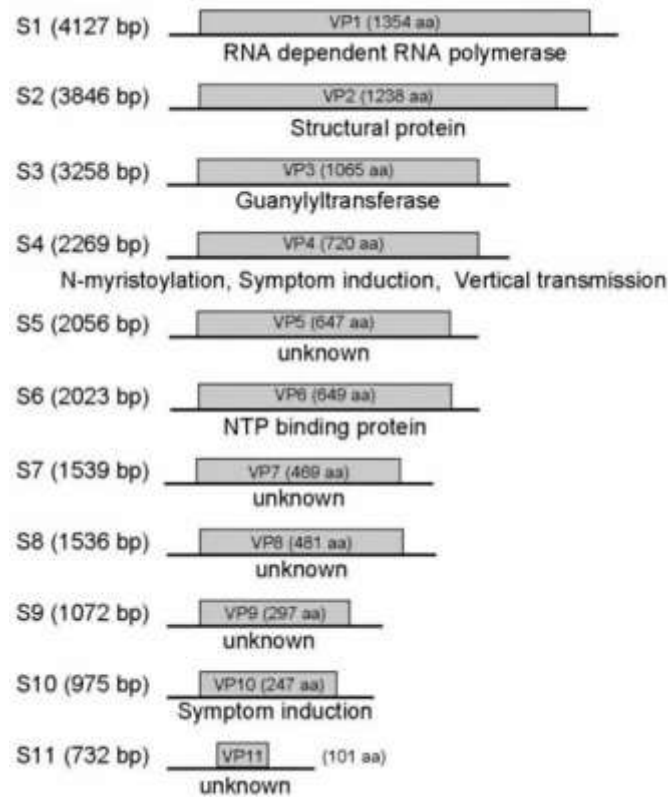


**Figure 1.7.** Genome organization of viruses belonging to family Mycoreoviridae. (Tanaka et al., 2012).

### 1.5.7 Endornaviridae (+) sense ssRNA

Members of this family were previously known as dsRNA viruses, however phylogenetic investigations revealed that they show more closeness to ssRNA viruses (Ghabrial and Suzuki, 2009). *Endornaviridae* is clearly designated as (+) sense ssRNA family having genome size varies from 9 - 18 kbp. The family contain two genera, *Alphaendornavirus* contain 24 species infecting wide host range such as plants, fungi and oomycotes and *Betaendornavirus* include 7 species infecting specifically ascomycete fungi. The genome of Endornaviruses contain single linear, large ORF (RdRP) (Fukuhara and Gibbs 2012, Stielow et al., 2011, Gibbs et al., 2000).

### 1.5.8 *Alphaflexiviridae* (+) sense ssRNA viruses

The members of *Alphaflexiviridae* contain +sense ssRNA genome, size ranging from 5.4 - 9 Kbp. The members of this family have flexuous filamentous virions and diameter is about 12 - 13 nm. Alphaflexiviruses infect both plants and phytopathogenic fungi. There is large single ORF encoding for RdRP. The *Alphaflexiviridae* contain 6 genera named as *Allexivirus*, *Botrexvirus*, *Lolavirus*, *Platypuvirus*, *Potexvirus* and *Sclerodnavirus*. Out of these six genera only 2 genera Botrexvirus and Sclerodnavirus infect fungi (Figure 1.8).

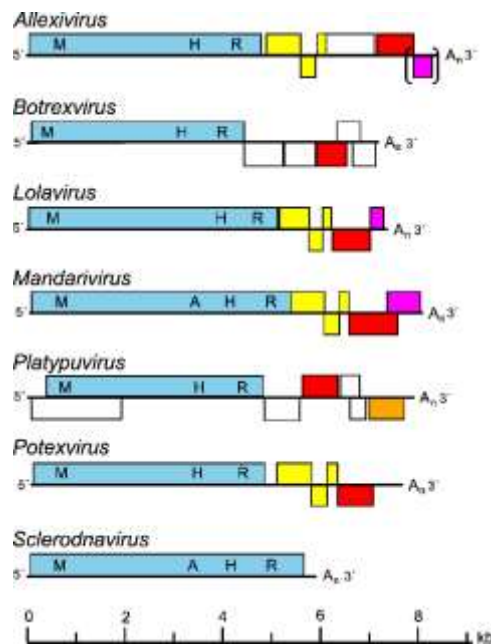


**Figure 1.8.** Genome organization of some representative members belonging to family *Alphaflexiviridae* ([https://talk.ictvonline.org/ictv-reports/ictv\\_online\\_report/positive-sense-rna-viruses/w/alphaflexiviridae](https://talk.ictvonline.org/ictv-reports/ictv_online_report/positive-sense-rna-viruses/w/alphaflexiviridae))

### 1.5.9 *Botourmiaviridae* (+) sense ssRNA viruses

The members of *Botourmiaviridae* infect both plants and filamentous fungi. The genome size is 2 - 3.4 kbp of viruses belonging to this family. Single ORF is present which encodes for RdRP. *Botourmiaviridae* contain six genera, *Botoulivirus*, *Ourmiavirus*, *Magoulivirus*, *Rhizoulivirus*, *Penoulivirus* and *Scleroulivirus*. Out of these six genera viruses of only three genera such as *Botoulivirus*, *Rhizoulivirus* and *Penoulivirus* infect fungi. The genome of ourmiaviruses is tripartite which remaining other genera have monopartite genomes (Figure 1.9).

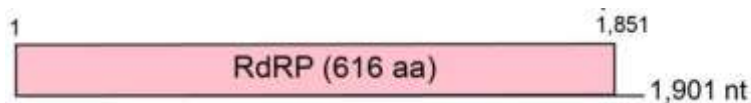


**Figure 1.9.** Genome organization of typical Botourmiavirus ([https://talk.ictvonline.org/ictv-reports/ictv\\_online\\_report/positive-sense-rna-viruses/w/botourmiaviridae](https://talk.ictvonline.org/ictv-reports/ictv_online_report/positive-sense-rna-viruses/w/botourmiaviridae)).

### 1.5.5 *Hypoviridae* (+) sense ssRNA

*Hypoviridae* contains only one genus Hypovirus, viruses of said family have genome size ranging from 9.1-12.7 Kbp and most of these viruses are capsid less. Viruses either possess single large ORF or two ORFs. In both ascomycetes and basidiomycetes, hypoviruses have been detected so far. Classified hypoviruses induce hypovirulence on chestnut trees and multiple unclassified mycoviruses have little or no effect. Hypovirus-related viruses also infect *Valsa ceratosperma* (Yaegashi et al., 2011), *Fusarium* spp. (Osaki et al., 2016; Wang et al., 2013), *S. sclerotiorum* (Marzano et al., 2016b) *Agaricus bisporus* (Dobbs et al., 2021) and *M. phaseolina* (Marzano et al., 2016a).

### **1.5.6 *Mymonaviridae* (-) sense ssRNA**

Viruses belonging to family *Mymonaviridae* are enveloped filamentous virions, have - sense ssRNA genome. Sclerotimonavirus is the only single known genus of *Mymonaviridae* and members of said family infect filamentous fungi. No 3'-terminal poly (A) tail is present, and the 5'-terminal does not contain a cap. The genome of mymonavirus contain six non-overlapping ORFs which are arranged linearly and these are separated by intergenic regions. There are total 9 genera present in *Mymonaviridae*. Members of this family solely infects fungi.

### **1.5.7 *Metaviridae* (Reverse Transcribing Viruses)**

Members of family *Metaviridae* include retrotransposons which have the ability to reverse-transcribe and also have long terminal repeats in their genomes. Members of this family has wide host range infecting fungi, plants and animals. Details of all mycoviral families are shown in Table 1.1.

**Table 1.1** List of reported mycoviral families with their molecular features

Family	Genus	Size	Envelope	Genome	Genome Size
<i>Metaviridae</i>	Metavirus	Unknown	Yes/No	ssRNA-RT	4-10 kb
<i>Pseudoviridae</i>	Pseudovirus, Hemivirus	60–80 nm	No	ssRNA-RT	5-9 kb
<i>Chrysoviridae</i>	Chrysovirus	65 nm	No	dsRNA	2.9-3.6 kb
<i>Endornaviridae</i>	Endornavirus	No virions	NA	dsRNA	14-18 kb
<i>Partitiviridae</i>	Partivirus	30-43nm	No	dsRNA	1.4-2.4 kb
<i>Reoviridae</i>	Mycoreovirus	60-85nm	No	dsRNA	19-32 kb
<i>Totiviridae</i>	Totivirus Victorivirus	33-40nm	No	dsRNA	4-7 kb
<i>Alphaflexiviridae</i>	Botrexvirus, Sclerodarnavirus	10-15nm x 470-800nm	No	ssRNA	6-9 kb
<i>Gammaflexiviridae</i>	Mycoflexivirus	13-720nm	No	ssRNA	7 kb
<i>Barnaviridae</i>	Barnavirus	48-53nm x 18-20nm	No	ssRNA	4 kb
<i>Hypoviridae</i>	Hypovirus	No virion	NA	ssRNA	9-13 kb
<i>Narnaviridae</i>	Narnavirus, Mitovirus	NA	NA	ssRNA	2-3 kb
<i>Mymonaviridae</i>	Sclerotimonavirus	25–50nm	Yes	-sense ssRNA	10 kb
<i>Botourmiaviridae</i>	Ourmiavirus	18nm	No	ssRNA	1-3 kb

<i>Quadriviridae</i>	Quadrivirus	45nm	No	dsRNA	16-17 kb
<i>Megabirnaviridae</i>	Megabirnavirus	80nm	No	dsRNA	16 kb

## 1.6 Vertical and horizontal transmission in mycoviruses

Currently two types of mycoviral mode of transmission are known for mycoviruses i.e. vertical transmission ([Nuss, 2005b](#)), horizontal transmission ([Milgroom and Cortesi, 2004](#)). Extracellular transmission of DNA mycoviruses has been established, but not RNA mycoviruses. The sexual or asexual transfer of viruses from parents to offspring is known as vertical transmission ([Nuss, 2005a](#)). Vertical transmission, on the other hand, is common in asexual reproduction ([Ghabrial et al., 2015](#)). The frequency of viral transmission varies depending on the mycovirus and the host fungus. Mycoviruses are transferred horizontally between two individual fungi by hyphal contact or anastomosis ([Ghabrial, 1998](#)). The propagation of RNA mycoviruses is inhibited due to formation of heterokaryon incompatibility or vegetative incompatibility, which behaves as a barrier during horizontal transmission. If many VCGs are present among fungal strain mycoviruses can't propagate horizontally. Interspecific transmission of mycoviruses across distinct fungal species has been seen in *A. niger/A. nidulans* and *S. sclerotiorum/S. minor* ([Yaegashi et al., 2013](#)). Purified RNA mycovirus particles, such as the *B. cinerea* RNA virus 1 (BcRV1) and *B. porri* RNA virus 1 (BpRV1), have been successfully transfected to *B. cinerea* and *B. porri*, respectively ([Castro et al., 2003](#); [Wu et al., 2012](#)).



## **1.7 Mycoviruses in *Botrytis* species**

Mycoviruses may be detected in almost every major taxonomic group of plant pathogenic fungus, such as *B. porri* and *B. cinerea* ([Ghabrial and Suzuki, 2009](#)). The presence of dsRNAs in mycelial extracts and the identification of virus-like particles (VLPs) led to the first completely characterized mycovirus from *B. cinerea* ([Howitt et al., 2001](#)). A wide diversity has been observed in *B. cinerea* reported VLPs (isometric, bacilliform, and flexuous). The presence of dsRNAs in *B. cinerea* mycelia is frequently confirmed by the presence of matching virus like particles (VLPs), implying that the dsRNAs are mycovirus genomes. With the evolving sequencing technologies, multiple species of RNA mycoviruses, including BVF (Botrytis virus F), BVX (Botrytis virus X), BcMV1 (Botrytis cinerea mitovirus 1), BfTV1 (Botryotinia fuckeliana totivirus 1), BfPV1 (Botrytis cinerea partitivirus 1), and Bc378V1 (Botrytis cinerea CCg 378 virus 1) infecting *B. cinerea*, and BpRV1 (Botrytis porri RNA virus 1) infecting *B. porri* (Table 1.2).

### **Geographic Distribution and Incidence of RNA Mycoviruses in Botrytis**

Although we currently know very little about the epidemiology of mycoviruses, they may have a broad geographical distribution like viruses that infect other hosts (animals and plants). According to evidence (Pearson and Bailey 2013; Rodriguez-Garcia et al. 2013; Kecskeméti et al. 2014; Wu et al. 2014), the RNA mycoviruses BVF, BVX, BcMV1 and BpRV1 have a widespread distribution. According to research by Howitt et al. (2001, 2006), BVF and BVX were present in 17.2 and 18.8% of *B. cinerea* isolates from New Zealand, respectively. In contrast to BVX, which was shown to be present alone in *B. cinerea* isolates from Belgium, Greece, Italy, Portugal, Switzerland, and the United States, BVF was found to be present alone or in combination with BVX in *B. cinerea* isolates from England, France, and Israel (Pearson and Bailey 2013). Among the analyzed isolates of *B. cinerea* from the aforementioned nations,

the average proportions of BVF and BVX were 16.1 and 29%, respectively. In Germany, neither of the two mycoviruses (BVF nor BVX) were found in 53 isolates of *B. cinerea* in 2008, but in 2010, 31 (3%) and 3% of the 100 isolates of *B. cinerea* (n = 100) were found to be infected with BVF alone, BVX alone, or BVF + BVX, respectively (Kecskeméti et al. 2014). It appears that the *B. cinerea* infection caused by BVF or BVX varies depending on the year and the region. *B. cinerea* was first discovered to be infected by the mycovirus BcMV1 in China (Wu et al. 2007, 2010). According to Rodriguez-Garcia et al. (2013), BcMV1 was found in about 30.2% of the *B. cinerea* isolates (n = 96) obtained from southern and central Spain. These investigations imply that BcMV1 might be widely distributed geographically. *B. porri* was first discovered to be infected with the mycovirus BpRV1 in China (Wu et al. 2012). In this nation, it has been shown to infect *B. squamosa* and *Sclerotinia sclerotiorum* (L. J. Liu and D. H. Jiang, unpublished data). These findings imply that BpRV1 might have a large host range.

**Table 1.2.** Mycoviruses identified from Botrytis species so far

Fungal Host	Virus shape	Genome Type	Reference
<i>B. cinerea</i>	Isometric	dsRNA	( <a href="#">Howitt et al., 2006</a> )
<i>B. cinerea</i>	Bacilliform	dsRNA	( <a href="#">Howitt et al., 2006</a> )
<i>B. cinerea</i>	Unencapsidated	dsRNA	( <a href="#">Howitt et al., 2006</a> )
<i>B. cinerea</i>	Isometric	dsRNA	( <a href="#">Vilches and Castillo, 1997</a> )
<i>B. cinerea</i>	Unencapsidated	dsRNA	( <a href="#">Vilches and Castillo, 1997</a> )
<i>B. cinerea</i>	Unencapsidated	dsRNA	( <a href="#">Vilches and Castillo, 1997</a> )
<i>B. cinerea</i>	Botrytis virus X	ssRNA	( <a href="#">Howitt et al., 2006</a> )
<i>B. cinerea</i>	Botrytis virus F	ssRNA	( <a href="#">Howitt et al., 2001</a> )
<i>B. cinerea</i>	Isometric	dsRNA	( <a href="#">Castro et al., 2003</a> )
<i>B. cinerea</i>	Isometric	dsRNA	( <a href="#">Castro et al., 2003</a> )
<i>B. cinerea</i>	Isometric	dsRNA	( <a href="#">Vilches and Castillo, 1997</a> )
<i>B. fuckeliana</i>	Partitivirus	dsRNA	( <a href="#">De Guido et al., 2007</a> )
<i>B. fuckeliana</i>	Totivirus	dsRNA	( <a href="#">De Guido et al., 2007</a> )
<i>B. cinerea</i>	Mitovirus	dsRNA	( <a href="#">Wu et al., 2010a</a> ; <a href="#">Wu et al., 2007</a> )
<i>B. cinerea</i>	Isometric	dsRNA	( <a href="#">Wu et al., 2012</a> )
<i>B. cinerea</i>	Endornavirus	dsRNA	( <a href="#">Hao et al., 2018</a> )
<i>B. porri</i>	RNA virus	dsRNA	( <a href="#">Wu et al., 2012</a> )
<i>B. cinerea</i>	Narnavirus	ssRNA(+sense)	( <a href="#">Donaire and Ayllón, 2017</a> )
<i>B. cinerea</i>	Mymonavirus	ssRNA(-sense)	( <a href="#">Hao et al., 2018</a> )

### **Effects of mycoviruses on host fitness**

Mycoviruses from different families can affect their hosts in various ways, but they are often latent (without symptoms) in nature, according to Buck (1988). Here, nearly all of the significant impacts brought on by mycoviruses are covered. The presence of fungal viruses and its impact on the fungal hosts are intricately correlated. These consist of the following.

- Cryptic
- Hypervirulent
- Hypovirulent

How mycoviruses control the ecology of their hosts is still a mystery (Hyder et al., 2013). Mycovirus impact analysis is extremely straightforward for a single infection, but it is quite challenging to connect several infections with understudied mycoviruses to a certain phenotypic.

### **Mycoviral infections that are cryptic (symptomless or latent)**

The term 'cryptic' means mysterious / obscure. Infections with cryptic mycoviruses are frequently seen in the kingdom Fungi. The mycoviruses' evident influence despite their absence of symptoms revealed that they are typically cryptic. One cannot rule out the chance that the effect will differ under all hypothetical environmental circumstances when keeping this element in mind. According to (van Diepeningen et al., 2006), a very slight change in colony diameter was noticed in isogenic lines of virus-free and infected cells. This result suggests that these mycoviruses may have a very small impact on host growth. The statement that mycoviruses "don't disturb their host fitness" doesn't imply that they are going unnoticed by their fungi hosts. A lengthy co-evolutionary process may have led to cryptic coexistence (Araujo et al., 2003; May and Nowak, 1995). When environmental

factors alter and the internal cellular balance is upset, symptoms may develop. Change may result from an internal stimulus (cytoplasmic) or an external stimulus (environmental). What mechanism underlies these symptomless and symptom-inducing interactions is still unknown.

### **Hypovirulence: A decrease in the pathogenicity of fungi**

Hypovirulence is a condition when a fungus's capacity to spread illness is reduced. Mycoviruses that are low in virulence cause a variety of symptoms in their hosts. Reduced pigmentation, spore production (both sexual and asexual), and mycelial growth are common signs (Ihrmark et al., 2002; Moleleki et al., 2003; Nuss, 2005; Suzaki et al., 2005). There is no recognised metabolic mechanism that specifically causes hypovirulence, and no known genetic trait that is connected with the hypovirulent phenotype (Xie et al., 2006). The region p29 that is in charge of hypovirulence is only known to exist in members of the family Hypoviridae. The region p29 that is in charge of hypovirulence is only known to exist in members of the family Hypoviridae. Further research is needed to identify the areas responsible for hypovirulence in additional families. The earliest description of mycoviral hypovirulence came from a mushroom called *Agaricus bisporus* that was home to the La France isometric virus (LIV) (Romaine and Schlagnhauser, 1995; Hollings, 1962; Ro et al., 2006). Later, other mycoviruses such as the oyster mushroom spherical virus (OMSV) from *Pleurotus florida* and the oyster mushroom isometric virus from *P. pulmonarius* also shown these effects in mushrooms. In addition to preventing sporulation in the *Diaporthe perijuncta* fungus, *Diaporthe* RNA virus also has growth-retarding effects (Moleleki et al., 2003). A totivirus called HmTV1-17 caused *Helicobasidium mompa* to have an attenuated phenotype (Suzaki et al., 2005) and *Heterobasidion annosum* to exhibit reduced basidiospore germination (Ihrmark et al., 2002). According to Wu et al. (2007), *Botrytis cinerea* mitoviruses have also demonstrated hypovirulence. Reduced sporulation, laccase activity, and fungus invasiveness are among the symptoms (Castro et al., 2003). *Fusarium graminearum*'s

growth and virulence on wheat were lowered, but the pigmentation was raised along with a 60-fold reduction in the synthesis of trichothecene mycotoxins (Chu et al., 2002). Similar to this, one isolation among 668 *Aspergillus* species that were mycovirus-positive displayed reduced development without sporulation (van Diepeningen et al., 2006). According to Doherty et al. (2006), mitoviruses that infected *Ophiostoma novo-ulmi* had hypovirulent effects as well. This fungus was shown to produce various sized dsRNAs that impaired the capacity of the fungus to cause disease by inhibiting the action of the mitochondrial cytochrome c oxidase enzyme. The fungus *S. sclerotiorum* virome, which causes white stem rot, has been the subject of extensive research. This investigation has revealed numerous hypovirulent viruses. These fungal viruses may have the ability to act as biocontrol agents (Xie and Jiang, 2014). Nevertheless, these effects can be exploited as biocontrol because they are economically significant (particularly in the case of phytopathogens).

### **Hypervirulence: Increased fungal pathogenicity**

Hypervirulence is the term used to describe the upregulation of fungal pathogenicity (Marquez et al., 2007). Consider the example of *Nectria radicicola* (a root pathogen) harbouring 6 kbp dsRNA, which interferes with signal transduction pathways and promotes fungal virulence (Ahn and Lee, 2001). Mycoviruses can boost fungal pathogenic characteristics. Fungal virulence is not always increased by hypervirulence, but it can also benefit the fungus and its host plant. *Curvularia thermal tolerance virus* (CThTV), the endophytic fungus *Curvularia protuberata*, and the virus of panic grass *Dichanthelium lanuginosum* form an intriguing three-way symbiosis. The panic grass *Dichanthelium lanuginosum* was given heat tolerance by this virus (Marquez et al., 2007). Furthermore, the tomato plant was able to acquire heat tolerance thanks to the virus-infected endophyte (Al-Hamdani et al., 2015). *Saccharomyces cerevisiae* is the fungus that is the most well-known example of the hypervirulence killer phenomenon (Bevan, 1963). The Totiviridae member *Saccharomyces cerevisiae*

virus L-A, which manifests a lethal phenomenon due to the production of protein toxins encoded by its satellite dsRNAs, is one of the mycoviruses that are advantageous to their host. According to Schmitt and Breinig (2002), these poisons are lethal for closely related species, giving the host an advantage over rivals. Other yeasts with killer phenotypes have also been reported, including *Hanseniaspora uvarum*, *Zygosaccharamyces bailii*, *Kluyveromyces lactis*, as well as the maize smut fungi *Ustilago maydis*, *Torulaspota delbrueckii*, and *Wickerhamomyces anomalus* (Schmitt and Breinig, 2002; Schmitt and Neuhausen, 1994). Killer isolates have potential uses in agriculture, the food industry, and medicine (Dawe and Nuss, 2001; Schmitt and Breinig, 2002). *Ustilago* and killer phenotypes in yeasts are extreme examples of advantageous interactions in the yeast *Saccharomyces cerevisiae*. Killer protein toxins are fatal to delicate strains and have antimycotic properties. This characteristic is not just related to dsRNA viruses; linear dsDNA plasmids can also encode it (Ahn and Lee, 2001). Three mycoviruses, ScV-M1, ScV-M2, and ScV-M28, have been found as having the ability to kill. All viruses carry the distinct deadly toxins K1, K2, and K28, along with an immunity gene that safeguards host strains that are harbouring them. Toxin-coding (M) killer virus and its helper virus (L-A) were needed as two distinct dsRNA viruses (Abu-Mejdad et al., 2020).

## Neoviral behaviours of mycoviruses

Mycoviruses have a wide range of lifestyles, according to research on them. While some mycoviruses can replicate on their own, others depend on other mycoviruses. Yadokari virus 1 (YkV1) and Yado-nushi virus 1 (YnV1) are carriers of one such way of life (Hisano et al., 2018). Here, YkV1 encodes its own separate RdRP protein for replication, but it depends on YnV1 for encapsidation. It was thought that YkV1's replication and transcription were carried in the YnV1 capsid, which is why it is grouped with dsRNA mycoviruses (Das et al., 2021; Zhang et al., 2016). This is an illustration of a synergistic interaction where YkV1 receives capsid for its genome and raises the amounts of YnV1 accumulation in exchange. According to Zhang et al. (2016), YnV1 is a self-sufficient dsRNA virus that can carry out its replication on its own. These interactions, in which YnV1-like viruses associate with other dsRNA viruses, have been seen in filamentous fungi (Luque et al., 2018). Another example of a mycovirus with a neo lifestyle is the *Aspergillus fumigatus* polymycovirus (also known as the tetra segmented mycovirus; Kanhayuwa et al., 2015; Zoll et al., 2018). The putative catalytic amino acid sequence GDNQ that this virus's genome encodes is comparable to other (+) ssRNA viruses (mostly mononegaviruses), but phylogenetic study revealed that it is more closely related to calciviruses (+) ssRNA viruses. It also encodes PASrp, which encases its genome (not a true capsid) and is resistant to RNase A (Jia et al., 2017; Kotta-Loizou and Coutts, 2017a; Mahillon et al., 2019). HadV1-7n and HadV1-1NL, members of the proposed family *Hadakaviridae*, have relationships to polymycoviruses, but they lack the ability to encode a PASrp that can encapsulate their genome, leaving it naked and vulnerable to RNase A (Khan et al., 2021; Sato et al., 2020b).



### **1.8 Mycoviruses can alter host fitness (In case of *Botrytis cinerea*)**

Different effects have been observed on host phenotype due to presence of mycoviral infections which could be healthy, harmful or symptomless ([Nuss and Koltin, 1990](#)). Yeast Killer system is the best example of these effects ([Magliani et al., 1997](#)). The uninfected strains are sensitive to the proteins produced by killer strains. Phytopathologists are interested in investigations on mycoviral infections that affect fungal virulence attenuation or deliberation. Infection of many of these viruses has been observed fungi, including *B. cinerea* and *B. porri*, so far. *B. cinerea* infection by BcMV1 is closely connected to *B. cinerea* hypovirulence ([Wu et al., 2010b](#); [Wu et al., 2007](#)). Infection would result in altered phenotype, changes in growth and pigmentation. The etiology of *B. porri* hypovirulence has been identified by another BpRV1 mycovirus. In comparison to virus-free *B. porri* isolates, the BpRV1-infected isolate propagated more slower on potato dextrose agar and developed multiple mycelial sectors along colony boundaries.

### **1.9 Techniques in mycoviral identification for molecular characterization**

The most basic method of pathogen identification is visual observation of symptoms and confirmation through microscopy ([Ward et al., 2004](#)). Irrespective of low-cost procedure, it does necessitate the use of particularly trained and professional personnel. Approaches are available for detecting viral proteins or viruses using serological and molecular techniques for detection of viral nucleic acids.

### **1.9.1 RT-PCR for detection of mycoviruses**

Reverse transcription PCR employs genome-specific primers to generate complementary DNA (cDNA) from viral RNA before amplifying a specific section of the genome. The result of electrophoresis on stained gels becomes apparent exponentially. The resultant amplicon is sequenced using sanger sequencing ([Schaad and Frederick., 2002](#)). Because most plant viruses have a DNA sequence, PCR is used to identify them. Because their genomes are extremely sensitive and specific, RNA PCR-based detection systems can identify a wide range of diseases. PCR-based detection methods are very sensitive and specific. They may be multiplexed to detect different diseases ([Ward et al., 2004](#)).

### **1.9.2 Metagenomics and Next-generation sequencing**

Metagenomics is a technique for sampling and studying the complete population of organisms that share the same habitat ([Hugenholtz and Tyson., 2008](#)). Scientists can now assess the complexity of microbial communities in single environments. Metagenomic analysis involves extracting total RNA from under studied samples and shearing it into small fragments. These fragments are further cloned in a vector and a library is prepared for sequencing ([Hugenholtz and Tyson., 2008](#)). Traditional Sanger sequencing was used in the early days of metagenomic research, but was not fast ([Adams et al., 2009b](#)). Next Gen Sequencing was introduced in 2005 which eliminate time consuming vector cloning ([Adams et al., 2009a](#)).

NGS also called high-throughput sequencing and deep sequencing. The basic procedure is same; shredding the total RNA into small fragments and adaptor ligation, which are further immobilized on specific platform. Adaptors complementary sequences are used to amplify the fragments on the platform also called pyrosequencing ([Ware et al., 2012](#)). This is now a trending approach in characterizing different microbial genomes including viral,

bacterial and fungal samples ([Dolja and Koonin, 2012](#)). It is very much sensitive as it can sequence low titered viruses which are even not visible on agarose gel ([Al Rwahnih et al., 2009](#)). Although sequencing takes just a minimal quantity of beginning material, it must be of excellent quality to get high-quality results. The RNA sequences of a range of infections might be sequenced by starting with RNA and synthesizing cDNA with random primers. This method is state of the art procedure for mycoviral genomic characterization.

### **1.10 Objectives of the research Project**

1. Molecular identification of environmental species of *Botrytis* to retrieve the information about the prevalence of *Botrytis* species existing in Pakistan and causing infection in environment
2. Characterization of novel mycovirus genomes identified during the screening process in order to understand the nature of mycoviruses
3. Phylogenetic analysis of the novel mycoviruses to verify the lineage of viruses
4. Studying the infection and its effect on the fungal samples so to identify the hypovirulent mycoviruses as a potential tool to control *Botrytis* infecting different crops
5. The strains with debilitating colonies will be mainly selected for their effects on the fitness of their hosts
6. The mycoviruses conferring harmful effects on the fungi will be used either cured or transfected to produce isogenic lines for potential biocontrol.

## **2. Materials and Methods Used:**

## 2.1 Fungal Isolates collection from Punjab and KPK, Pakistan

A total of 102 samples were collected Punjab & KPK province of Pakistan (Figure 2.1) The location of sampling sites can be seen in Figure 2.2. Muridke, Kamoke and Mardan fields were the main cultivation sites where these samples were seen. Samples of fungus infected strawberry fruits were collected from strawberry fields. Complete list of collection of fungal samples which have been identified is mentioned in Table 2.1.



**Figure 2.1** Sample collection of infected strawberry fruits from strawberry fields which showed symptoms of grey mold infestation.



**Figure 2.2.** Map of Pakistan showing the collecting sites of understudied fungal samples. The samples were collected from Mardan, Muridke and Kamoke from different farms of strawberry.

**Table 2.1.** Details of fungal isolates collected and screened during this study. Genetic diversity

analysis showed almost all fungal samples belongs to group II

Isolate Code	Fungal Morphology	Molecular Identification	Mycovirus	Genetic Group
A ST 1	White	<i>Geotrichum candidum</i>	Yes	II
A ST 2	White	<i>B. cinerea</i>	No	II
A ST7	White	<i>B. cinerea</i>	No	II
A ST 13	White	<i>B. cinerea</i>	No	II
A ST 15	White	<i>B. cinerea</i>	No	II
A St 9	White	<i>B. cinerea</i>	Yes	II
M ST1	White	<i>B. cinerea</i>	No	II

M ST 2	White	<i>B. cinerea</i>	No	II
M ST 3	White	<i>B. cinerea</i>	No	II
M ST 4	White	<i>B. cinerea</i>	No	II
M ST 8	White	<i>B. cinerea</i>	No	II
M ST 9	White	<i>B. cinerea</i>	No	II
M ST12	White	<i>B. cinerea</i>	No	II
M ST 15	White	<i>B. cinerea</i>	No	II
M ST 16	White	<i>B. cinerea</i>	No	II
A ST 16	White	<i>B. cinerea</i>	No	II
A ST 18	White	<i>B. cinerea</i>	No	II
M ST a1	White	<i>B. cinerea</i>	No	II
M ST a2	White	<i>B. cinerea</i>	No	II
M ST a4	White	<i>B. cinerea</i>	No	II
M ST a5	White	<i>B. cinerea</i>	No	II
M ST a7	White	<i>B. cinerea</i>	No	II
M ST a11	White	<i>B. cinerea</i>	No	II
M ST a12	White	<i>B. cinerea</i>	No	II
M ST a14	White	<i>B. cinerea</i>	No	II
A ST 35	White	<i>B. cinerea</i>	No	II
KST1	White	<i>B. cinerea</i>	No	II
KST2	White	<i>B. cinerea</i>	No	II
KST4	White	<i>B. cinerea</i>	No	II
KST5	White	<i>B. cinerea</i>	Yes	II
KST6	White	<i>B. cinerea</i>	No	II
KST7	White	<i>B. cinerea</i>	No	II
KST8	White	<i>B. cinerea</i>	No	II
KST9	White	<i>B. cinerea</i>	No	II
KST10	White	<i>B. cinerea</i>	Yes	II
KST12	White	<i>B. cinerea</i>	No	II
KST14	White	<i>B. cinerea</i>	Yes	II

KST15	White	<i>B. cinerea</i>	No	II
KST16	White	<i>B. cinerea</i>	No	II
KST18	White	<i>B. cinerea</i>	Yes	II
KST19	White	<i>B. cinerea</i>	No	II
KST20	White	<i>B. cinerea</i>	No	II
KST21	White	<i>B. cinerea</i>	No	II
KST22	White	<i>B. cinerea</i>	No	II
KST23	White	<i>B. cinerea</i>	No	II
KST25	White	<i>B. cinerea</i>	No	II
KST28	White	<i>B. cinerea</i>	No	II
KST29	White	<i>B. cinerea</i>	No	II
KST31	White	<i>B. cinerea</i>	Yes	II
KST33	White	<i>B. cinerea</i>	Yes	II
KST35	White	<i>B. cinerea</i>	No	II
KST36	White	<i>B. cinerea</i>	No	II
KST37	White	<i>B. cinerea</i>	No	II
KST38	White	<i>B. cinerea</i>	No	II
KST39	White	<i>B. cinerea</i>	No	II
KST40	White	<i>B. cinerea</i>	Yes	II
KST41	White	<i>B. cinerea</i>	No	II
KST42	White	<i>B. cinerea</i>	No	II
KST44	White	<i>B. cinerea</i>	No	II
KST45	White	<i>B. cinerea</i>	No	II
KST46	White	<i>B. cinerea</i>	No	II
KST47	White	<i>B. cinerea</i>	No	II
KST48	White	<i>B. cinerea</i>	No	II
KST50	White	<i>B. cinerea</i>	No	II
KST51	White	<i>B. cinerea</i>	No	II
KST52	White	<i>B. cinerea</i>	No	II
KST53	White	<i>B. cinerea</i>	No	II



KST54	White	<i>B. cinerea</i>	No	II
KST55	White	<i>B. cinerea</i>	No	II
KST56	White	<i>B. cinerea</i>	No	II
KST57	White	<i>B. cinerea</i>	No	II
KST58	White	<i>B. cinerea</i>	No	II
KST59	White	<i>B. cinerea</i>	No	II
KST60	White	<i>B. cinerea</i>	No	II
KST61	White	<i>B. cinerea</i>	No	II
KST62	White	<i>B. cinerea</i>	No	II
KST63	White	<i>B. cinerea</i>	No	II
KST64	White	<i>B. cinerea</i>	No	II
KST65	White	<i>B. cinerea</i>	No	II
KST66	White	<i>B. cinerea</i>	No	II
KST67	White	<i>B. cinerea</i>	No	II
KST69	White	<i>B. cinerea</i>	No	II
KST70	White	<i>B. cinerea</i>	No	II

## 2.1 Isolation and culture conditions for *B. cinerea* isolates

Surface sterilization was performed on samples containing infected fruits or foliage using 1% sodium hypochlorite solution. Afterwards the plugs from infected parts were taken and placed on the potato dextrose agar (PDA) plate to get the mother plate. Pure colonies were then collected in 2 ml stock tubes containing 40% glycerol. Glycerol stocks were stored at -80°C. For growth purposes. For preparing PDA media, we used 39 g of PDA (Sigma) powder in 1000 ml of distilled water and later it was autoclaved at 121°C for 15-20 mins. PDA was solidified at room temperature. PDA plates were prepared in biosafety cabinet. A suitable antibiotic ampicillin (100 mg/ml) was added to avoid bacterial contamination and incubated at 37°C overnight to confirm that plates are not contaminated. On PDA plates, the fungal stocks were point inoculated and cultured for 72 hours at 25°C. Potato dextrose broth was used as liquid media for mycelia growth. For preparing PDB, we mixed 200 g potato

infusion, 20 g anhydrous dextrose and pH was maintained at 5.1. It was followed by sterilization at 15 psi pressure at 121°C in an autoclave. Fungal mycelia were grown by inoculation of fungus from plate in 200 ml PDB in 500 ml conical flask. The flasks were placed on shaker for 7-10 days at 25°C. Cultured mycelia were filtered using Mira cloth and stored at -80°C.

### **Total Nucleic acid extraction**

The mycelia were pulverized into fine powder using liquid nitrogen. The grounded mycelia were transferred into 2 ml microfuge tube and placed at -80°C until processed. The total nucleic acid content was extracted by addition of 350µl of extraction buffer (10 ml; 400µl of 20 mM EDTA [pH 8], 200 µl of 20 mM Tris-HCl [pH 7.5], 1ml of 1% SDS, 5ml 1% NaCl and 3.4ml sterile water) followed by brief vortex to homogenize the mixture. For 1 hour, the microfuge tubes were incubated at 70°C. Prior to centrifugation at 11000 x g for 15 minutes, 350µl of phenol and an equal volume of sevag (chloroform and isoamyl alcohol [24:1]) were added. The supernatant was decanted onto new microfuge tubes, and 500 µl of sevag was added before centrifugation (11000 X g; 10 mins). The top phase was transferred into clean microfuge tubes and nucleic acids were precipitated by 800µl of 100% chilled ethanol. At -20°C, the microfuge tubes were incubated for 4 hours. Centrifugation at 11000 x g was used to pellet down nucleic acids (20 mins). The pellets were air dried before being resuspended in a 25 µl autoclaved water bath ([Bhatti et al., 2011](#)). The nucleic acids were kept at a temperature of -20°C. The extracted RNA fractions were fractionated on 1% agarose gel to visualize the presence of viral genome.

## **2.2 DsRNA extraction and agarose gel electrophoresis**

The mycelia were pulverized into fine powder using liquid nitrogen. After vortexing, the ground mycelia were placed into a 2ml microfuge tube, 1ml extraction buffer was added, the tube was vortexed, and 1ml phenol was added, followed by centrifugation at 13000 rpm for 15 mins. The supernatant was poured into a new microfuge tube. After vortexing, 1 ml sevag (Choroform (24): Isoamyl alcohol (1)) was added, and the tube was centrifuged. The supernatant was transferred to a new 1.5 ml tube, which was then filled with 0.3 g cellulose powder and 100% ethanol. Tubes were placed in spinner with slow spinning for one hour. After that, the tube was centrifuged for five minutes at 10k rpm. The supernatant was discarded, and the cellulose powder was washed three times with a 3:1 mixture of sodium Chloride-Tris-EDTA buffer (STE) and 100% ethanol (84:16). Each time the tube was washed, it was centrifuged for at least 2-5 mins. After the third washing, the tube was filled with 400 µl 1X STE buffer, centrifuged, and the supernatant was transferred to a fresh tube. After that, the supernatant tube was filled with 1 ml of 100% chilled ethanol and 40µl of 3M sodium acetate. The microfuge tubes were incubated for 4 hours at -20°C. dsRNA was pelleted by centrifugation at 11000 x g for 20 mins. An extra washing step with 70% ethanol was also performed. The pellets were resuspended in 25 µl of autoclaved water after being air dried. The temperature of the dsRNA was held at -20°C. The samples were examined for the presence of mycoviral by fractionating the dsRNAs on a 1% agarose gel.

### 2.3 Identification of fungal strains using ITS region

Fungal strains were cultured on PDA medium. For harvesting mycelia, the plugs were cultured in liquid culture media (PDB). The initial identification was done on morphological features but species level identification was further confirmed by amplification of ITS (Internal transcribed spacers) and sequencing of those species described by ([Bellemain et al., 2010](#)).

The ITS Primers used for this study are mentioned in the Table 2.2:

**Table 2.2.** Sequences of primers used for amplification of ITS region and Bc-hch Gene.

Sr.#	Primer name	Primer sequence (5'-3')
1	ITS1 F	TCCGTAGGTGAACCTGCGG
2	ITS4 R	TCCTCCGCTTATTGATATGC
3	ITS3 F	GCATCGATGAAGAACGCAGC
4	ITS2 R	GCTGCGTTCTTCATCGATGC
5	ITS5 F	GGAAGTAAAAGTCGTAACAAGG
6	ITS86 (F)	GTGAATCATCGAATCTTTGAA
7	ITS86 (R)	TTCAAAGATTCGATGATTCAG
8	262	AAGCCCTTCGATGTCTTGGA
9	520L	ACGGATTCCGAACTAAGTAA

In the amplification, a total volume of 50  $\mu$ l (recipe described in Table 2.3) of reaction mixture was employed, followed by PCR amplification. The amplification was carried out in an Applied Biosystems thermal cycler with the following settings: pre-denaturation at 94°C

for 3 minutes, denaturation at 94°C for 45 seconds, annealing at 58°C for 45 seconds, extension at 72°C for 45 seconds, and final extension at 72°C for 7 minutes. Amplicons size ranges from 350 to 700 bp, were analyzed on 1% agarose gel using 1X TAE buffer. The amplicons were purified using PCR purification kit (Thermoscientific, USA).

**Table 2.3.** Recipe of PCR mixture used in this study

Sr. #	Reagent name	Volume (µl)
1	Nuclease free water	33
2	10X taq buffer	5
3	2mM Magnesium chloride	3
4	2mM dNTPs	2
5	Primer F	2
6	Primer R	2
7	Template	2
8	Taq polymerase	1
	Total Volume	50

The purified DNA was sent for sequencing using Sanger dideoxy method. The sequenced genomes were assembled using software SeqMan Pro of DNASTAR Laser Gene software suite (Version 14.1) and submitted to GenBank in NCBI. Double stranded DNA was purified by carrying out DNase treatment and S1 nuclease treatment by modified method reported Bhatti *et al.*, 2012.

## **2.7 Detection of mycoviruses from *Botrytis* isolates**

The prevalence of mycoviral infection was determined using a traditional method of total nucleic acid extraction ([Bhatti et al., 2011](#); [Coenen et al., 1997](#)) with a positive and negative control for the extraction process. The virus-positive strains were then processed with DNase 1 and S1 nuclease to confirm that the virus was double-stranded RNA.

## **2.8 DNase Treatment of Isolated RNA**

The standard protocol of DNase1 was followed as per manufacturer instructions with slight modification in the volume of nucleic acid treated. A total of 30 µl of nucleic acid was taken in fresh microfuge tube, 5 µl 10 X nuclease buffer, 63 µl double distilled (dd) water and 2 µl of DNase were also added in that tube. For 1 hour, the microfuge tube was incubated at 37°C. The volume was then increased to 350 µl. The liquid was vortexed after an equal volume of phenol was added. Centrifugation was done at 13000 x rpm for 5 mins. The top phase was moved to a new microfuge tube. Prior to centrifugation at 13000 rpm for 5 minutes, 350 µl of sevag was added. Supernatant was shifted to new microfuge tube. 10% Sodium acetate of total volume of supernatant was added in tube along with 2.5 volume of supernatant, 100% ethanol was also added. Microfuge tube was incubated at -20°C for overnight. Next day, centrifugation was done at 13000 rpm for 20 mins. Ethanol was discarded, later rewashing was done 70% ethanol. For the second time, centrifugation was carried out at 13000 rpm for 20 minutes. The ethanol was discarded, and the pellets were dried in the open air. Pellet was resuspended in nuclease-free NF water.

## **2.9 S1 Nuclease Treatment of isolated Nucleic acid Prep.**

Standard procedure of S1 nuclease was adapted as per manufacturer instructions with slight modification in the volume of nucleic acid treated in a microfuge tube, 40 µl of RNA, 2 µl of S1 nuclease, 5 µl of 10X nuclease buffer, and 13 µl of sterile distilled water were added. Incubation was done for 1 hour at 37°C. The volume was then increased to 350 µl. The liquid was vortexed after an equal volume of phenol was added. Centrifugation was done at 13000 rpm for 5 mins. The top phase was moved to a new microfuge tube. Prior to centrifugation at 13000 rpm for 5 minutes, 350 µl of sevag was added. Supernatant was shifted to new microfuge tube. 10% Sodium acetate of total volume of supernatant was added in tube along with 2.5 volume of supernatant, 100% ethanol was also added. Microfuge tube was incubated at -20°C for overnight. Next day, centrifugation was done at 13000 rpm for 20 mins. Ethanol was discarded, later rewashing was done 70% ethanol. For the second time, centrifugation was carried out at 13000 rpm for 20 minutes. The ethanol was discarded, and the pellets were dried in the open air. Pellet was resuspended in NF water.

## **2.10 Genomic Characterization of isolated mycoviruses**

### **2.10.1 Next Generation Sequencing of Total RNA**

Purified RNA was extracted from a sample to construct a library. Quality check was performed using Bio analyzer. Library was prepared by fragmentation of total RNA and adaptors were ligated at terminals. Oligos complementary to adopter's sequences were used to amplify the fragments through bridge amplification. Illumina SBS technology (Macrogen) was used to detect the sequence of nucleotides.

### **2.10.2 Raw data & Quality Control**

The raw data obtained from sequencer was sent for quality control check to assess the quality of sequences obtained.

### **2.10.3 Preprocessing**

Adaptors were trimmed from the sequences and further filtered using standard parameters to reduce biases in the analysis.

### **2.10.4 K-mer Analysis & De novo assembly**

This procedure yields data on k-mer coverage, heterozygosity, and genome size estimation. De novo assembly was conducted using filtered reads. With the use of several stats from the assembly outcomes, the best k-mer was chosen.

### **2.10.5 Assembly validation**

Using a mapping technique and BUSCO analysis, the assembled genome was validated against the assembled genome.

### **2.10.6 Validation of NGS data**

Presence of mycoviruses was further confirmed by performing the RT-PCR (Reverse Transcription). As the data of NGS was received, results were analyzed and genome annotation was done. Contig specific primers were designed from aligned NGS data. Following the manual instructions, cDNA was produced using Thermo Fisher Scientific RevertAid First strand cDNA synthesis kit. Total RNA was heat denatured (90 $\mu$ l) with 100 % dimethyl sulfoxide(DMSO) (10 $\mu$ l) and random hexamer primers (1 $\mu$ l) at 65 °C for 20 minutes. The denatured dsRNA was snap cooled on ice and precipitated with 3M sodium acetate and absolute ethanol followed by incubation at -80 °C for 30 mins or -20 °C.



overnight. After centrifugation at 15k rpm for 20 minutes, the pellet was washed with 70% ethanol and the dried pellet was re-suspended in in first strand cDNA synthesis reaction mixture (4  $\mu$ l nuclease free water, 4  $\mu$ l RT buffer [5X], 2  $\mu$ l DTT [0.1M], 5  $\mu$ l dNTPs [2 mM], 3  $\mu$ l random hexamer primers [10 pmol]). The first cDNA strand was synthesized using Moloney Murine Leukemia Virus (MMLV) reverse transcriptase (RTase). After re-suspending the pellet, the mixture was incubated for 10 mins on ice followed by addition of 1  $\mu$ l RNase inhibitor (Thermo Fisher Scientific) and 1  $\mu$ l MMLVRTase. Next the reaction mixture was incubated at 37 °C for 90 mins. Reactions were performed in a (Applied Biosystem) thermal cycler conditions are as follows: 1 cycle of 30 s at 96 °C, followed by 30 cycles of 20 seconds at 94 °C, 30 seconds at 56 °C, 1 min and 30 s at 72 °C. The amplified product was of 650 bps.

### **2.10.7 Sequence and phylogenetic analysis**

Sequences retrieved were aligned through MAFFT (version 3.0) and GeneDoc. (Version 2.7). The complete genomic characterization of each mycovirus is mentioned in detail. After confirmation of the genomic sequences Maximum Likelihood tree were constructed using RdRP amino acid sequences for each mycovirus using Phylml online webserver.

### **2.10.8 RLM-RACE for viral terminal confirmation**

After internal validation of genomic data, viral termini were confirmed using RNA linked mediated random amplification of cDNA ends (RLM-RACE) ([Coutts and Livieratos, 2003](#)), to determine the sequencing of terminal sequences. In order to determine the terminal sequences of the dsRNAs, RLM-RACE was performed by a method described by Suzuki et al. (2004). The dsRNA was used as a template for cDNA synthesis. It was heat denatured with 100% DMSO at 65 °C for 20 mins, snap cooled on ice and precipitated with 100% ethanol. 5' phosphorylatedoligo deoxynucleotide (3' RACE adapter 5'-PO<sub>4</sub>-CAATACCTTCTGACCATGCAGTGACAGTCAGCATG-3') was ligated to both the 3' ends of the

viral denatured dsRNA with T4 RNA ligase (Takara) at 17 ° C for 16 to 18 hours.

**Table 2.4. Recipe of RACE.**

<b>Adapter ligation</b>	<b>ddH<sub>2</sub>O to 50 <math>\mu</math>l</b>
10 x T4 RNA ligase buffer	5 $\mu$ l
0.1 % BSA	3 $\mu$ l
T4 RNA Ligase (33 U)	2 $\mu$ l
PEG 6000	Final concentration 25%
Adapter oligo nucleotide	2 $\mu$ l

The ligates were used as templates for cDNA synthesis using M-MLV reverse transcriptase (Invitrogen, Carlsbad, CA, USA) in which 3' RACE 1st primer (5'-CATGCTGACTGTCACTGCAT-3') is used which is actually complementary to the 3' half of the 3' RACE adaptor. The reaction mixture was incubated at 37 ° C for 90 mins or 42 ° C for 60 mins. The products were diluted (10 – 50 times; as required) and were amplified by PCR with 3' RACE 2nd primer (5'-TGCATGGTCAGAAGGTATTG-3') that is complementary to the 5' half of adapter and a gene specific primer. The PCR products of predicted size were purified followed by ligation into pGEM-T Easy vector. The primer sequences are listed in Table 2.4.

### 2.10.9 Ligation of PCR products

**Table 2.5** The purified PCR products of RACE were ligated into pGEM-T Easy vector (Promega, Madison, WI, USA). The ligation reaction was set as follows:

Chemicals / Reagents	Amount
2 X ligation buffer	7.5 $\mu$ l
pGEM-T easy vector	1 $\mu$ l
Insert	5.5 $\mu$ l
T4 DNA ligase	1 $\mu$ l
Total	15 $\mu$ l

The mixture was incubated at 4°C overnight.

### 2.10.10 Transformation of ligated PCR products colony PCR and sequencing

The ligation mixture was transformed in *E.coli* competent cells (*dh5 $\alpha$* ). The ligation mixture (5  $\mu$ l) was mixed gently by still movement to 25 -30 $\mu$ l competent cells and incubated for 20 mins on ice. The mixture was then heat shocked at 42°C for 45 seconds and snap cooled on ice for 2 mins. Add 900 $\mu$ l of SOC broth to the tubes on clean bench followed by incubation at 37°C for one hour at 140 rpm. After mini spin, 800 $\mu$ l of SOC broth was removed from the tubes and the pellet was resuspended in the remaining SOC and spread on LB ampicillin plates and incubated at 37°C overnight. To confirm the transformants, colony PCR was performed and sequenced for confirmation.

## 2.7 Impact of botrytis mycovirus on the fitness of their host.

### 2.7.1 Genotypic Differentiation in Botrytis species finding compatible strain for mycovirus transmission

To assess the diversity among the botrytis strains Bc-hch Gene was amplified to see which isolates are suitable for mycovirus transmission. Approximately fragment of 1100 - 1200 bp size was amplified from specific region of Bc-hch gene using already reported primers (Table 2.4). A total volume of 50µl was used in the amplification and followed by PCR conditions (Table 2.3). The reactions were carried out in a (Applied Biosystem) thermal cycler with the following settings: 1 cycle of 20 seconds at 96°C, followed by 30 cycles of 20 seconds at 94°C, 30 seconds at 56°C, 1 minute and 30 seconds at 72°C, and 1 minute and 30 seconds at 72°C. The amplified product was of 1171 bp size was purified by Thermo scientific gene jet PCR purification kit and finally eluted with 40 µl elution buffer.

By combining 10 µl of purified PCR product with 2 µl of FastDigest® Hha-I restriction enzyme (Fermentas), the amplified gene was digested. Digestion took place for 2 hours at 37°C. The fragments were separated on a 1% agarose gel and visualized with ethidium bromide on a UV Transilluminator. In Group II, the restriction enzyme has five restriction sites, while Group I have four. The upper band in Group I was around 600 bp, while the upper band in Group II was 500 bp ([Fournier et al., 2003](#)).

**Table 2.5.** Sequences of primers used for amplification of Bc-hch Gene.

Sr.#	Primer name	Primer sequence (5'-3')
1	262	AAGCCCTTCGATGTCTTGGA
2	520L	ACGGATTCCGAACTAAGTAA

## **Development of isogenic lines**

Different techniques are used for the curing the mycoviruses some of them are highlighted below.

1: Cold Treatment

2: Temperature shock

3: Hyphal Tipping

4: Antibiotic Treatment

5: Hyphal anastomosis

The technique used in this study include hyphal anastomosis. Two plugs were co-cultured on the same PDA plate. One mycelial plug was taken from donor (Kst31) and one from potential recipient of mycovirus (Kst51). The plugs were closely placed and plate was incubated at 25 °C. 3 plugs (named as Near (N), Middle (M) and Far (F) were taken 72 h after hyphal anastomosis. Control plates were used to monitor growth. Virus was transferred into N and M region which was confirmed by Reverse Transcription PCR.

N: Near region

M: Middle region

F: Far region

### **2.11.2. Method for Biological Impact Assessment on PDA Media**

The un infected isolated of Botrytis strains or virus free strains were compared on PDA media and also used simultaneously for Apple assays to check the biological impact of mycovirus on the pathogenicity of fungal strains. For comparison on PDA growth media, equal size plug of virus infected and virus free strains were placed on PDA and assessed for its growth for 5-7 days. The test was performed with 3 replicates. Student T-test was applied and at a confidence interval of 0.05. Hence p- values less than 0.05 were considered significant.

### **2.11.3 Fungal Pathogenicity Test on Apple Fruits**

Pathogenicity of the fungi was further assessed through Apple Assay. Apples were collected from fruit store; 10 fresh apples of approximately equal size were purchased. Surface sterilization of apples was performed using a 1% sodium hypochlorite solution. With the use of sterilized corkborer, holes were drilled in apples. MAPs were also extracted from the colony margin of each isolate of *B.cinerea* (VF and VI isolates) and PDA cultures (as control). These plugs were inoculated on each apple (One mycelial plug agar plug and one was only potato agar plug as control). Individual trays were sealed with clear plastic film and incubated in a growth chamber at 25°C under fluorescent light (12 h light/12 h dark). Measurements were taken after the 72 hours of inoculation. The diameter of lesion caused by each MAP and PDA was measured. The test along with its replicates were repeated twice for verification. Student T-test was applied and at a confidence interval of 0.05. Hence p- values less than 0.05 were considered significant.

## **3. Results:**

### **3.1 Molecular identification of environmental species of *Botrytis* Using ITS marker**

#### **(Objective 1)**

A total 102 samples of *Botrytis* spp. were isolated so far (Figure 3.1). All isolates were morphologically similar to *Botrytis* species, as revealed by sclerotia (colony appearance) and molecular identification (ITS based identification).

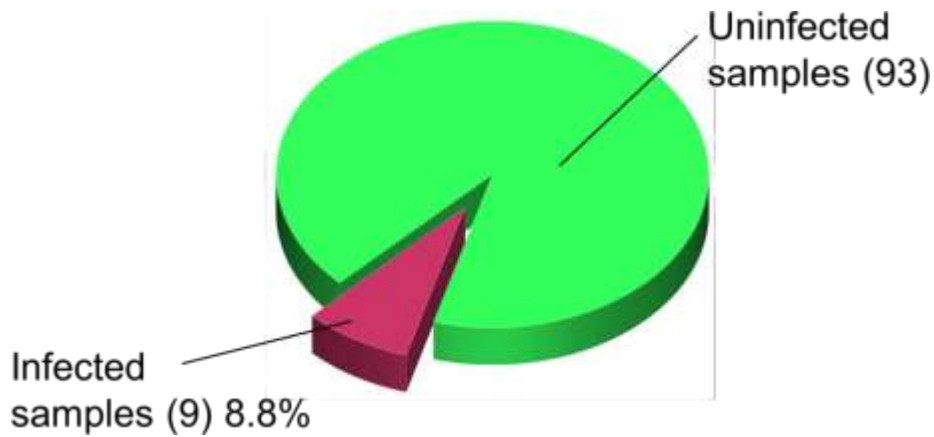


**Figure 3.1** A pie graph showing the percentage of dsRNA positive fungal samples. A total of 102 fungal samples were collected from which only nine showed dsRNA positive profile showed an incidence rate of 8.8%.

Total nucleic acid was extracted using protocol described by ([Bhatti et al., 2012](#)). Molecular identification of only those fungal isolates was performed which show morphological similarity to *Botrytis*. Internally Transcribed Spacer (ITS) regions were amplified by using ITS

primers. The size of amplicon was 350-700 bp (Figure 3.2). The purified amplicons were purified and sequenced. Resulting sequences were assembled and submitted to NCBI GenBank. So far 30 isolates have been sequenced using Classical dsRNA extractions prep followed by agarose gel electrophoresis. The molecular characterization of multiple viruses has been done. Sequence were in GenBank with their respective accession numbers are mentioned in Table 3.1

**Table 3.1** List of viruses infected fungal isolates with their sampling location and GenBank accession numbers

Isolate Name	Place of Isolation	Accession No.
St13	Muridke, Punjab	MG270185
St15	Muridke, Punjab	MG270570
St 7	Muridke, Punjab	MG101817
St2	Muridke, Punjab	MG263462
Mst2	Mardan, Kpk	MK342567
Mst9	Mardan, Kpk	MK346204
Mst4	Mardan, Kpk	MK346329
Mst15	Mardan, Kpk	MK346332
Mst1	Mardan, Kpk	MK611795
Mst8	Mardan, Kpk	MK611818
Mst16	Mardan, Kpk	MK417799
Msta4	Mardan, Kpk	MK417796
Msta7	Mardan, Kpk	MK415691
Msta12	Mardan, Kpk	MK415690
Msta14	Mardan, Kpk	MK415775
Kst5	Kamoke, Punjab	MN055820
Kst8	Kamoke, Punjab	MN055897
Kst10	Kamoke, Punjab	MN055900
Kst33	Kamoke, Punjab	MN055973
Kst44	Kamoke, Punjab	MN055982
Kst52	Kamoke, Punjab	MN055983



Kst53	Kamoke, Punjab	MN055992
Kst61	Kamoke, Punjab	MN056024

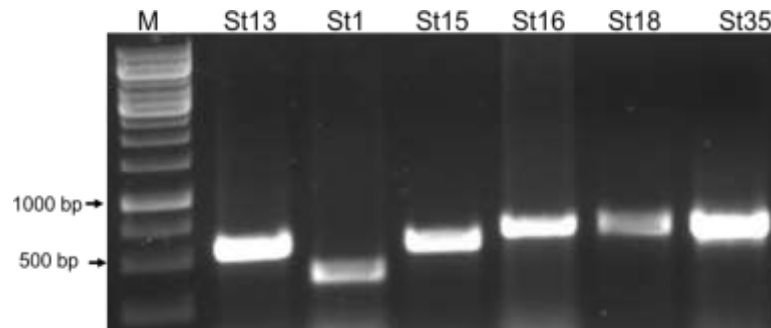


**Figure 3.2** ITS region amplification of different fungal isolates using two primers: ITS5F &ITS4.

### 3.1.2 Screening of mycoviruses from identified Botrytis strains

In order to identify mycoviral infection in Botrytis species. All isolates were subjected to total nucleic acid isolation procedure in the presence of positive and negative control (section 2.3). A total of 9 isolates were found positive for mycoviral infection Colony morphologies and can be seen in Figure 3.3 and mycoviral profiles can be seen in Figure 3.4. The isolated mycoviruses were subjected to DNases and S1 Nuclease treatment to get rid of DNA and single stranded RNA.

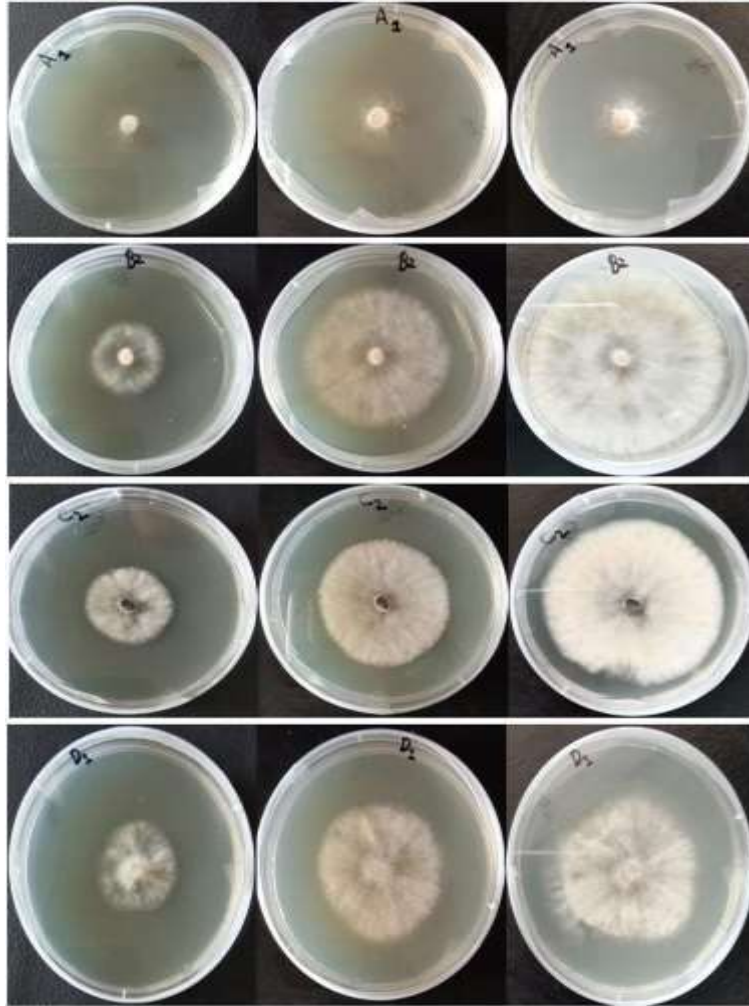


**Figure 3.3** Colony morphology of *Botrytis* isolates, (A1; Kst5C, B2; Kst10A, C2; Kst14A & D1; Kst31C) on PDA medium over a period of 2-4 days.

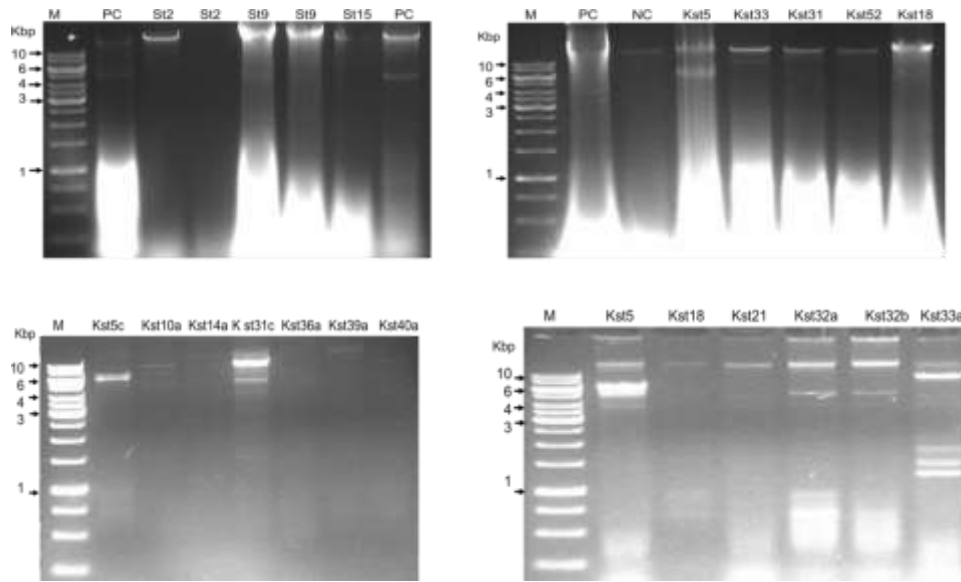


**Figure 3.4** Agarose gel electrophoresis indicating total nucleic acid extraction for the screening of mycoviral infection. Lane M indicate molecular weight marker DNA; PC indicate the Positive control and other lane include the sample screened for mycoviral infection.

### 3.2 Characterization of novel mycovirus genomes identified during the screening process in order to understand the nature of mycoviruses (Objective 2) along with their

## **phylogeny (Objective 3)**

### **3.2.1 Molecular Characterization of mycoviruses from Fungal Isolates**

This objective was achieved by deciphering of the sequence of the viral genome present inside the *Botrytis*. This was carried out designing primers based on specific family of dsRNA mycoviruses, for either reverse transcription (RT) PCR cDNA library construction or NGS. The complete genome of fungi including **mitogenomes** were sequenced. However, the other data not related to this report is not mentioned. Only information related to mycoviruses is mentioned in this report. The families were identified through NGS based contigs (Table 3.2) assembly and genome walking strategy that helped in revealing the viral genomic sequence in both directions of termini (Both 3' and 5') The sequence obtained through NGS was subjected to internal confirmation through RT-PCR (Coutts and Livieratos., 2003). Amplicons generated were confirmed through sequencing (Eurofin, USA & Macrogen, China). Sequences retrieved were checked through MAFFT (version 3.0) and GeneDoc. (version 2.7). The complete genomic characterization of each mycovirus is mentioned in detail. After confirmation of the genomic sequences Maximum Likelihood tree were constructed using RdRP amino acid sequences for each mycovirus.

**Table 3.2** List of Contigs and virus Names (Virus detected in six NGS processed Botrytis isolates)

Contigs Isolate Name	Length (nt)	Virus Name	Status
<b>CONTIGS OF KST10A</b>			
contig2(KST10A)	2459	Sclerotinia sclerotiorum umbra-like virus 2	Partial
<b>CONTIGS OF KST14A</b>			
contig7(KST14A)	8370	Botrytis cinerea fusarivirus 2	Complete
contig8(KST14A)	7863	Botrytis cinerea mymonavirus 1	Complete
contig20(KST14A)	5047	Monilinia ourmiavirus	Complete
contig49(KST14A)	3302	Plasmopara viticola lesion associated orfanplasmovirus 5	Complete
contig15(KST14A)	6424	Botrytis cinerea Fusarivirus 3	Complete
contig5(KST14A)	10241	New Negative stranded RNA Virus	Complete
contig43(KST14A)	3421	Plasmopara viticola lesion associated orfanplasmovirus 4	Complete
contig16(KST14A)	5576	Sclerotinia sclerotiorum deltaflexivirus 2	Complete
contig4(KST14A)	10683	Sclerotinia sclerotiorum hypovirus 1-A isolate	Complete
contig25(KST14A)	4676	Sclerotinia sclerotiorum hypovirus 1-A isolate SsHV1-A2	Partial
contig12(KST14A)	7309	Sclerotinia sclerotiorum mycotymovirus 1	Complete
contig17(KST14A)	5426	Sclerotinia sclerotiorum negative-stranded RNA virus 6 isolate SsNSRV6	Complete
contig23(KST14A)	4779	Sclerotinia sclerotiorum umbra-like virus 2 isolate SsULV2	Complete
<b>CONTIGS OF KST31C</b>			
contig1(KST31C)	13748	Endornavirus	Complete
contig2(KST31C)	6721	Botrytis cinerea hypovirus 1 strain BcHv1.HBstr-470	Partial
contig6(KST31C)	2687	Sclerotinia nivalis mitovirus 1 isolate SsSn-1.m1	Complete
contig9(KST31C)	2501	Sclerotinia nivalis mitovirus 2 isolate SsSn-1.m2	Partial
contig18(KST31C)	1758	Sclerotinia sclerotiorum dsRNA mycovirus-L	Partial
<b>CONTIGS OF KST5C</b>			

contig89(KST5C)	2059	Sclerotinia sclerotiorum endornavirus 3	Partial
contig71(KST5C)	2275	Botrytis cinerea birnavirus	Complete
contig65(KST5C)	2372	Botrytis cinerea mitovirus 2	Partial
contig39(KST5C)	3051	Botrytis cinerea mitovirus 4	Complete
contig2(KST5C)	8037	Botrytis cinerea orthrobonya like virus	Complete
contig7(KST5C)	5127	Botrytis cinerea victorivirus 1 strain BcVv1.HBstr-470	Partial
contig55(KST5C)	2556	Plasmopara viticola lesion associated narnavirus	Complete
contig37(KST5C)	3092	Plasmopara viticola lesion associated orfanplasmovirus 5	Complete
contig57(KST5C)	2478	Plasmopara viticola lesion associated ourmia-like virus	Complete
contig4(KST5C)	5909	Sclerotinia sclerotiorum botybirnavirus 1 segment 1	Partial
contig6(KST5C)	5201	Sclerotinia sclerotiorum botybirnavirus 1 segment 2	Partial
contig46(KST5C)	2854	Sclerotinia sclerotiorum ourmia-like virus 3	Complete
contig18(KST5C)	3933	Sclerotinia sclerotiorum umbra-like virus 3 isolate SsULV3	Complete
<b>CONTIGS OF KST32B</b>			
contig22(KST32B)	2458	Botrytis cinerea victorivirus 1 strain BcVv1.HBstr-470	Partial
contig17(KST32B)	2611	Botrytis cinerea victorivirus 1 strain BcVv1.HBstr-470	Partial
contig4(KST32B)	6298	Grapevine associated mycovirus-3 isolate Ctg454(Fusarivirus)	Complete
contig11(KST32B)	3102	Plasmopara viticola lesion associated Orfanplasmovirus	Complete
contig16(KST32B)	2701	Sclerotinia nivalis mitovirus 1 isolate SsSn-1.m1	Complete
contig59(KST32B)	1026	Sclerotinia sclerotiorum umbra-like virus 3 isolate SsULV3	Partial
<b>CONTIGS OF KST33A</b>			
contig1(KST33A)	4836	Botrytis cinerea negative stranded RNA virus	Partial
contig4(KST33A)	4243	Botrytis cinerea negative stranded RNA virus 2	Partial
contig24(KST33A)	1300	Botrytis cinerea negative stranded RNA virus 3	Partial

### 3.2.1 .1 Characterization of Novel Endornavirus from Kst 31

DsRNA profile on agarose gel showed the presence of single segment (Figure 3.4). NGS analysis yielded 583,356 short reads from Illumina sequencing. Prior to being assembled, short Illumina reads were trimmed, and quality filtered using the GLC Genomic work bench 11. Filtered readings from *Botrytis cinerea* isolate kst31 dsRNAs were assembled into 1 contig. The sequence was internally validated with the help of contig sequence specific primers. Figure 3.5).

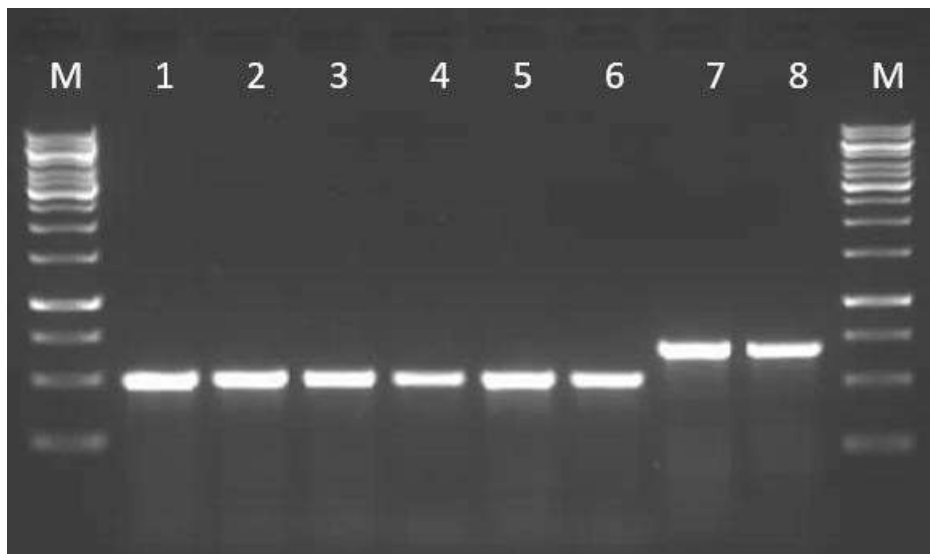


**Figure 3.5:** Lane M shows molecular marker, lanes 1-6 show bands of DNA amplified by using Primer set End1F & End1R while 7 and 8 show bands which were amplified by using End1F and End2R.

The virus was named *Botrytis cinerea* endornavirus 4. The full genome sequence of the dsRNA was 13,765 bp long, with a GC content of 41.48 percent, and comprised a single large ORF and two short untranslated regions (UTRs), 48 nt and 77 nt in length, respectively, at the 5' and 3' termini. The 3'-UTR had eight cytosine residues at the end, which are common in endornaviruses. Both terminal sequences (5' and 3') were conserved with already reported endornaviruses from *Botrytis cinerea*. A putative polypeptide of 4546 amino acids was predicted to be encoded by single large ORF (predicted molecular mass: 508.06 kilodaltons)

(Figure. 3.6). An RNA dependent RNA Polymerase (RdRp 2 superfamily domain), two helicase domains (a DEXDc domain (DExH box) and a viral MTR domain) were identified using CDD and pfam search. Multiple alignment study of the CRRs in BcEV4 and other endornaviruses revealed that BcEV4 has no cysteine rich repeats (CRRs), which may have an enzymatic function during polyprotein digestion (Figure. 3.7). RdRP amino acid multiple sequence alignment showed eight (A - F) conserved regions, which are common in all endornaviruses (Figure. 3.8). According to the findings of a BlastP search, this polypeptide is most closely linked to endornavirus-encoded polypeptides, notably those of the particular those of *Sclerotinia sclerotiorum* endornavirus 9 (SsEV9/JZJL2, 49.05 % aa identity) and *Sclerotinia minor* endornavirus 1 (SmEV1, 51.32 % aa identity). Based on the most up to date Endornaviridae species delimitation criteria > 75 % sequence identity, BcEV4 should be considered a novel endornavirus. BcEV4 has conserved terminals with other viruses from botrytis genus (Figure 3.9).



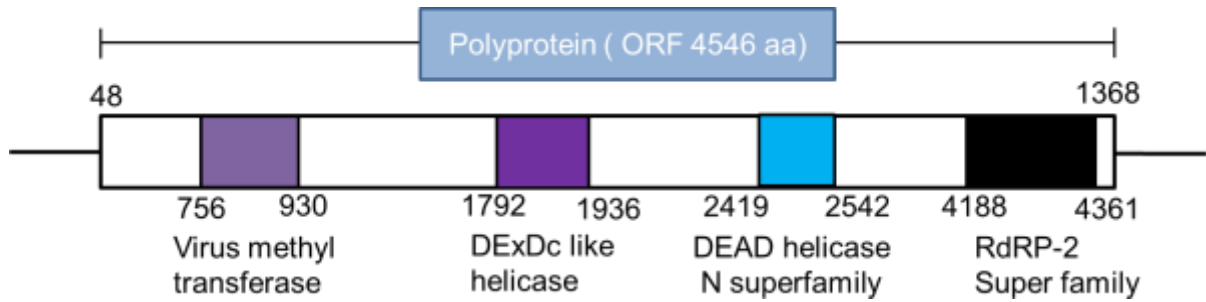


**Figure 3.6** Genome organization of *Botrytis cinerea* endornavirus 4 showing conserved regions with already reported endornaviruses.



**Figure 3.7** No conserved cysteine regions were observed in BcEV4 when compared within already reported endornaviruses.

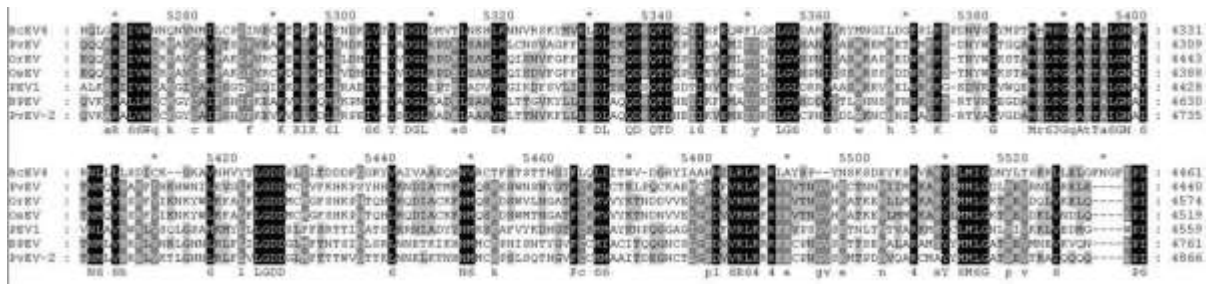


**Figure 3.8** Conserved regions identified in RdRP region using multiple alignment.

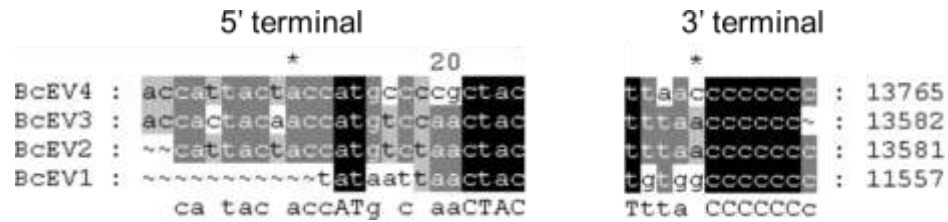
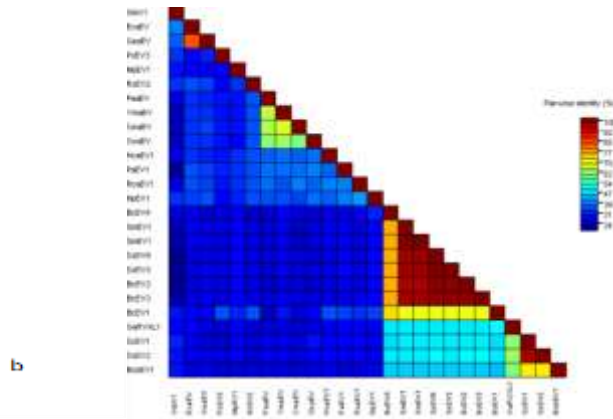


**Figure 3.9** Conserved (5' and 3') terminals in Botrytis cinerea endornavirus 4.

### 3.2.1.2 Phylogenetic analysis of Botrytis cinerea endornavirus 4 (Objective 3)

Phylogenetic analysis showed that it made a clade with already reported alpha-endornaviruses (Figure 3.10).





**(b) Identity matrix of viruses used in phylogenetic tree. The scale represents the level of identity.**

### 3.2.2.1 Characterization of Novel Fusariviruses in Kst14a strain

Isolate Kst14a NGS data revealed the presence of Fusariviruses. The full-length genome sequence of *Botrytis cinerea* fusarivirus BcFV8 and BcFV9 comprised of 6424 and 8370 nucleotides (nt), encoding two ORFs as detected by ORF Finder available at the National Centre for Biotechnology Information (NCBI). ORF1 of BcFV8 start from nt 110 and ends at nt 4741 was found to encode a polyprotein having a conserved RdRP domain and helicase (Hel) domain. Helicase domain also functions in replication (Figure 3.11).

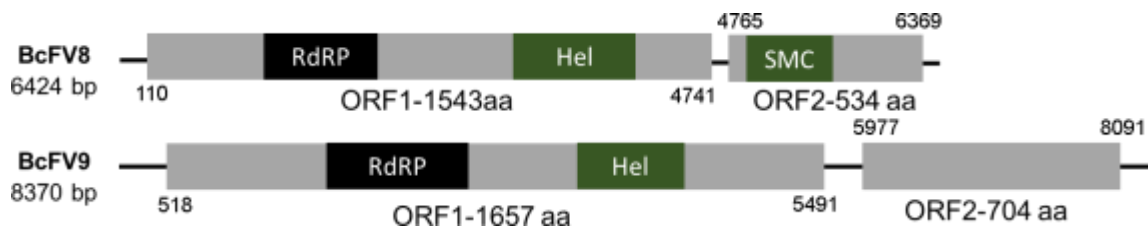


**Figure 3.11** Genome organization of both fusariviruses identified from *Botrytis cinerea* isolate Kst- 14a. Black regions shows the conserved RdRP and green regions shows the other conserved regions present in the genome.

The predicted molecular weight of protein encoded by ORF1 was 174 kDa. BLASTp search using NCBI non-redundant protein sequence database showed that this protein is 51%, 49% and 48% identical to the RdRP of *Rutstroemia firma fusarivirus 1* (RfFV1), *Botryosphaeria dothidea fusarivirus 1* (BdFV1) and *Neofusicoccum luteum fusarivirus 1* (NIFV1), respectively. ORF2 starts from nt 4765 and terminates with a UAG at nt 6369 with a 23-nt-long intergenic region separating ORF2 from ORF1. It was found to encode a hypothetical protein having a conserved domain of SMC (structural maintenance of chromosomes, which has been reported from many fusariviruses. It was identified in N terminal half of ORF2. SMC domains are mainly found in bacteria, archaea and eukaryotes. It has also been reported from coat protein of some plant viruses including *Lygus lineolaris virus 1* (putative Iflavirus) and some fungal viruses including *Fusarium graminearum hypovirus 2* and *Macrophomina phaseolina virus 2* ([Hrabáková et al., 2017](#)). The deduced protein of ORF2 has a predicted molecular weight of 59 kDa. BLASTp search similarity with PaFV1, BdFV1 and ZtFV1, which share shares 24%, 24% and 25% aa sequence similarity.

For BcFV9, ORF1 starts from nt 517 and ends with a UAA at nt 5491. The predicted protein of ORF1 has a molecular weight of 189 kDa. BLASTp search using NCBI non-redundant protein sequence database showed that this protein is 62%, 35% and 36% identical to the RdRP of *Botrytis cinerea* fusarivirus 1 (BcFV1), *Rhizoctonia solani* fusarivirus 2 (RsFV2) and *Morchella importuna* fusarivirus 1 (MiFV1), respectively, but less than 35% amino acid sequence identity to RdRP of other fusariviruses. This indicates that ORF1 encodes the RdRP, and helicase (Hel) conserved domains as predicted by CDD (Figure 3.11). ORF2 starts from nt 5976 and terminates with a UAG at nt 8091. The 485 nt long intergenic region separating ORF2 from ORF1. The deduced protein of ORF2 has a predicted molecular weight of 78kDa. A BLASTp search revealed only one similar protein which was from *Botrytis cinerea* fusarivirus 1. Eight conserved motifs were observed in both BcFV8 and 9. The 5'-UTR of BcFV8 and 9 had 110, 518 nt in length and 3'-UTRs had 55, 279 in length. A conserved poly A tail was observed in both viruses having a size of 28 and 21 bp respectively. Conserved domains were also identified in both viruses (Figure 3.12). A conserved poly A tail was also observed at 3' terminal of both viruses (Figure 3.13).

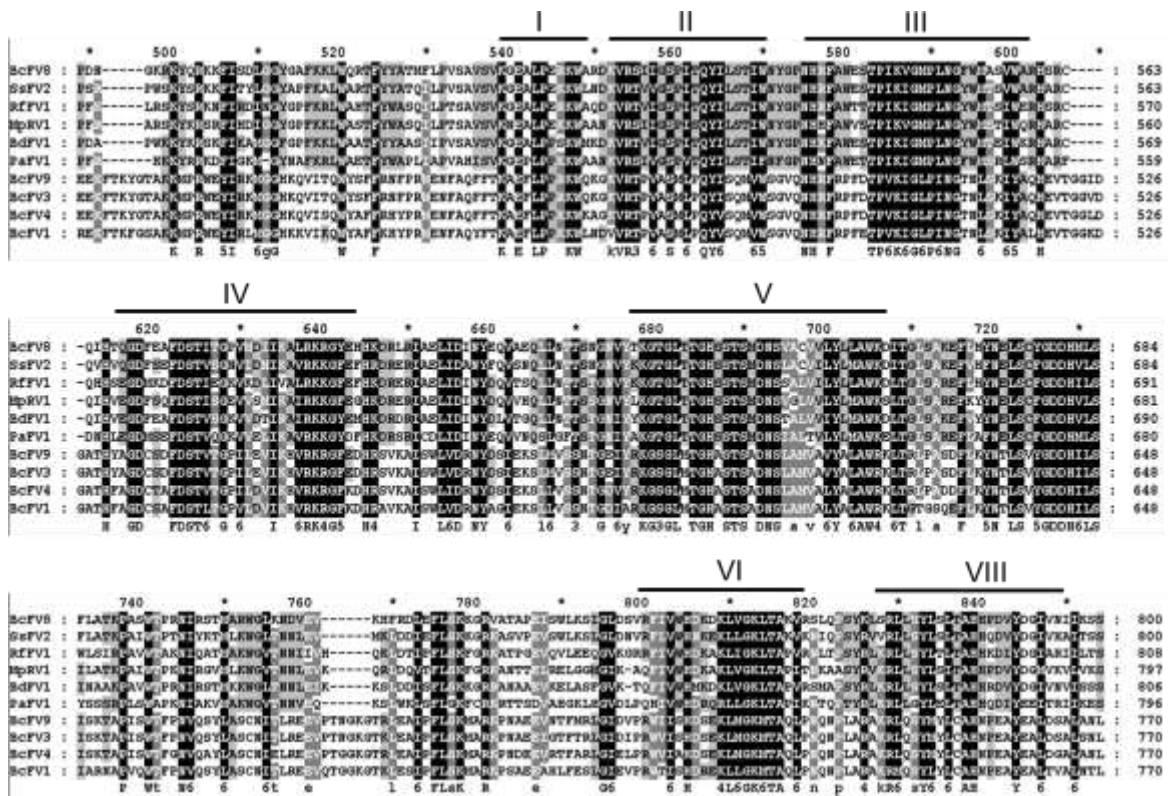


**Figure 3.12** Conserved regions predicted in the genome of both fusariviruses using multiple alignment.

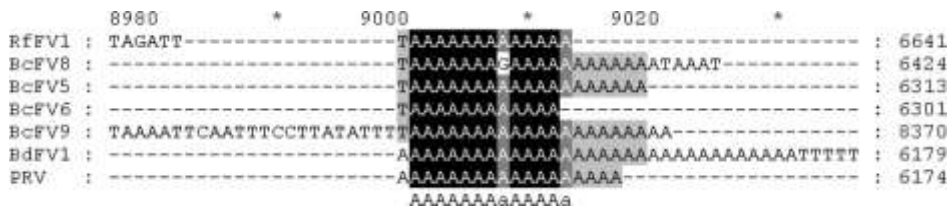


**Figure 3.13** Conserved poly A tail identified in both fusariviruses at 3' terminal

### 3.2.2.2 Phylogenetic analysis of both fusariviruses from Kst14a

Maximum Likelihood tree constructed using RdRP amino acid sequences showed BcFV8 and BcFV9 fall in sister clades within the family *Fusariviridae* (Figure 3.14). As the species demarcation criteria for fusariviruses threshold has not been established yet, BcFV8 and BcFV9 should be considered as novel members of the family *Fusariviridae* which are related to RfFV1, BcFV1 and BcFV1. However, RfFV1 was recovered from a brown cup

fungus. BdFV1 and BcFV1 were identified in the pathogenic plant fungi *Botryosphaeria dothidea* and *Botrytis cinerea*, respectively, in China. This indicates that BcFV8 and BcFV9 differ significantly in its host range and geographic distribution from RfFV1, BdFV1 and BcFV1, and considering them as novel members of *Fusariviridae* is reasonable.

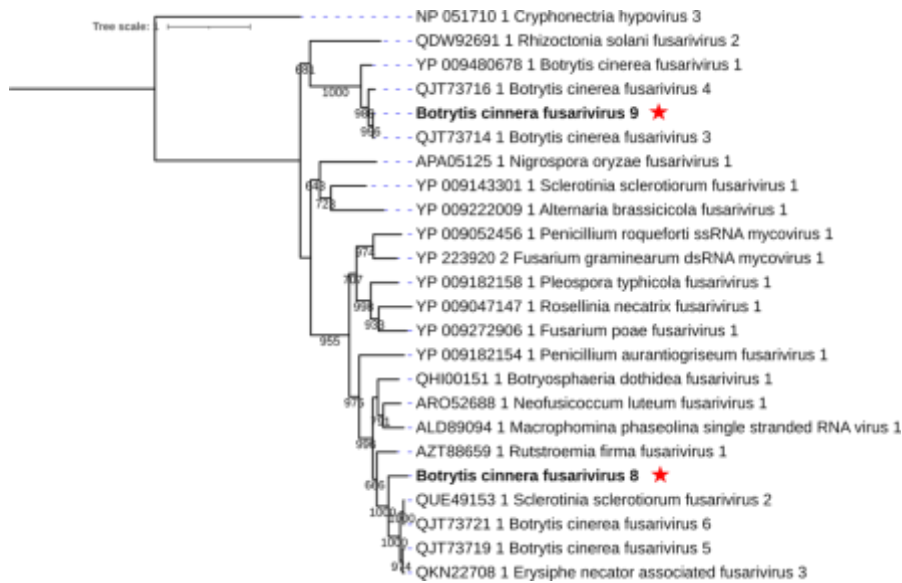




**Figure 3.14** Phylogenetic analysis of both fusariviruses identified from botrytis cinerea isolate Kst-14a

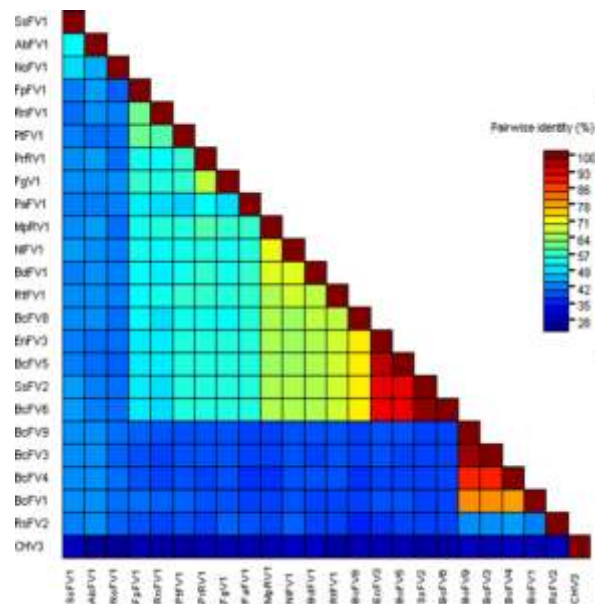


**Figure 3.15** Identity matrix of all fusariviruses used in phylogenetic analysis. The red in the scale represents the maximum identity.

### 3.3 Genomic features of other new viruses identified in this study

#### 3.3.1 Botrytis cinerea mymonavirus

The genome of the mymonavirus comprise of 7863 nucleotides (Figure 3.16). According to the ORF finder software provided by National Center for Biotechnology Information (NCBI), the genome contains three ORFs (Open Reading Frames). The predicted molecular weight of protein encoded by ORF1 was 224 kDa. BLASTp search using NCBI non-redundant protein sequence database showed this protein is 99%, 99% and 54% identical to the RdRP Botrytis cinerea mymonavirus 1 (BcMV1), Sclerotinia sclerotiorum negative-stranded RNA virus 7 (ScNRV7) and Penicillium cairnsense negative-stranded RNA virus 1 (PcNSRV1) respectively. ORF2 starts from nt 6022 and terminates at nt 6531 with a 48-nt-long intergenic region separating ORF2 from ORF1. The predicted protein of ORF2 has a molecular weight of 18 kDa. BLASTp search showed similarity with only BcMV1 which shares 98% aa

sequence similarity. Whilst ORF2 and ORF3 have 100-nt long intergenic region. ORF3 starts at nt 6631 and ends at nt 7383. The deduced protein of ORF3 had molecular weight of 28 kDa.

BLASTp search showed this protein is 96% and 33% similarity with *Botrytis cinerea* mymonavirus 1 (BcMV1) and *Plasmopara viticola* lesion associated mymonavirus 1 (PVlasMV1) respectively. Phylogenetic analysis showed that *Botrytis cinerea* mymonavirus fall in a clade with already reported mymonaviruses (Figure 3.17). A total of eight conserved motifs were observed (I-VIII) in RdRP amino acid sequence, with GDNQ instead of GDD (Figure 3.18). *Botrytis cinerea* mymonavirus shared conserved terminal with other reported viruses (Figure 3.19)

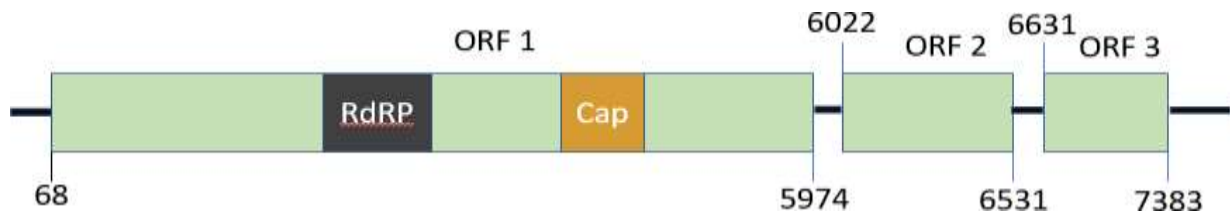
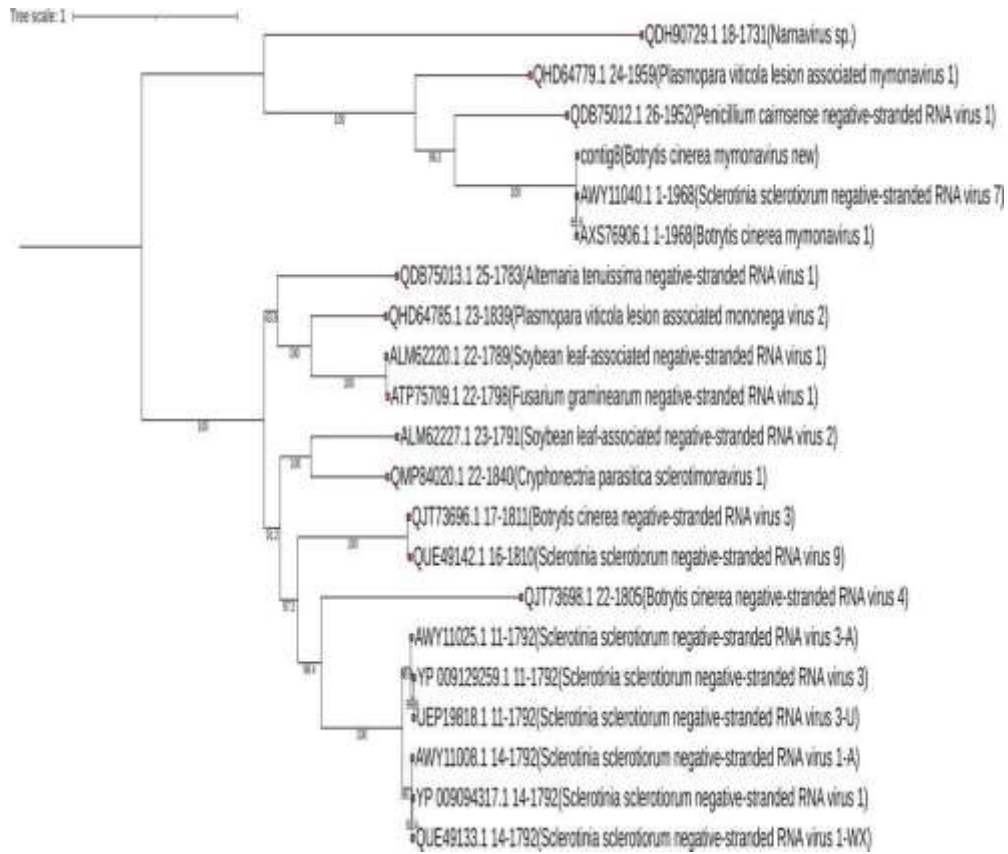


**Figure 3.16** Genome organization of *Botrytis cinerea* mymonavirus showing three different ORFs. ORF1 encodes for RdRP and cap protein while other ORFs encode hypothetical proteins.

# A



**B**

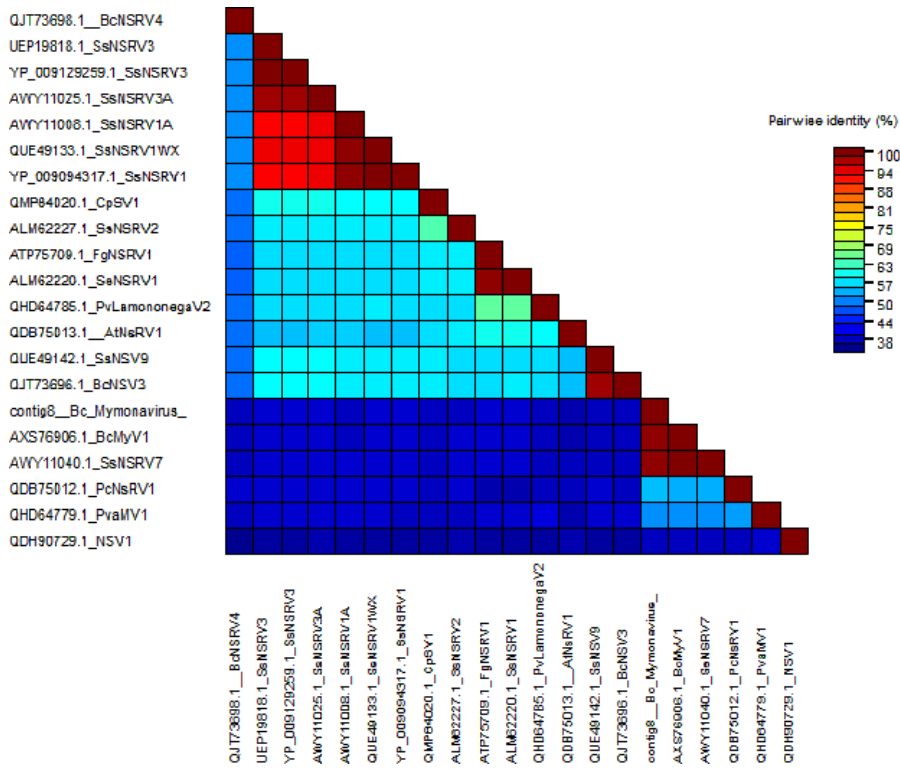


**Figure 3.17 A).** Phylogenetic analysis, based on the deduced amino acid sequences of RdRP, revealed that Contig 8 belongs to the family *Mymonaviridae*. B) Identity matrix of viruses used in phylogenetic tree. The scale represents the level of identity.

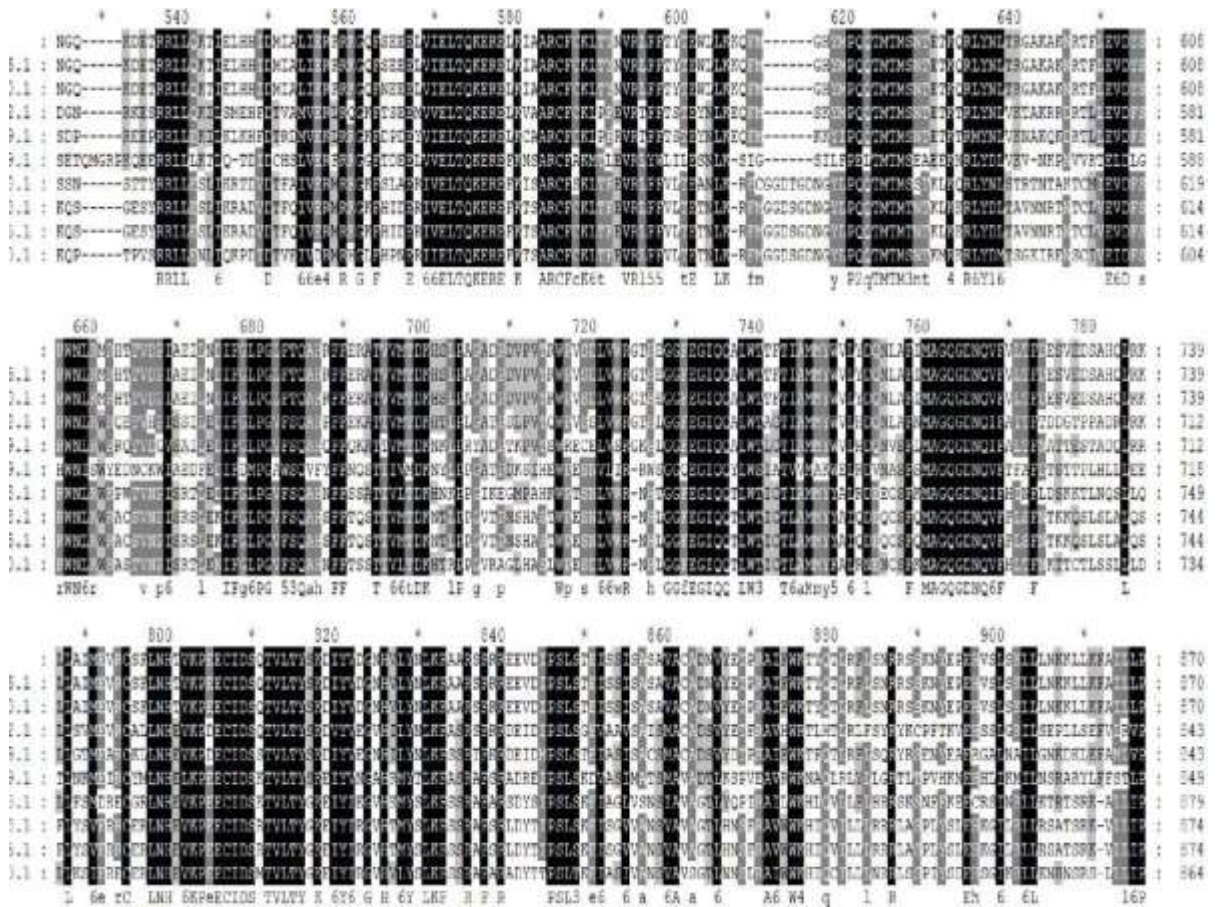


Figure 3.18 Conserved regions identified in RdRp region using multiple alignment.

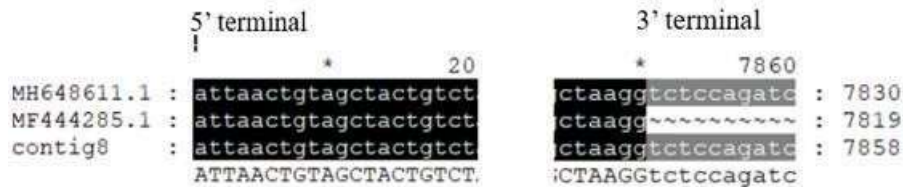
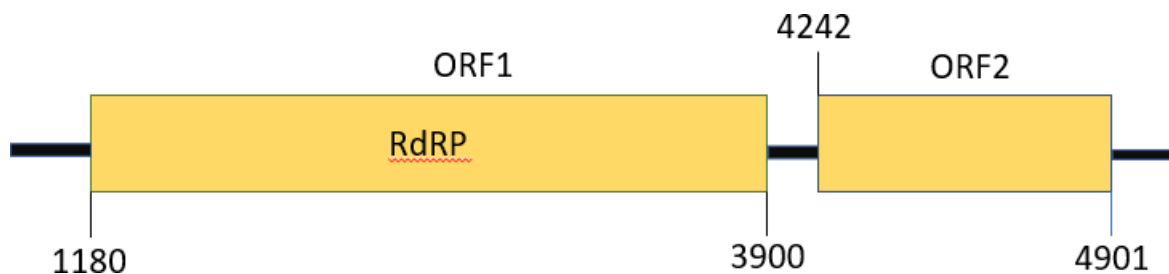


Figure 3.19 Conserved (5' and 3') terminals in Botrytis cinerea mymonavirus.

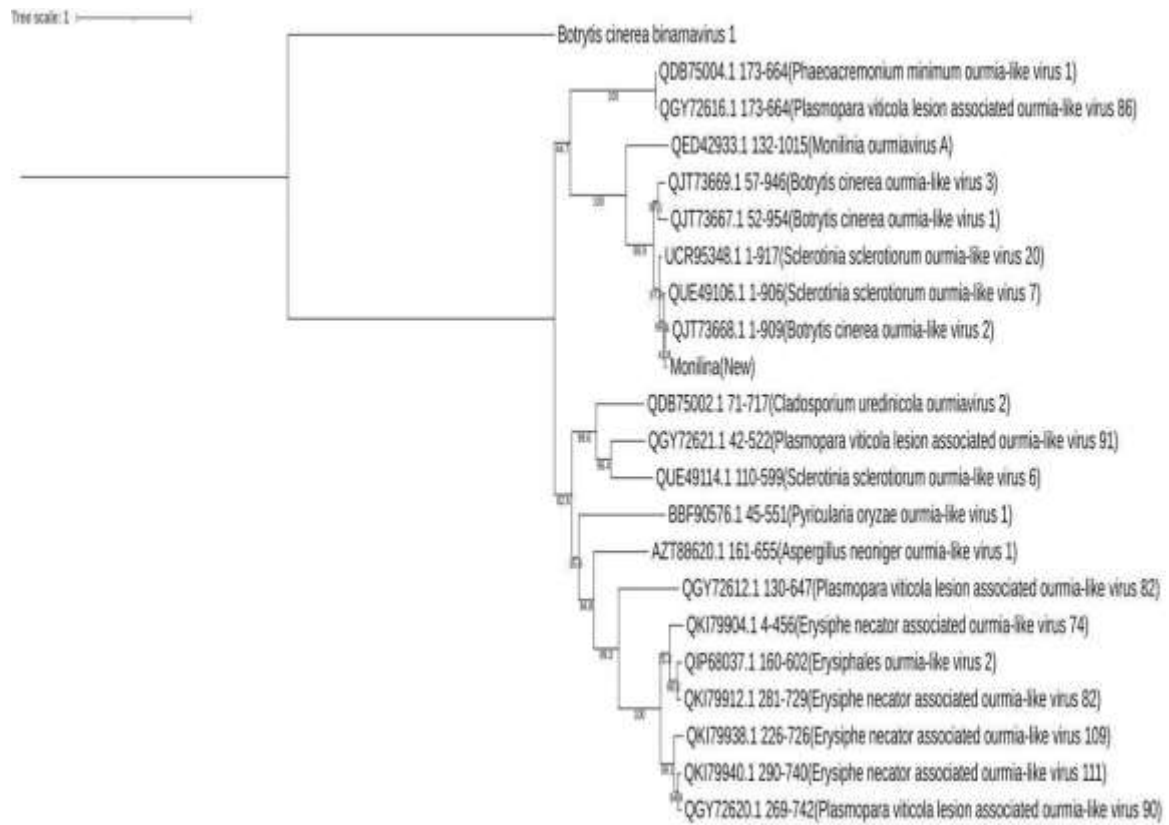
### 3.3.2 Botrytis cinerea ourmiavirus

*Botrytis cinerea* ourmiavirus has a genome of 5047 nt (Figure 3.20). The genome has two ORFs. The predicted molecular weight of protein encoded by ORF1 was 103 kDa. BLASTp search showed this protein is 96%, 94% and 90% identical to the RdRP of *Sclerotinia sclerotiorum* ourmia-like virus 7 (ScOLV7), *Botrytis cinerea* ourmia-like virus 2 (BcOLV2) and *Sclerotinia sclerotiorum* ourmia-like virus 20 (ScOLV20) respectively. ORF2 starts from nt 4242 and terminates at nt 4901 having 342-nt-long intergenic region separating ORF2 from ORF1. The predicted protein of ORF2 has a molecular weight of 24kDa. BLASTp search showed no significant result. Phylogenetic analysis showed that *Botrytis cinerea* ourmiavirus fall in a clade with already reported ourmiaviruses (Figure 3.21). A total of eight conserved motifs were observed (I-VIII) in RdRP amino acid sequence (Figure 3.22). *Botrytis cinerea* ourmiavirus didn't share conservation terminal with other reported viruses (Figure 3.23)



**Figure 3.20** Genome organization of *Botrytis cinerea* ourmiavirus showing two different ORFs. ORF1 encodes for RdRP while ORF2 encode for hypothetical protein.

A





**B**

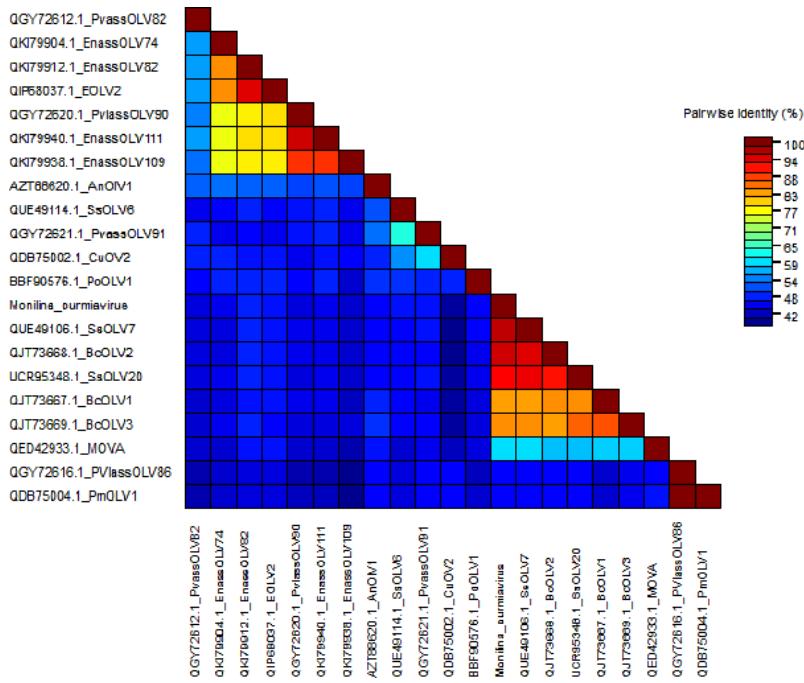


**Figure 3.21 (A).** Phylogenetic analysis, based on the deduced amino acid sequences of RdRP, revealed that Contig 20 (*Botrytis cinerea* ourmia-like virus) belongs to the ourmiavirus which is genus of *Botourmiaviridae*. (B). Identity matrix of viruses used in phylogenetic tree. The scale represents the level of identity.

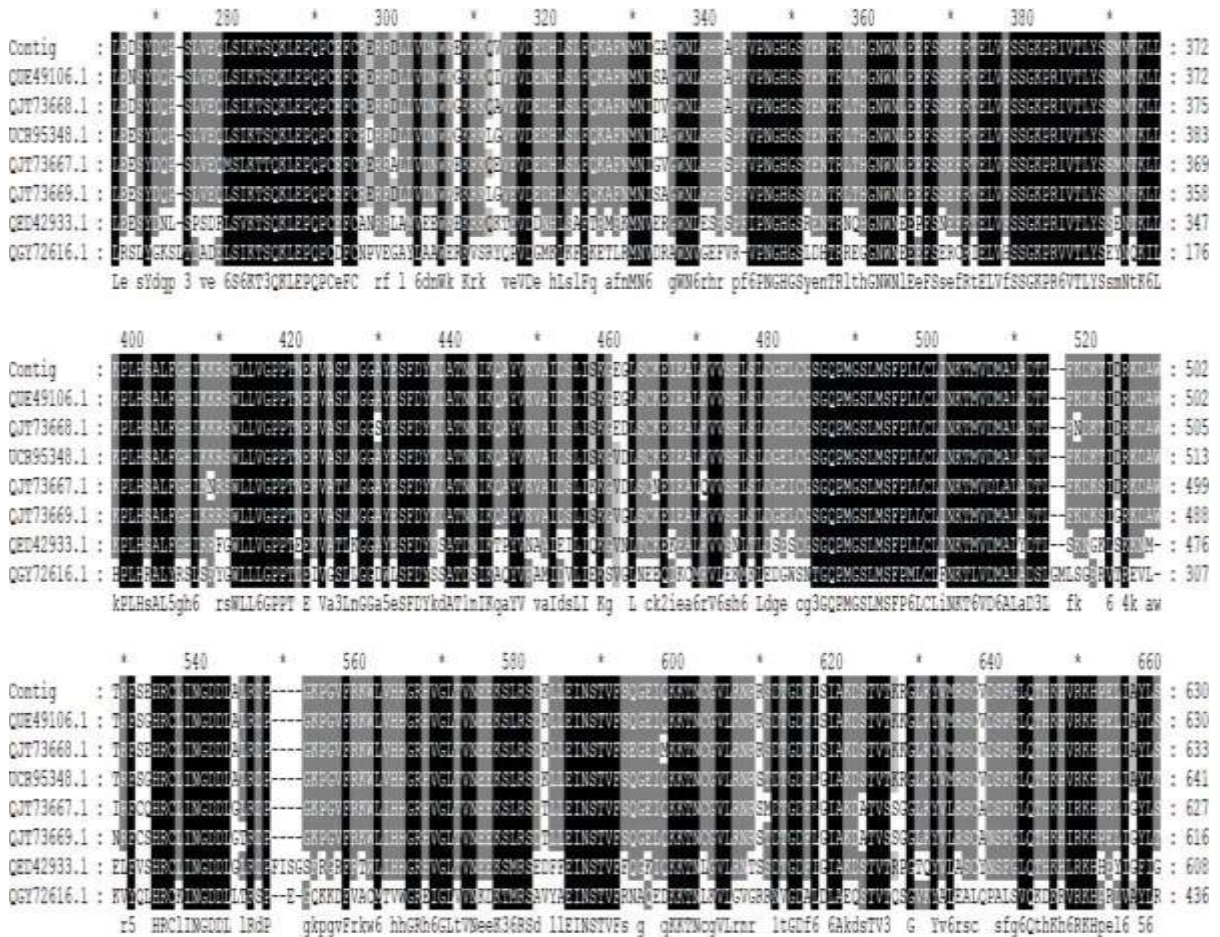


Figure 3.22 Conserved regions identified in RdRP region using multiple alignment.

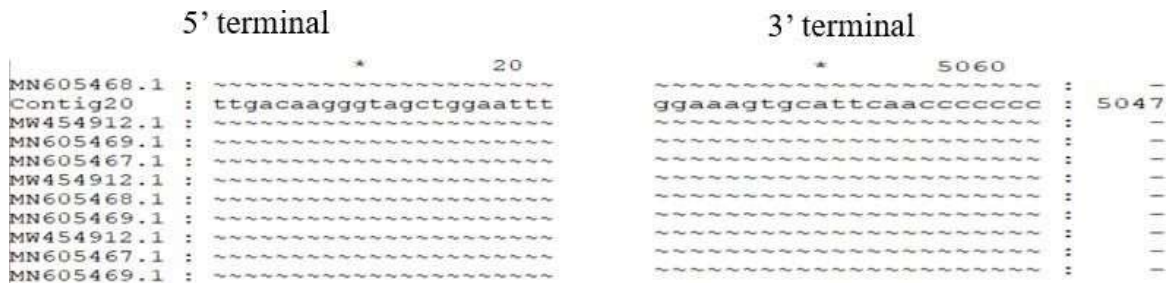
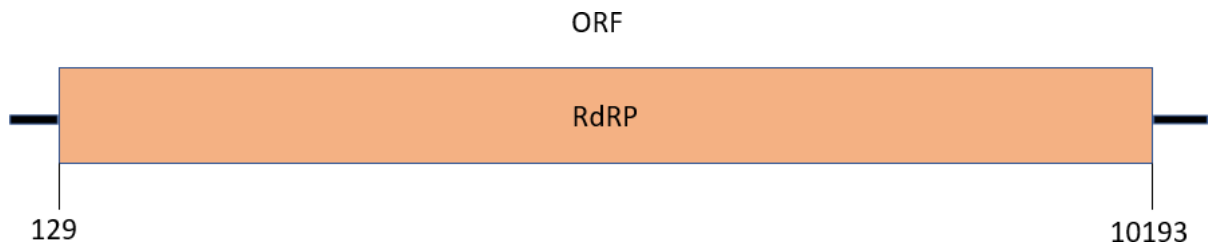


Figure 3.23 Conserved (5' and 3') terminals in Botrytis cinerea ourmiavirus Contig 20.

### 3.3.4 Botrytis cinerea negative stranded RNA virus

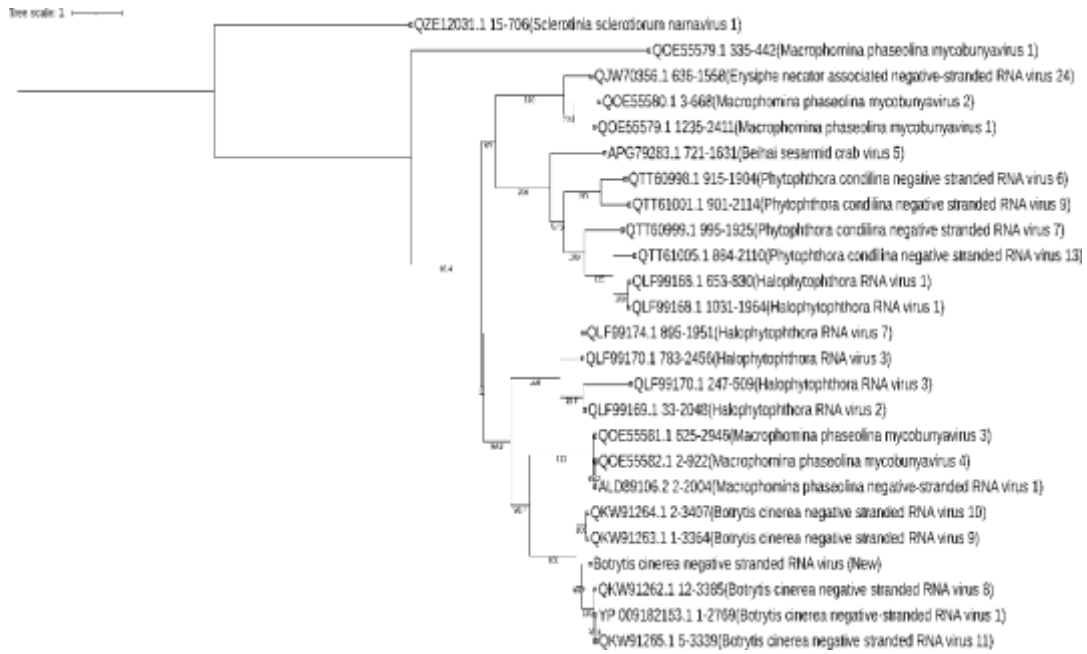
The full genome sequence of Negative-stranded RNA virus was 10241 bp long and it

comprised a single large ORF and two short untranslated regions (UTRs) (Figure 3.24). A putative polypeptide of 3354 amino acids was predicted to be encoded by single large ORF (predicted molecular mass 392 kilodaltons). According to the findings of BLASTp search, this polypeptide showed similarity 70%, 69% and 68% with Botrytis cinerea negative-stranded RNA virus 8 (BcNSRV8), Botrytis cinerea negative-stranded RNA virus 11 (BcNSRV 11) and Botrytis cinerea negative stranded RNA virus 9 (BcNSRV 9) respectively. Phylogenetic analysis showed that Botrytis cinerea negative stranded RNA virus made clade with already reported negative stranded RNA viruses (Figure 3.25). A total of eight conserved motifs were observed (I-VIII) in RdRP amino acid sequence (Figure 3.26). Botrytis cinerea negative stranded RNA virus shared conserved 5' terminal with already reported viruses but no conservations were observed at 3' terminal (Figure 3.27)



**Figure 3.24** Genome organization of *Botrytis cinerea* negative stranded RNA Virus.

A



## B

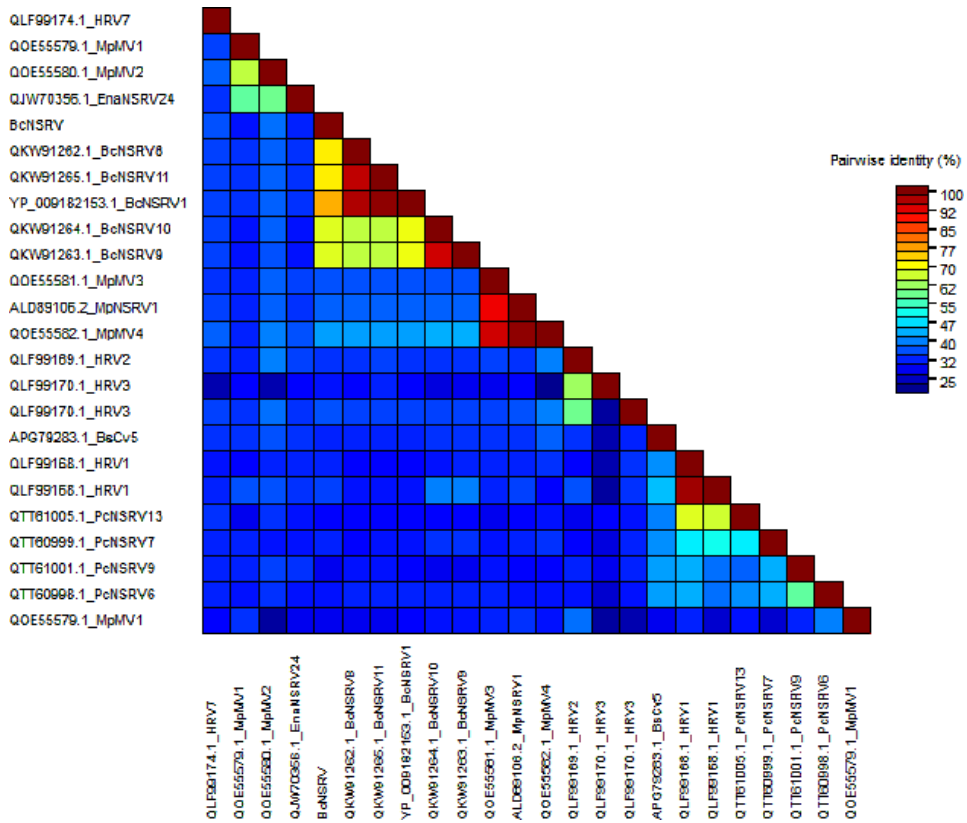


**Figure 3.25** Phylogenetic analysis, based on the deduced amino acid sequences of RdRP, revealed that Contig 5 belongs to the family Negative stranded RNA viruses. identity matrix of viruses used in phylogenetic tree. The scale represents the level of identity.

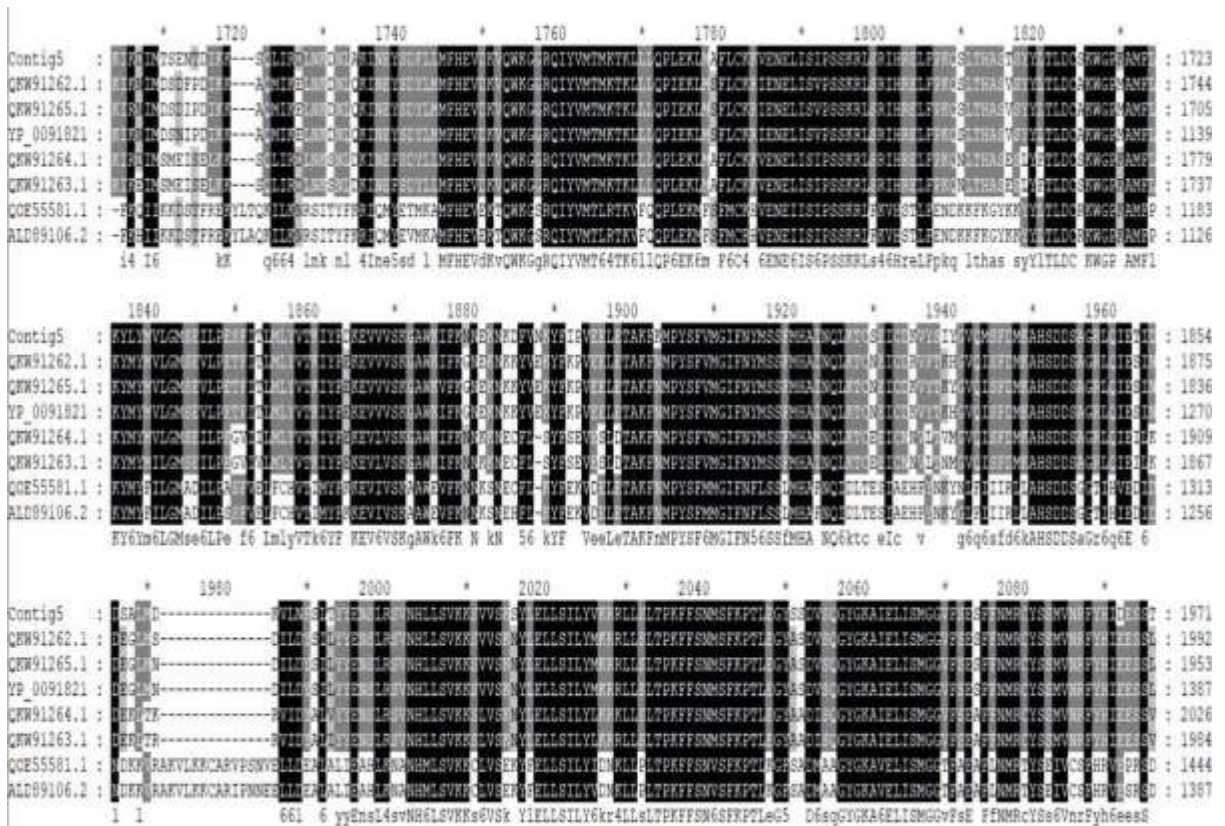


**Figure 3.26** Conserved regions identified in RdRP region using multiple alignment.

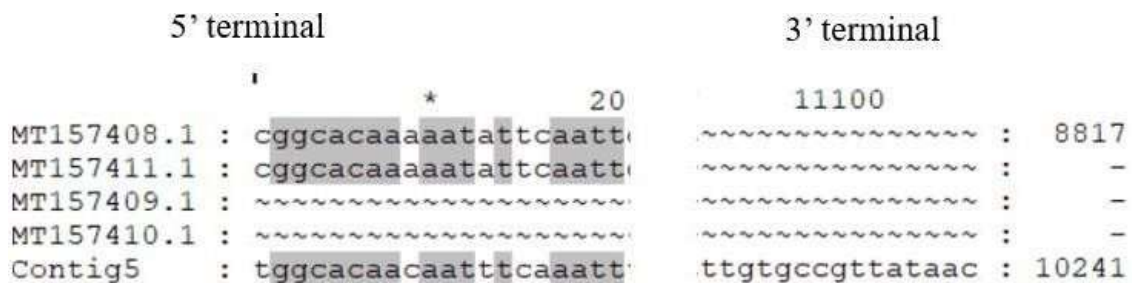


**Figure 3.27** Conserved (5' and 3') terminals in Botrytis cinerea negative stranded RNA Virus Contig 5.



### 3.3.5 *Plasmopara viticola* lesion associated orfanplasmovirus 4

*Plasmopara viticola* lesion associated orfanplasmovirus 4 has a genome of 3421 nt (Figure 3.28). The genome has single ORF and two short Untranslated regions (UTRs). ORF begins at nt 30 and continues through nt 3260. ORF is anticipated to have a molecular weight of 121 kDa. BLASTp search showed the similarity 80%, 34% and 33% with *Sclerotinia sclerotiorum* narnavirus 3 (SsNV3), *Plasmopara viticola* lesion associated orfanplasmovirus 4 (PvlaOPV 4) and *Plasmopara viticola* lesion associated orfanplasmovirus 2 (PvlasOPV2) respectively. The phylogenetic tree was constructed based on an alignment of the aa sequences of the conserved motifs in the RdRp domain to check relatedness of said mycovirus. Phylogenetic analysis showed that *Plasmopara viticola* lesion associated orfanplasmovirus 4 made clade with already reported viruses (Figure 3.29). A total of four conserved motifs were observed (I-IV) in RdRP amino acid sequence (Figure 3.30). *Plasmopara viticola* lesion associated orfanplasmovirus 4 shared conserved 5' and 3' terminals with already reported viruses (Figure 3.31).

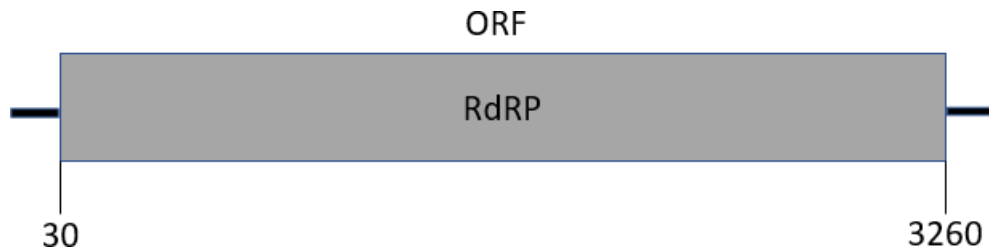
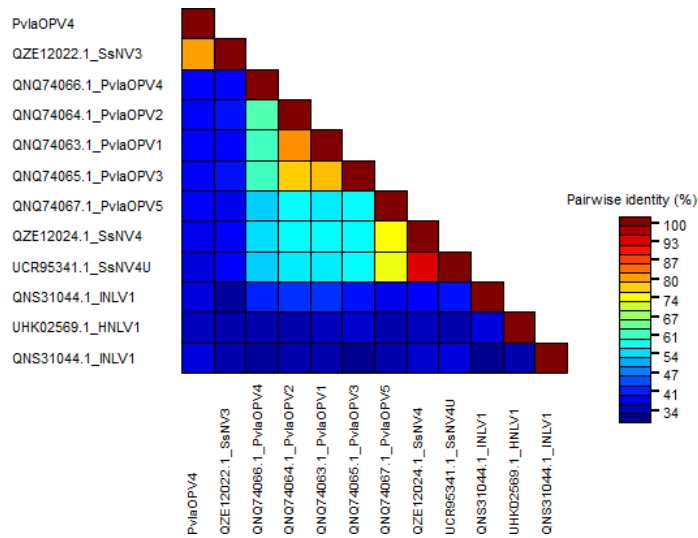
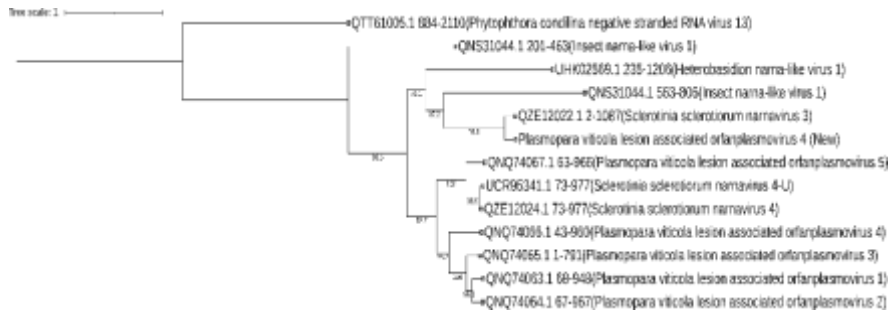


**Figure 3.28** Genome organization of *Plasmopara viticola* lesion associated orfanplasmovirus 4.



A



B

**Figure 3.29.** A). Phylogenetic analysis, based on the deduced amino acid sequences of RdRP, revealed that Contig 43 belongs *Plasmopara viticola* lesion associated orfanplasmoviruses. B). Identity matrix of viruses used in phylogenetic tree. The scale represents the level of identity.



### 3.3.6 Botrytis cinerea hypovirus

Botrytis cinerea hypovirus 1-A has a genome of 10683 nt (Figure 3.32). The genome has single ORF. ORF begins at nt 757 and concludes at nt 9675. ORF's predicted protein has a 339 kDa molecular weight. Polypeptide deduced by ORF contain two domains which Helicase and Peptidase. The findings of BLASTp showed similarity 94%, 93%, 93% and 94% with Sclerotinia sclerotiorum hypovirus 1-A (SsHV 1-A), Sclerotinia sclerotiorum hypovirus 1/SX276 (SsHV 1/SX276) and Botrytis cinerea hypovirus 3 (BcHV3) respectively. The phylogenetic tree was built using an alignment of the aa sequences of the conserved motifs in the RdRp domain to determine the mycovirus's relatedness. Phylogenetic analysis showed that Botrytis cinerea hypovirus made clade with already reported members of family *hypoviridae* (Figure 3.33). A total of six conserved motifs were observed (I-VI) in RdRP amino acid sequence (Figure 3.34). Botrytis cinerea hypovirus shared conserved 3' terminals with already reported viruses while no conservations were observed at 5' terminal (Figure 3.35)

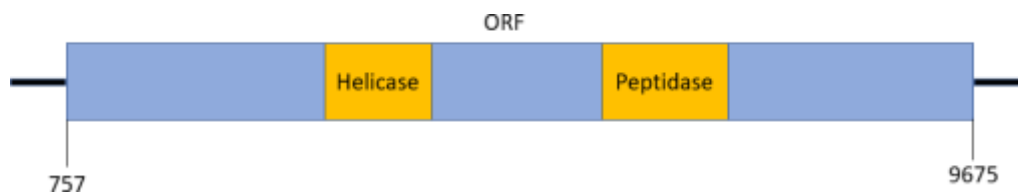
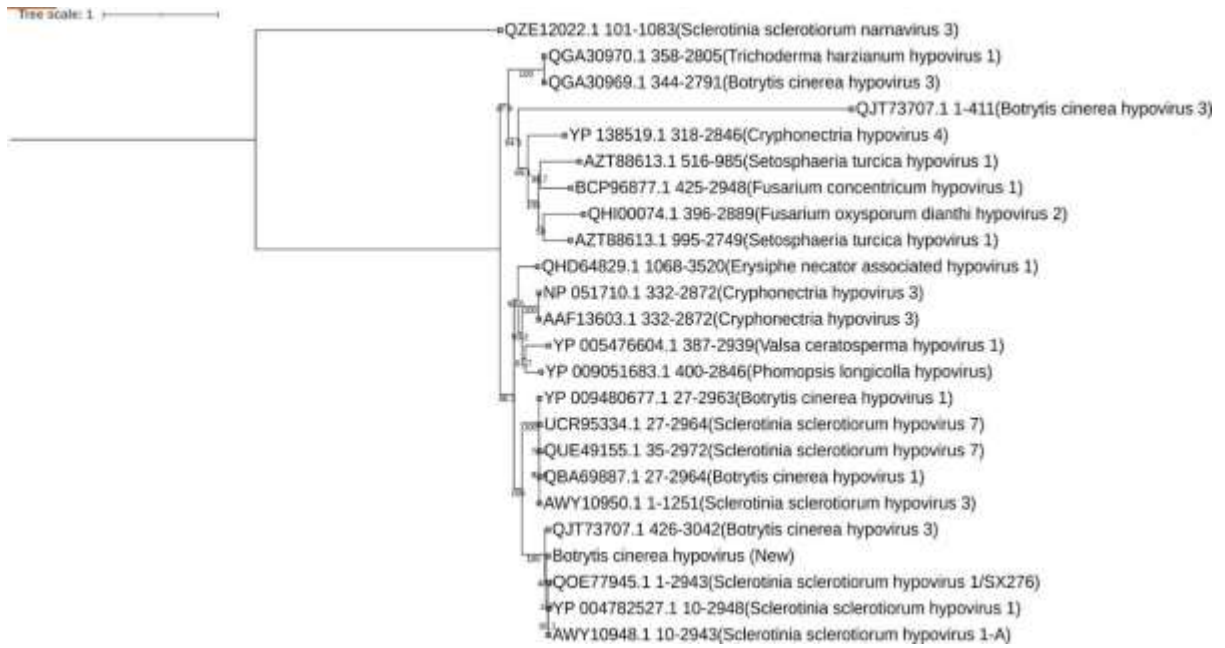


**Figure 3.32** Genome organization of Botrytis cinerea hypovirus.

### A



### B

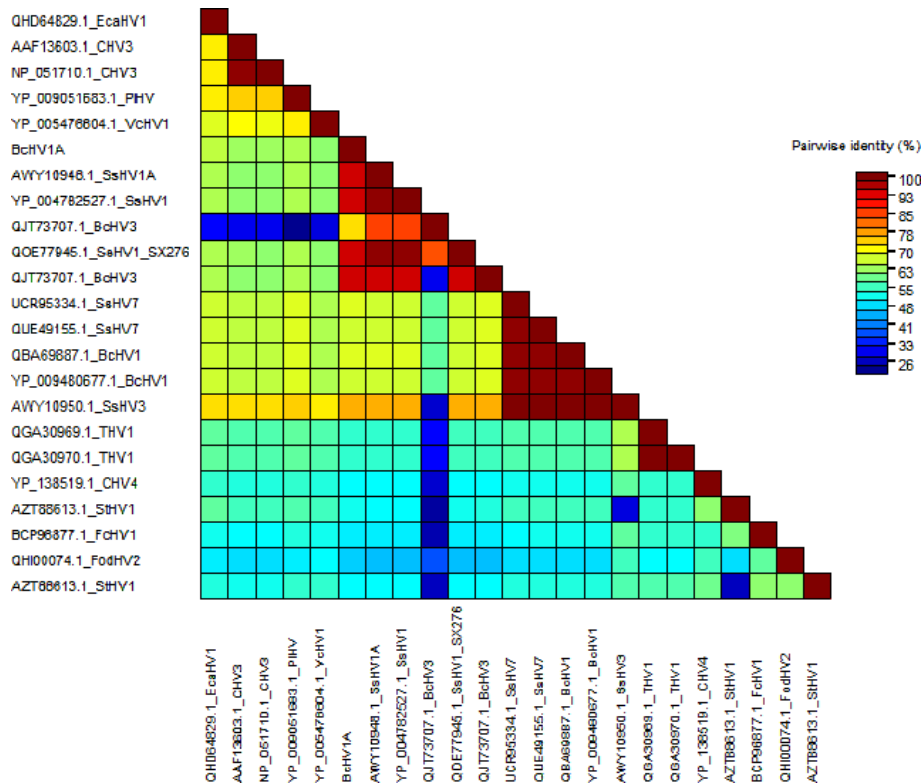




**Figure 3.33** Phylogenetic analysis, based on the deduced amino acid sequences of RdRP, revealed that Contig 4 belongs to the family *Hypoviridae*. identity matrix of viruses used in phylogenetic tree. The scale represents the level of identity.

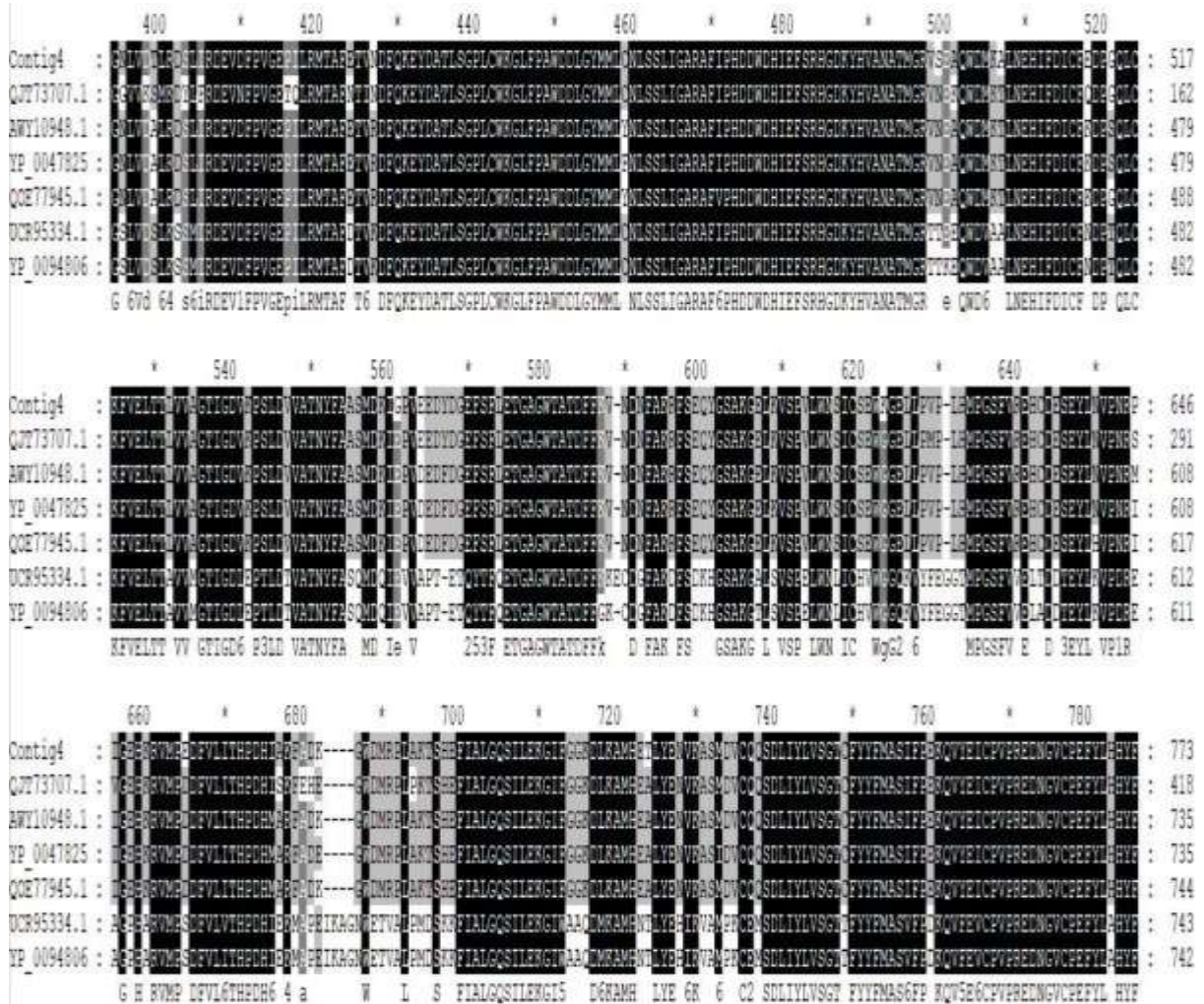


**Figure 3.34** Conserved regions identified in RdRP region using multiple alignment.

5' terminal		3' terminal	
			*
			20
JF781304.1	: ~~~~~	aggtagacgtcagca	: 9486
Contig4	: ttctttcatattgttttaa	aggtagacgtcagca	: 10683
MN617170.1	: ~~~~~	aggtagacgtcagca	: 8736
MN617170.1	: ~~~~~	~~~~~	: -
NC_037659.	: ~~~~~	~~~~~	: -
MW454885.1	: ~~~~~	~~~~~	: -

**Figure 3.35** Conserved (5' and 3') terminals in *Botrytis cinerea* hypovirus.

### 3.3.6 *Botrytis cinerea* mycotymovirus

*Botrytis cinerea* mycotymovirus has a genome of 7309 nt (Figure 3.36). The genome has single ORF. ORF starts from nt 28 And ends at nt 7071. ORF has multiple domains like V-methyltransferase, Helicase and RdRp. ORF's predicted protein has a 261 kDa molecular weight. BLASTp findings showed the similarity 98%, 98% and 95% with *Sclerotinia sclerotiorum* mycotymovirus 1-WX (SsMTV 1-WX), *Sclerotinia sclerotiorum* mycotymovirus 1-U (SsMTV 1-U) and *Botrytis cinerea* mycotymovirus 1 (BcMTV1) respectively. The phylogenetic tree was built using an alignment of the aa sequences of the conserved motifs in the RdRp domain to determine the mycovirus's relatedness. Phylogenetic analysis showed that *Botrytis cinerea* mycotymovirus made clade with already reported viruses (Figure 3.37). A total of eight conserved motifs were observed (I-VIII) in RdRP amino acid sequence (Figure 3.38). *Botrytis cinerea* mycotymovirus shared conserved 5' and 3' terminals with already reported viruses (Figure 3.39).

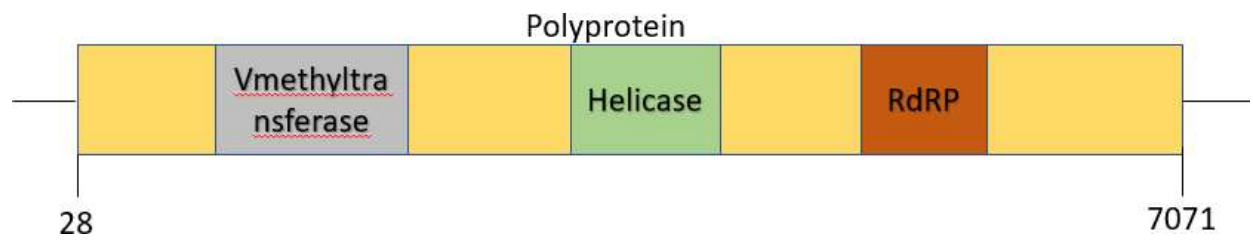
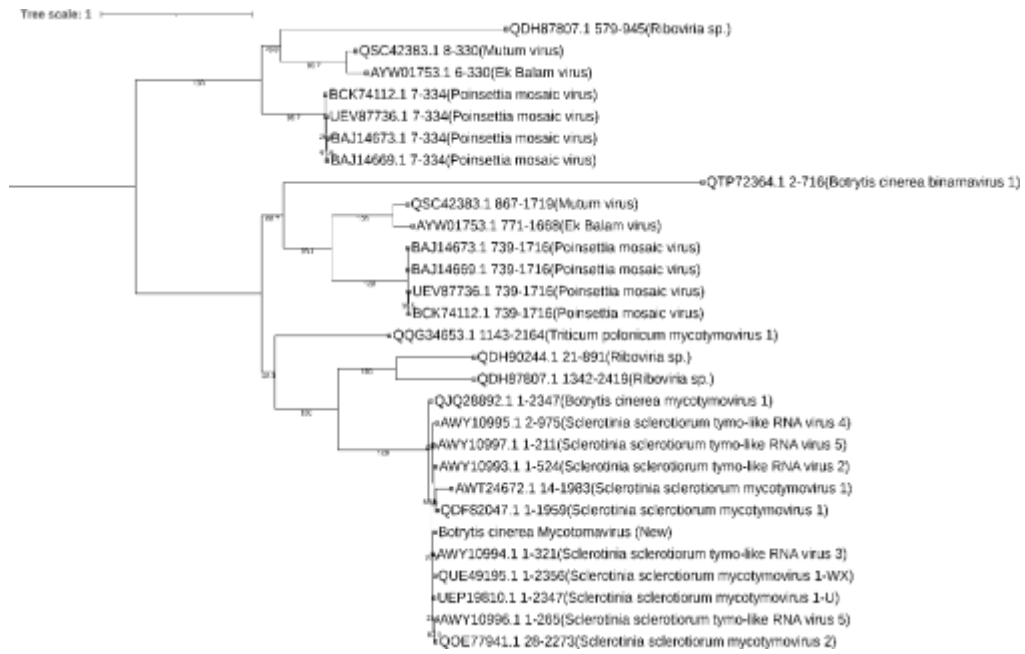


**Figure 3.36** Genome organization of *Botrytis cinerea* mycotymovirus.

# A





B

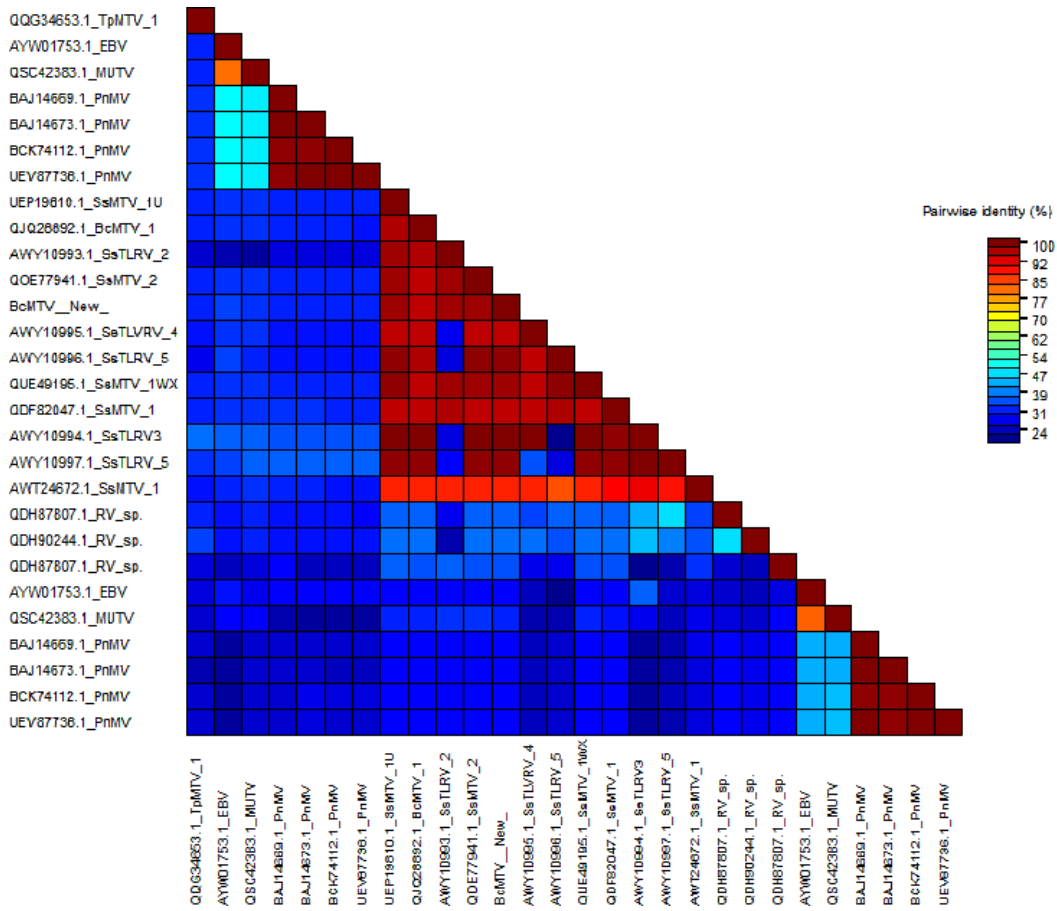


**Figure 3.37 (A).** Phylogenetic analysis, based on the deduced amino acid sequences of RdRP, revealed that Contig 5 belongs to the mycotymoviruses. (B). Identity matrix of viruses used in phylogenetic tree. The scale represents the level of identity.

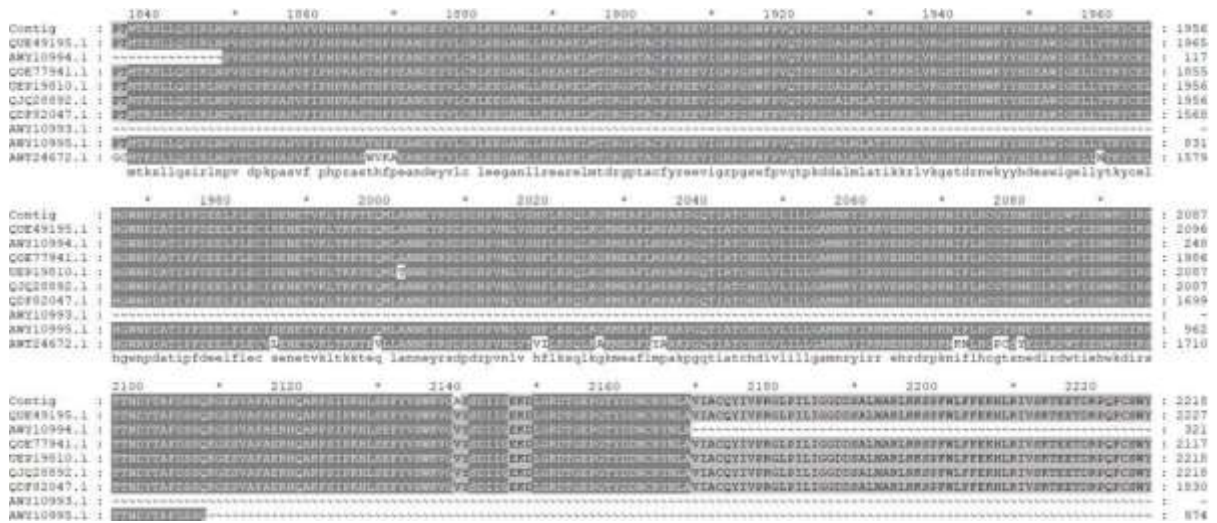


**Figure 3.38** Conserved regions identified in RdRP region using multiple alignment.

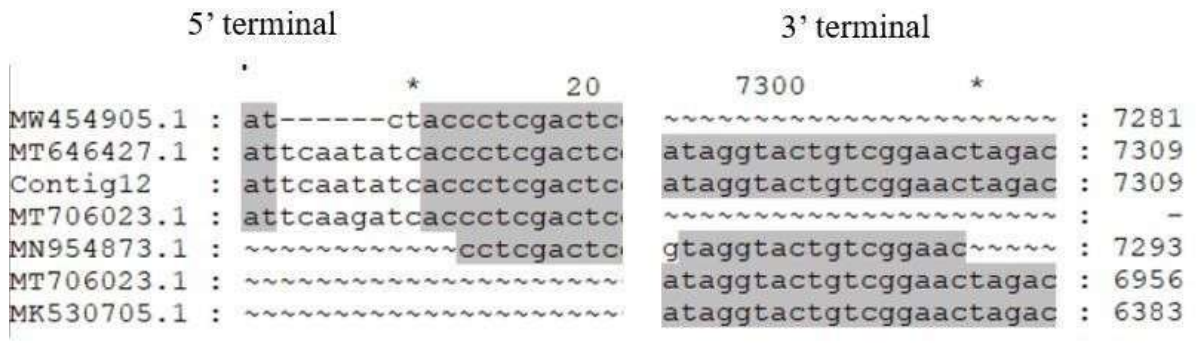


**Figure 3.39** Conserved (5' and 3') terminals in Botrytis cinerea mycovirus.

### 3.3.7 Botrytis cinerea birnavirus

The genome of *Botrytis cinerea* birnavirus is 2274 nucleotides long (Figure 3.40). There is only one ORF in the genome. ORF begins at nt 39 and concludes at nt 2192. ORF's predicted protein has an 80 kDa molecular weight. Results of BLASTp showed similarity *Botrytis cinerea* birnavirus 1 (BcBV1), *Botrytis cinerea* birnavirus 3 (BcBV3) and *Sclerotinia sclerotiorum* narnavirus 1 (SsNV1) respectively. The phylogenetic tree was built to see how closely it was linked to other mycoviruses. Phylogenetic analysis showed that *Botrytis cinerea* birnavirus made clade with already

reported birnaviruses (Figure 3.41). No conserved motifs were observed in RdRP amino acid sequence (Figure 3.42). *Botrytis cinerea* birnavirus shared conserved 5' and 3' terminals with already reported viruses (Figure 3.43).



**B**

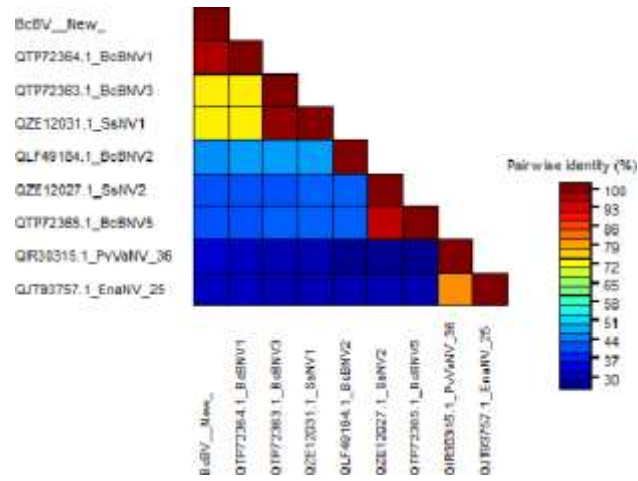


**Figure 3.41 (A).** Phylogenetic analysis, based on the deduced amino acid sequences of RdRP, revealed that Contig 5 belongs to the family *Birnaviridae*. **(B).** Identity matrix of viruses used in phylogenetic tree. The scale represents the level of identity.

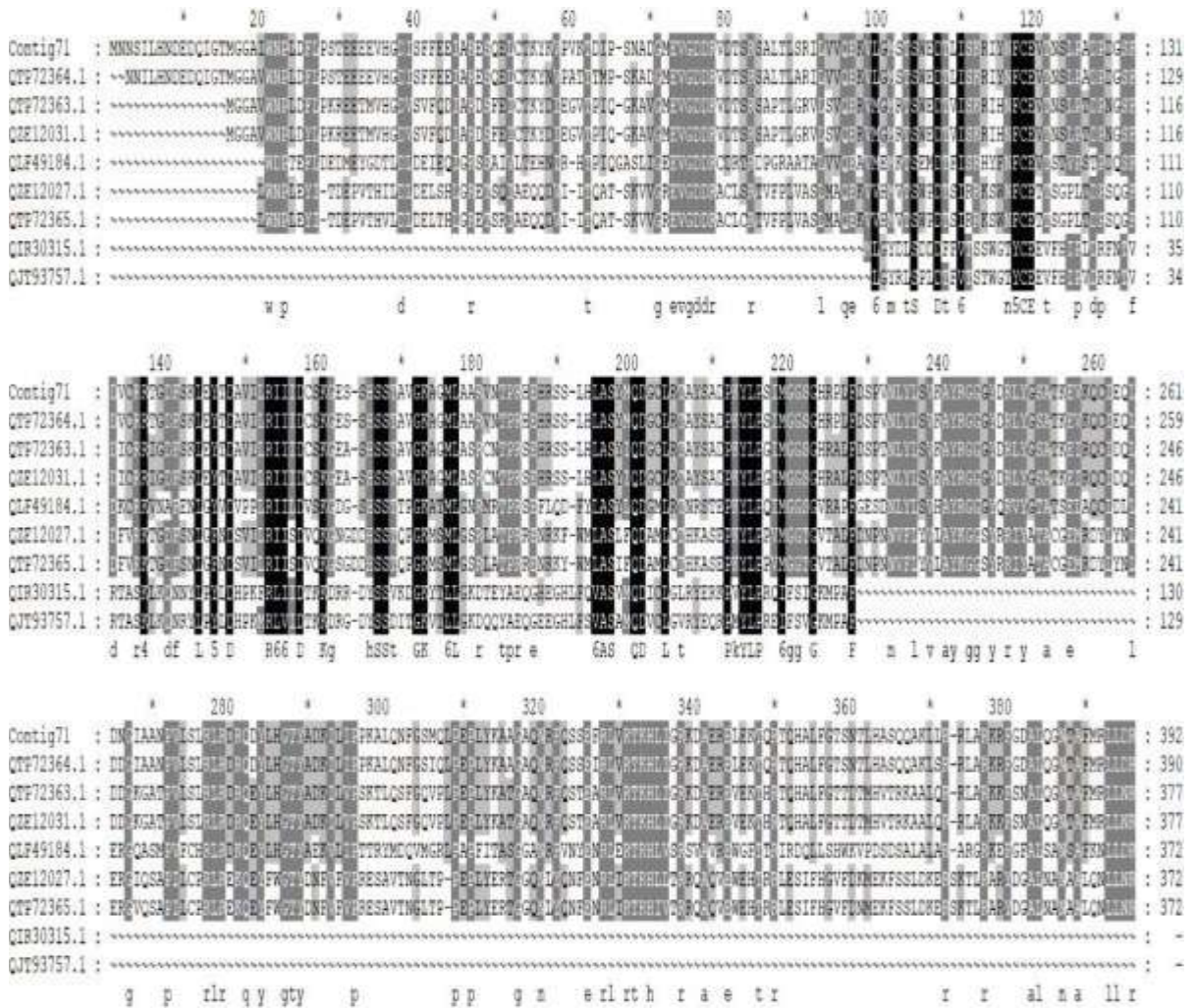


**Figure 3.42** Conserved regions identified in RdRP region using multiple alignment.

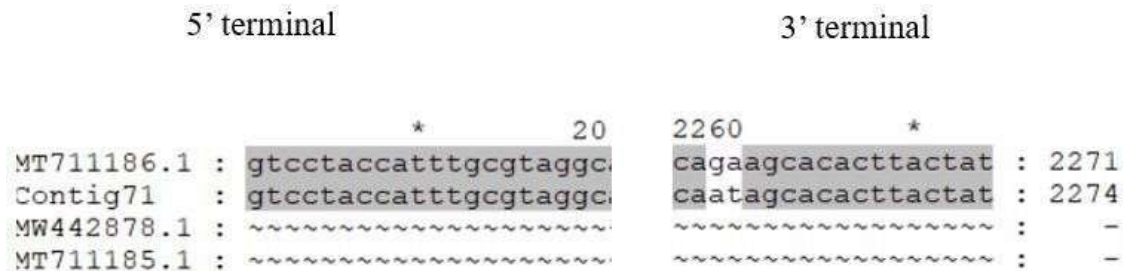


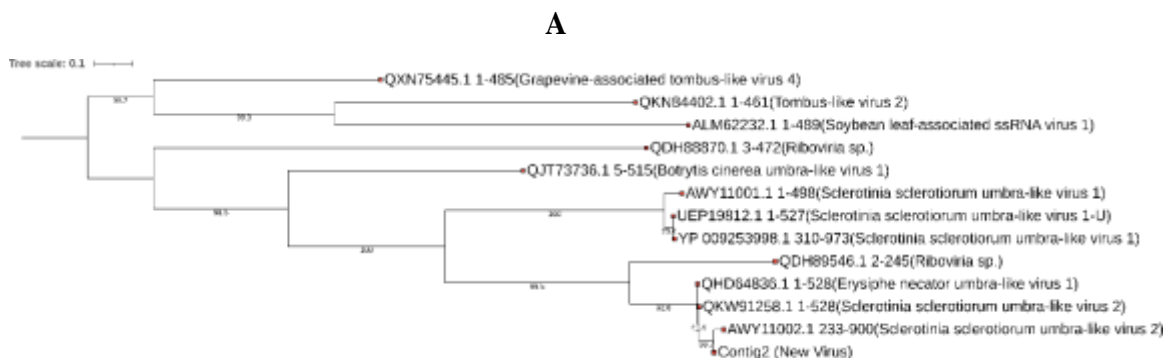
**Figure 3.43** Conserved (5' and 3') terminals in Botrytis cinerea birnavirus Contig12.

### 3.3.8 Botrytis cinerea umbra-like virus

The genome of Botrytis cinerea umbra like virus (Contig 2) is 2459 nucleotides long (Fig. 3.44). There is only one ORF in the genome. ORF starts at nt 421 and concludes at nt 2007. ORF's predicted protein has a 60 kDa molecular weight. Results of BLASTp showed similarity 92%, 90% and 55% with Sclerotinia sclerotiorum umbra-like virus 2 (SsULV2), Erysiphe necator umbra-like virus 1 (EnULV 1) and Sclerotinia sclerotiorum umbra-like virus 1 (SsULV1) respectively. The phylogenetic tree was built to see how closely it was linked to other mycoviruses. Phylogenetic analysis showed that Botrytis cinerea umbra-like virus made clade with already reported umbra-like viruses (Fig. 3.45). Presence of conserved motifs in RdRP amino acid sequence is shown in (Fig. 3.46).



**Figure 3.44** Genome organization of Botrytis cinerea umbra-like virus.



**B**

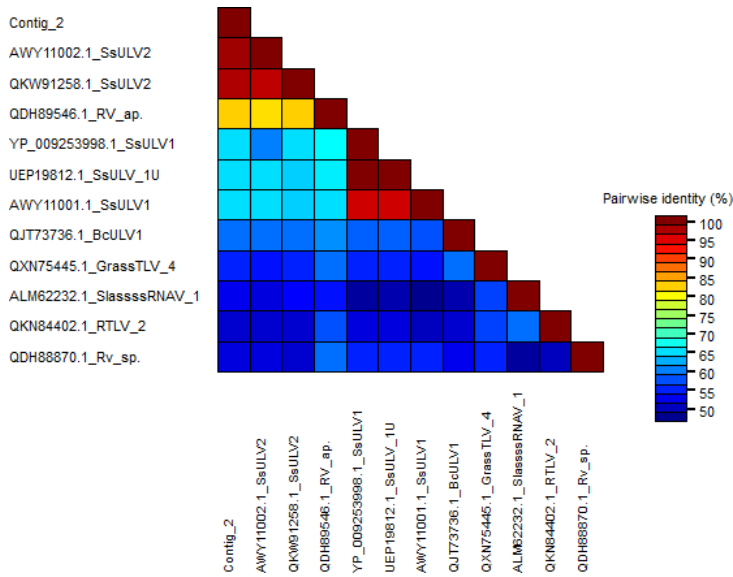


**Figure 3.45 (A).** Phylogenetic analysis, based on the deduced amino acid sequences of RdRP, revealed that Contig 5 belongs to the umbra-like viruses. **B).** Identity matrix of viruses used in phylogenetic tree. The scale represents the level of identity.





### 3.3.9 Botrytis cinerea Narnavirus

The genome of Botrytis cinerea narnavirus (Contig 55) is 2556 nucleotides long (Fig. 3.47). There is only one ORF in the genome. ORF begins at nt 28 and concludes at nt 2502. ORF's predicted protein has a 92 kDa molecular weight. Results of BLASTp showed similarity 86%, 84% and 74% with Botrytis cinerea birnavirus 1 (BcBNV 1), Erysiphe necator associated narnavirus 12 (EnassNV 12) and Erysiphe necator associated narnavirus 50 (EnassNV 50) respectively. The phylogenetic tree was built to see how closely it was related to other mycoviruses. Phylogenetic analysis showed that Botrytis cinerea narnavirus made clade with already reported narnaviruses (Fig. 3.48) Presence of conserved motifs is shown in (Fig. 3.49).

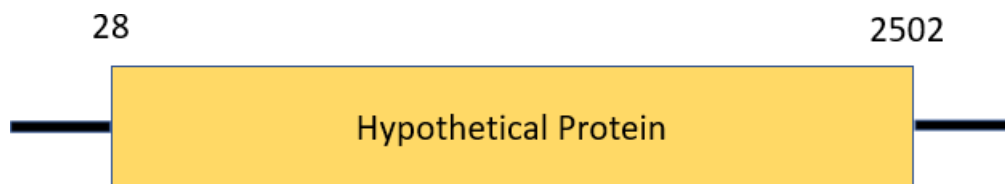
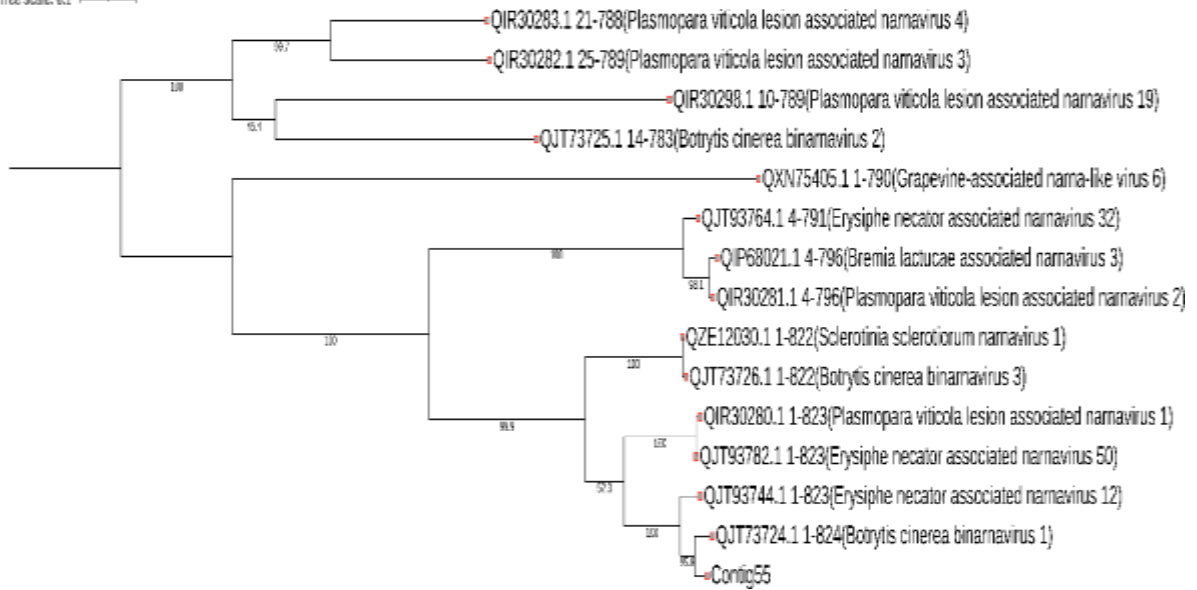


**Figure 3.47** Genome organization of Botrytis cinerea narnavirus.

Tree scale: 0.1



## B

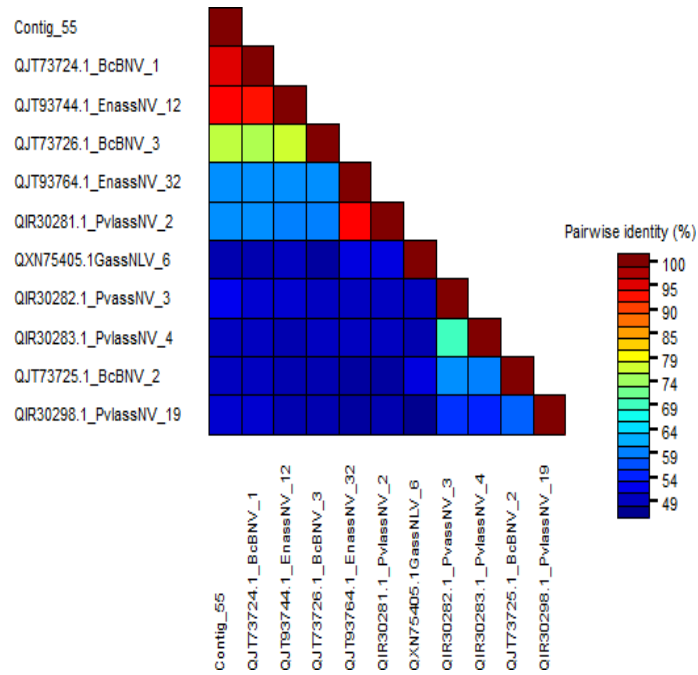


**Figure 3.48 A).** Phylogenetic analysis, based on the deduced amino acid sequences of RdRP, revealed that Contig 5 belongs to the family *Narnaviridae*. B). Identity matrix of viruses used in phylogenetic tree. The scale represents the level of identity.

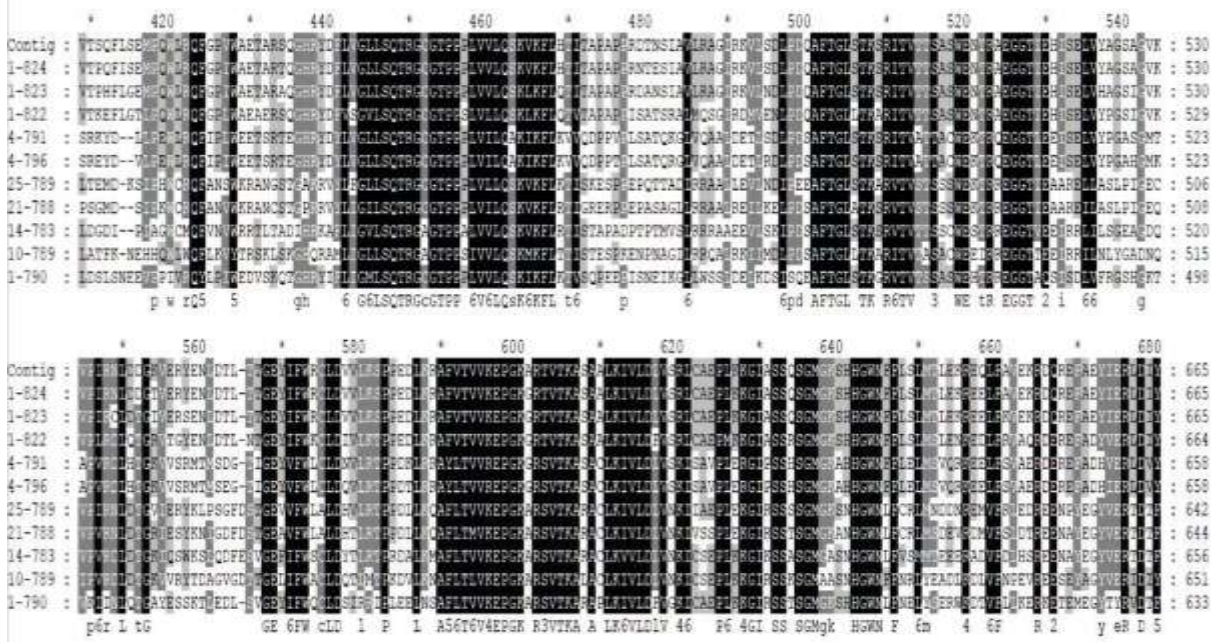


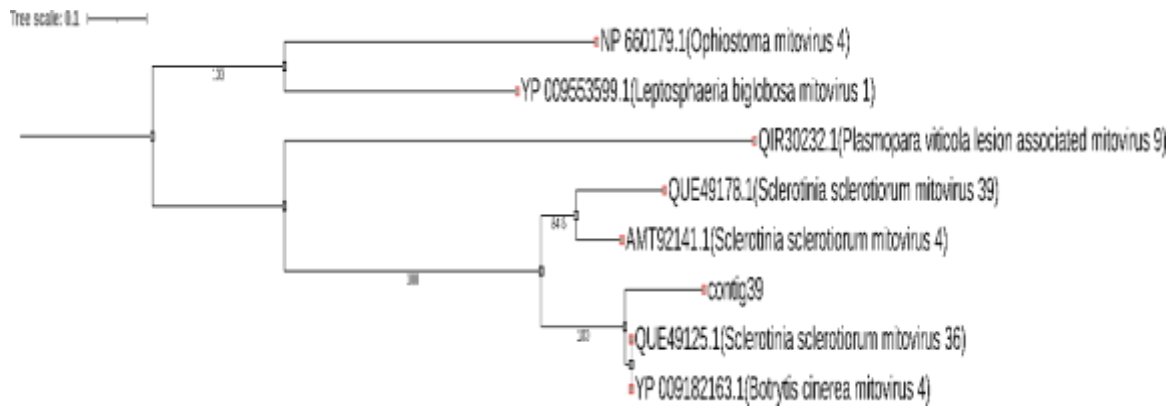
Figure 3.49 Conserved regions identified in RdRP region using multiple alignment.

### 3.3.10 Botrytis cinerea Mitovirus

The genome of *Botrytis cinerea* mitovirus (Contig 39) is 3051 nucleotides long (Fig. 3.50). There is only one ORF in the genome of said mycovirus. ORF begins at nt 592 and ends at nt 2787. ORF's predicted protein has an 85 kDa molecular weight. Results of BLASTp showed similarity 93%, 89% and 90% with *Botrytis cinerea* mitovirus 4 (BcMV4), *Sclerotinia sclerotiorum* mitovirus 36 (SsMV 36) and *Sclerotinia nivalis* mitovirus 1 (SnMV 1) respectively. The phylogenetic tree was built to see how closely it was linked to other mycoviruses. Phylogenetic analysis showed that *Botrytis cinerea* mitovirus made clade with already reported mitoviruses (Fig. 3.51). Presence of conserved motifs observed in RdRP amino acid sequence shown in (Fig. 3.52).



**Figure 3.50 Genome organization of *Botrytis cinerea* mitovirus.**



**B**

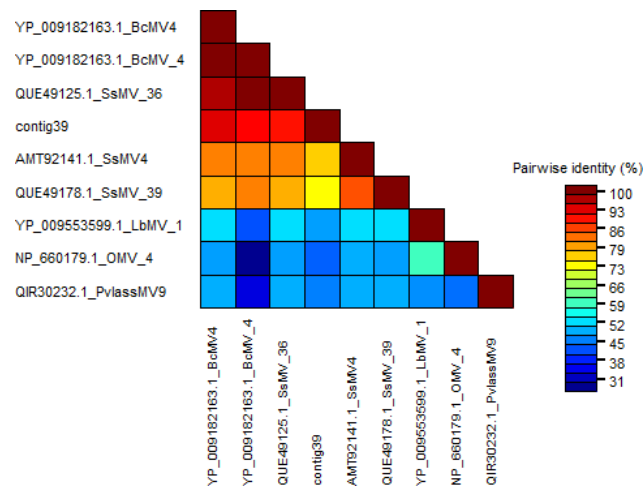


**Figure 3.51 A).** Phylogenetic analysis, based on the deduced amino acid sequences of RdRP, revealed that viral sequence belongs to the family *Birnaviridae*. **B).** Identity matrix of virus used in phylogenetic tree. The scale represents the level of identity.



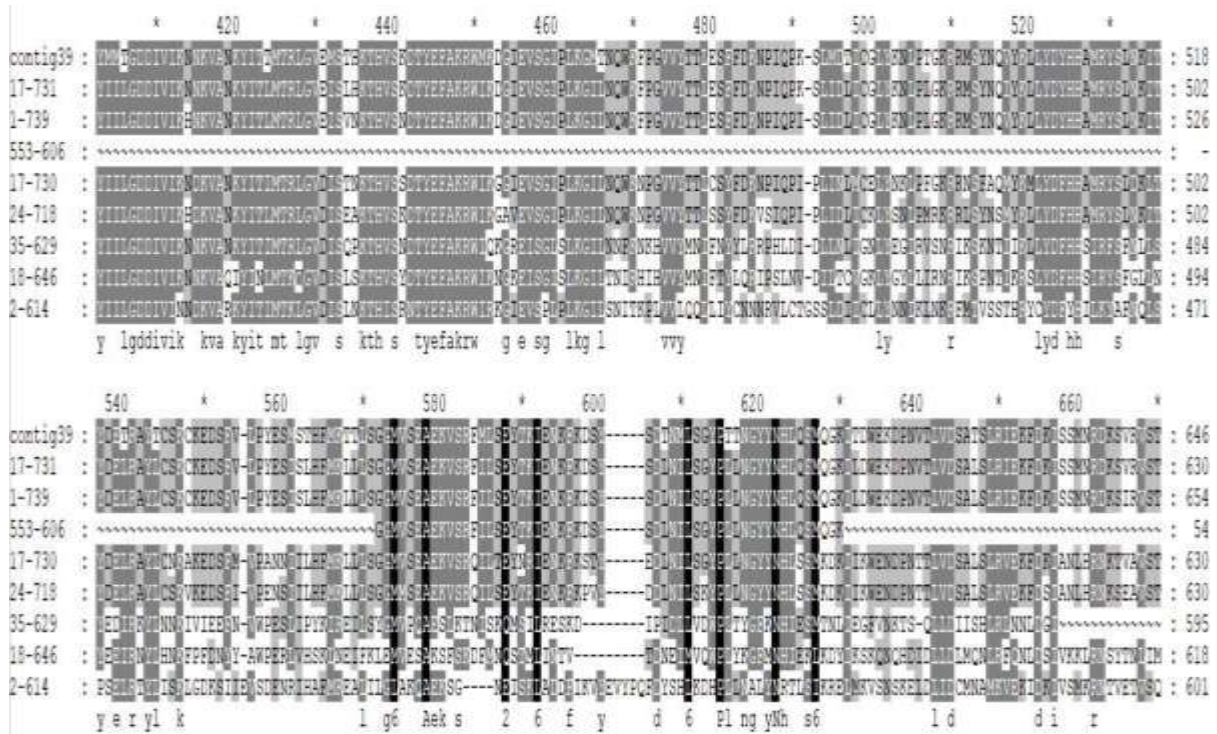


**Figure 3.52** Conserved regions identified in RdRP region using multiple alignment.

### 3.4 Studying the infection and its effect on the fungal samples to identify the hypovirulent mycoviruses as a potential tool to control *Botrytis* infecting different crops (Objective 4).

#### 3.4.1 Growth Comparison Test of viruses infected isolates with uninfected *Botrytis*

##### strains

Another growth comparison test was conducted by taking 8 *Botrytis* isolates (Kst5C, Kst10A, Kst14A & Kst51). Three isolates were virus infected (Kst5C, Kst10A & Kst14A) while isolate Kst51 was virus free and considered as positive control. By taking data on 2<sup>nd</sup>, 3<sup>rd</sup> and 4<sup>th</sup> day, it was observed that mycoviruses present in Kst10A and Kst14A have cryptic effect on their host because their growth pattern was just like the isolate Kst51. But in case of Kst5C the growth of isolate was slow due to mycoviral infection although growth conditions and growth media were same for all the isolates (Figure 3.53). Isolate Kst5C show abnormal and slow growth as compared to other isolates. Growth rate was also determined by measuring



the colony diameter over a 4 days period because at "the" 4<sup>th</sup> day the plate was completely filled with mycelia, the results have been presented as histograms (Figure 3.55 A-C). The results of histograms showed the exact pattern as there is present in pictures of fungal colony growth pattern. Similarly, growth comparison test was conducted by taking another batch of infected *Botrytis* isolates (Kst31C, Kst32B, Kst33A & Kst58). Three isolates were virus infected (Kst5C, Kst10A & Kst14A) while isolate Kst58 was virus free and considered as positive control. By taking data on 2<sup>nd</sup>, 3<sup>rd</sup> and 4<sup>th</sup> day, it was observed that mycoviruses present in Kst32B have cryptic effect on their host because their growth pattern was just like the isolate Kst58. But in case of Kst31C & Kst33A (Figure 3.54) the growth of isolates was slower due to its mycoviruses although growth conditions and growth media were same for all the isolates. Isolates Kst31C & Kst33A show abnormal and slow growth as compared to positive isolate. (Figure 3.56 A-C).

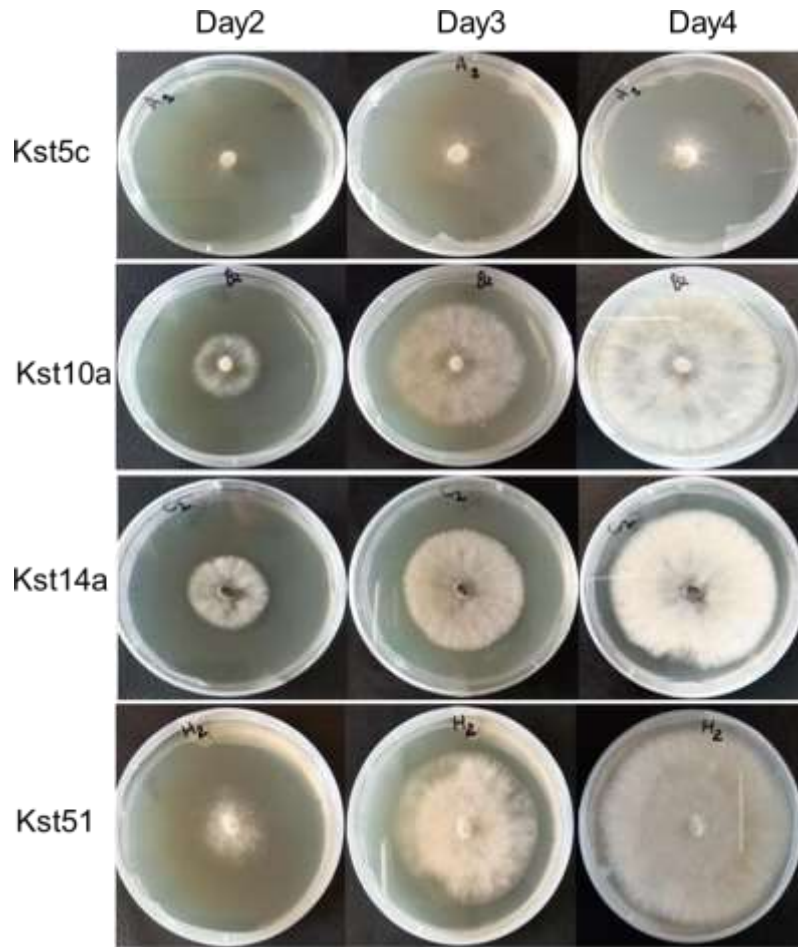


**Figure 3.53** show relative growth comparison test at 25 C for 4 days at regular 12-hour light and 12-hour dark period.

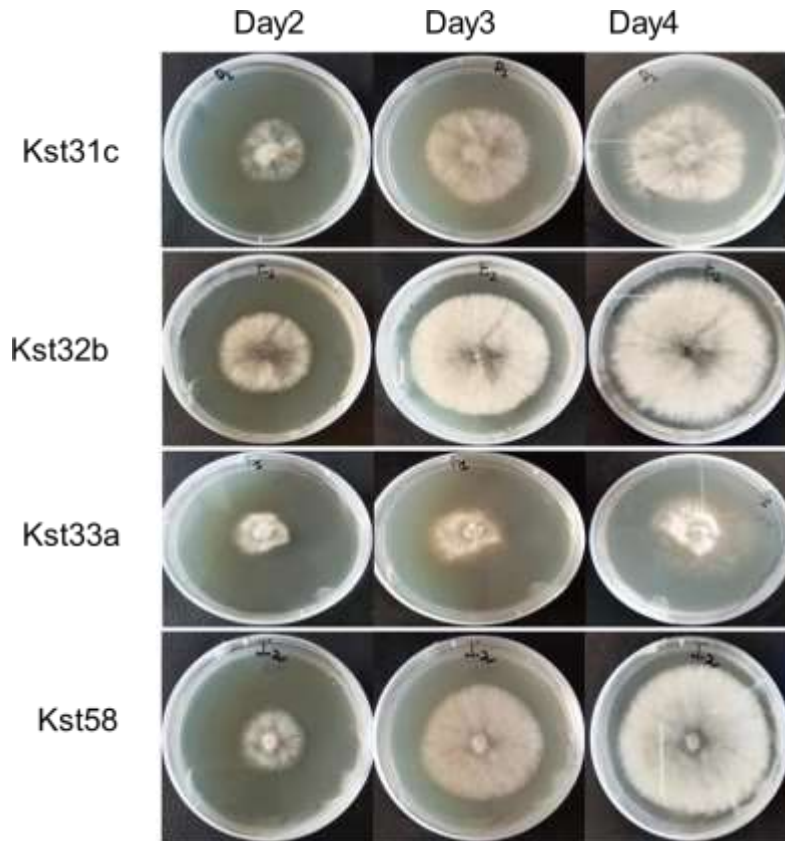


**Figure 3.54** Relative growth comparison test on PDA at 25 C for 4 days at regular 12-hour light and 12-hour dark period.

	R	Day 2	Day 3	Day 4
	1	0.2	0.5	1.3
Kst 5c	2	0.3	0.6	1.4
	3	0.4	0.7	1.5
Mean +SE		0.3+0.1	0.6+0.1	1.4+0.1
	R	Day 2	Day 3	Day 4
	1	2.1	3.9	5.3
Control	2	2.2	4	5.4
	3	2.3	4.1	5.5
Mean +SE		2.2+0.1	4+0.1	5.4+0.1
P value		0.001	0.001	0.001

**Growth Comparison of Kst5C**

Colony Diameter in Cm

**Figure 3.55 A.** Histogram showing a comparison of the growth rates of the virus-infected isolate (Kst5C) and virus-free isolate (Control, Kst51) on PDA plates. As the P value (0.02) calculated by T.test is less than  $\alpha$  (0.05) so the data is significant.

	R	Day 2	Day 3	Day 4
	1	1.7	3.9	5.1
Kst 10A	2	1.8	4	5.2

	3	1.9	4.1	5.3
Mean +SE		1.8+0.06	4+0.06	5.2+0.06
	R	Day 2	Day 3	Day 4
	1	2.1	4.1	5.2
Control	2	2.2	4.2	5.3
	3	2.3	4.3	5.4
Mean +SE		2.2+0.06	4.2+0.06	5.3+0.06
P value		0.004	0.03	014

### Growth Comparison of Kst10A

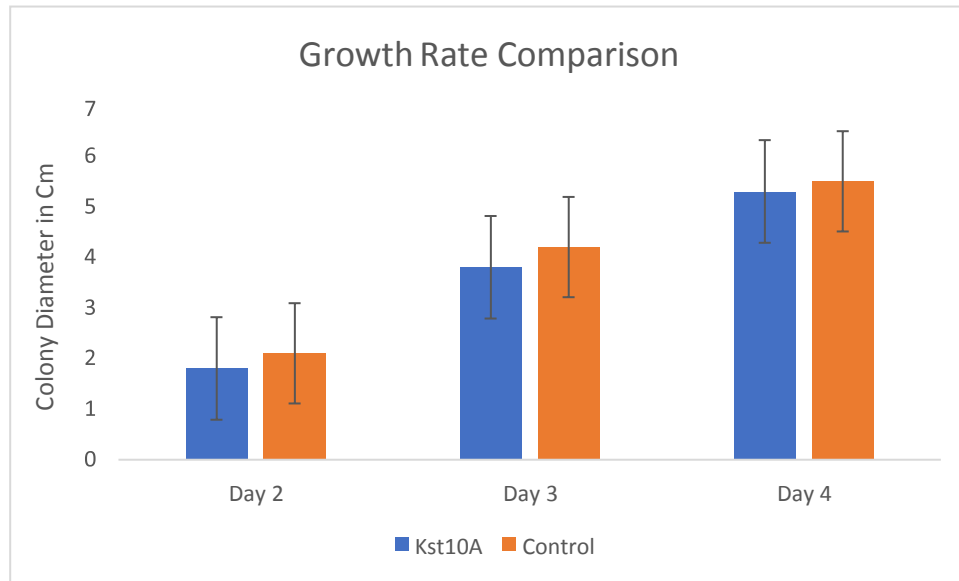


**Figure 3.55 B** Histogram showing a comparison of the growth rates of the virus-infected isolate (Kst10A) and virus-free isolate (Control, Kst51) on PDA plates. As the P value (0.17) calculated by T.test is greater than (0.05) so the data was not significant.

	R	Day 2	Day 3	Day 4
	1	2	3.6	4.8
Kst 14A	2	2.1	3.7	4.9
	3	2.2	3.8	5
Mean +SE		2.1+0.05	3.7+0.05	4.9+0.05
	R	Day 2	Day 3	Day 4
	1	1.8	3.9	5.3
Control	2	1.9	4	5.4
	3	2	4.1	5.5
Mean +SE		1.9+0.05	4+0.05	5.4+0.05
P value		0.03	0.01	0.001



### Growth Comparison of 14A

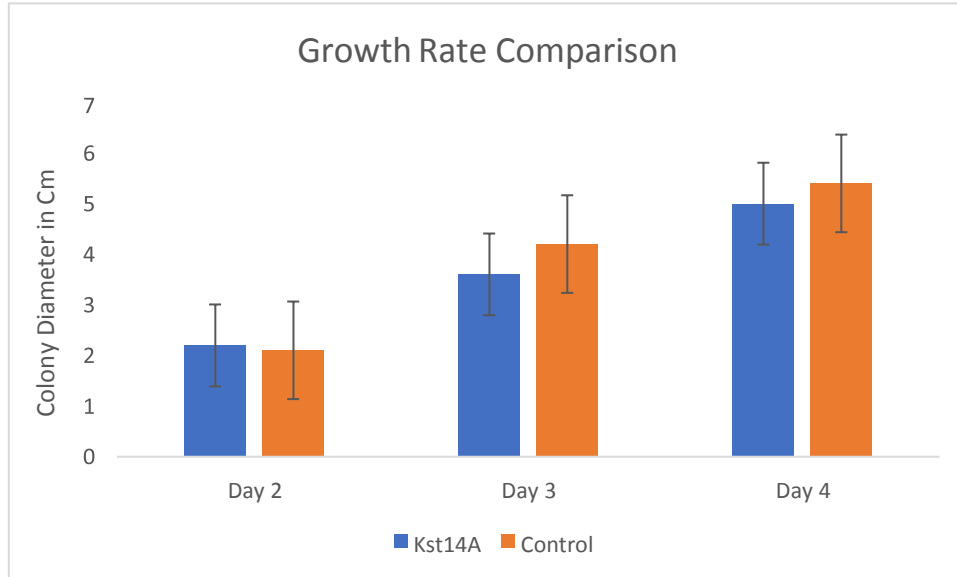


**Figure 3.55C** Histogram showing a comparison of the growth rates of the virus-infected isolate (Kst14A) and virus-free isolate (Control, Kst51) on PDA plates. As the P value (0.14) calculated was greater than (0.05) so the data was not-significant.

	R	Day 2	Day 3	Day 4
	1	1.8	3.1	3.9
Kst 31	2	1.9	3.2	4
	3	2	3.3	4.1
Mean +SE		1.9+0.05	3.2+0.05	4+0.05
	R	Day 2	Day 3	Day 4
	1	2.2	4.2	5.3
Control	2	2.3	4.3	5.4
	3	2.4	4.4	5.5
Mean +SE		2.3+0.05	4.3+0.05	5.4+0.05
P value		0.004	0.0009	0.003

**Growth Comparison of Kst31C**

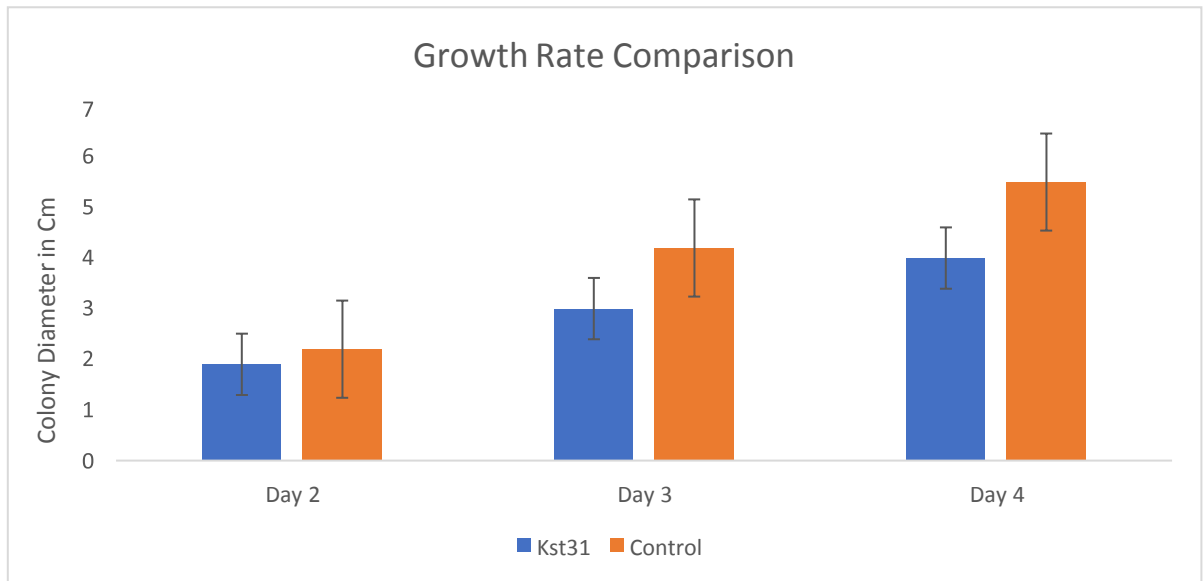


**Figure 3.56A** Histogram showing a comparison of the growth rates of the virus-infected isolate (Kst31C) and virus-free isolate (Control, Kst51) on PDA plates. As the P value (0.05) was equal to (0.05) so the data was significant.

	R	Day 2	Day 3	Day 4
	1	2.2	4	5.1

Kst 32B	2	2.3	4.1	5.2
	3	2.4	4.2	5.3
Mean +SE		2.3+0.05	4.1+0.05	5.2+0.05
	R	Day 2	Day 3	Day 4
	1	2	3.9	5.3
Control	2	2.1	4	5.4
	3	2.2	4.1	5.5
Mean +SE		2.1+0.05	4+0.05	5.4+0.05
P value		0.03	0.14	0.03

### Growth Comparison of Kst32B

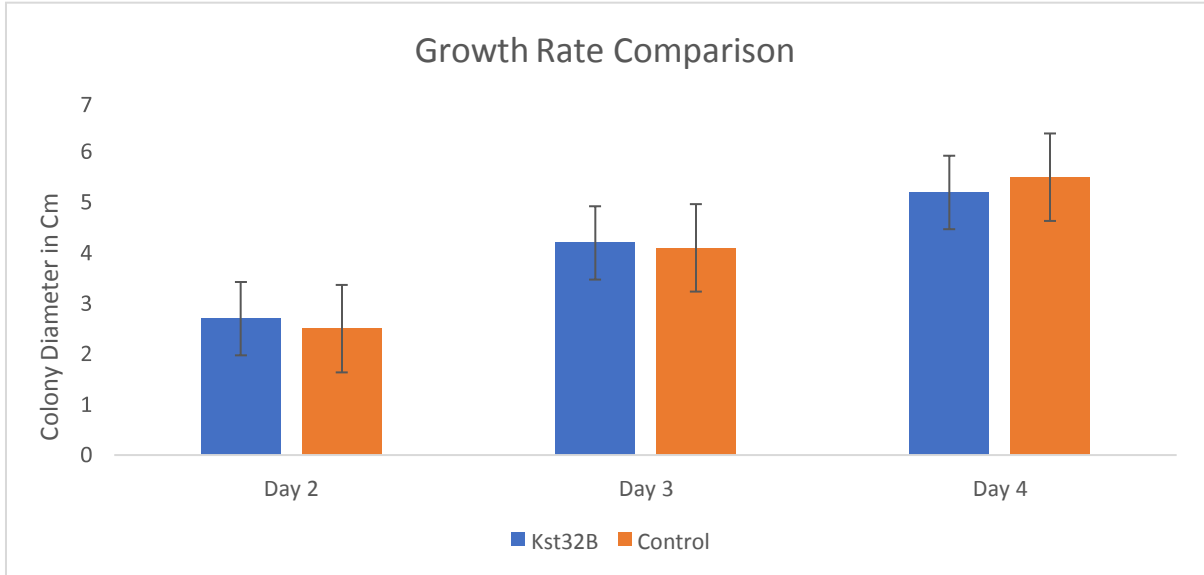


**Figure 3.56 B** Histogram showing a comparison of the growth rates of the virus-infected isolate (Kst32B) and virus-free isolate (Control, Kst51) on PDA plates. As the P value (0.5) calculated greater than  $\alpha$  (0.05) so the data was not-significant.

	R	Day 2	Day 3	Day 4
	1	1.8	2.6	3
Kst 33A	2	1.9	2.7	3.1
	3	2	2.8	3.2
Mean +SE		1.9+0.06	2.7+0.06	3.1+0.06
	R	Day 2	Day 3	Day 4
	1	2	4.3	5.3
Control	2	2.2	4.5	5.4
	3	2.3	4.6	5.5
Mean +SE		2.2+0.06	4.5+0.06	5.4+0.06
P value		0.03	0.004	0.00007

### Growth Comparison of Kst33A

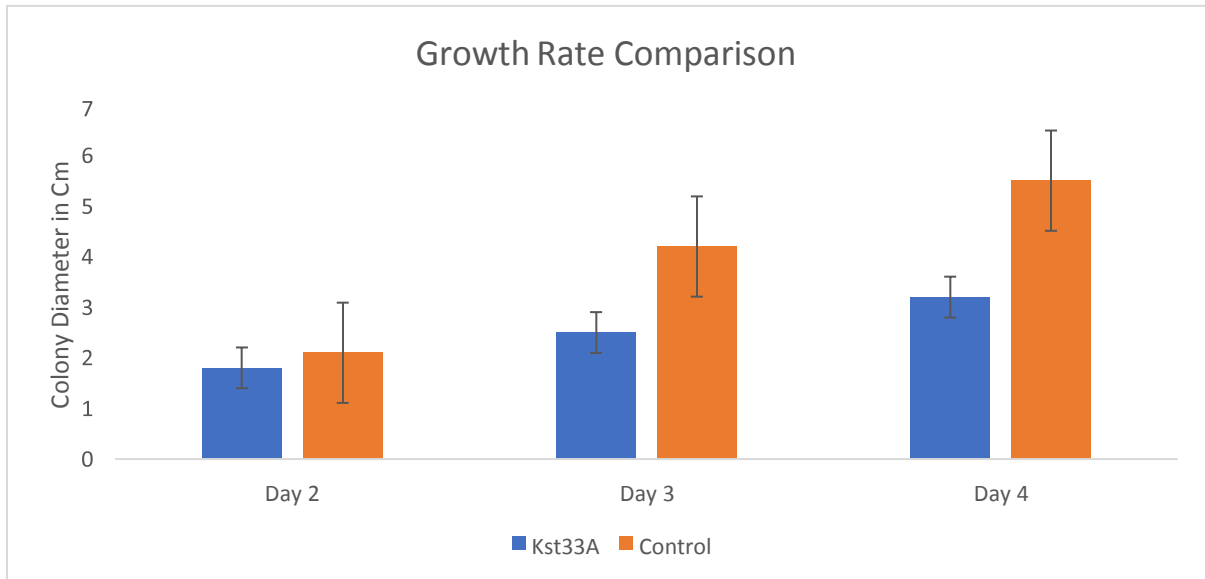


**Figure 3.56 C** Histogram showing a comparison of the growth rates of the virus-infected isolate (Kst33A) and virus-free isolate (Control, Kst51) on PDA plates. As the P value (0.06) was greater than  $\alpha$  (0.05) so the data was non-significant.

### **3.4.2 Pathogenicity Tests of virus infected and uninfected isolates (Apple Assay)**

Pathogenicity test 1 was performed by taking 4 *Botrytis* isolates (Kst5C, Kst10A, Kst14A & Kst51). Three isolates (Kst5c, Kst10A, Kst14A) were infected with mycoviruses and the 4<sup>th</sup> one (Kst51) was virus free and considered as positive control. Mycelial plugs of same size were placed in holes of surface sterilized apples. Data was taken for 4 days. As in the Growth Comparison Assay, we observed slow growth of Kst5c so same case was observed in lesion spread on apple (Both were slow; Figure 3.57). While lesion size in case of Kst10A and Kst14A were same as compared to lesion size caused by Kst51. So, it was also confirmed here that even the virulence capacity of Kst5c was also halted by its mycoviruses.



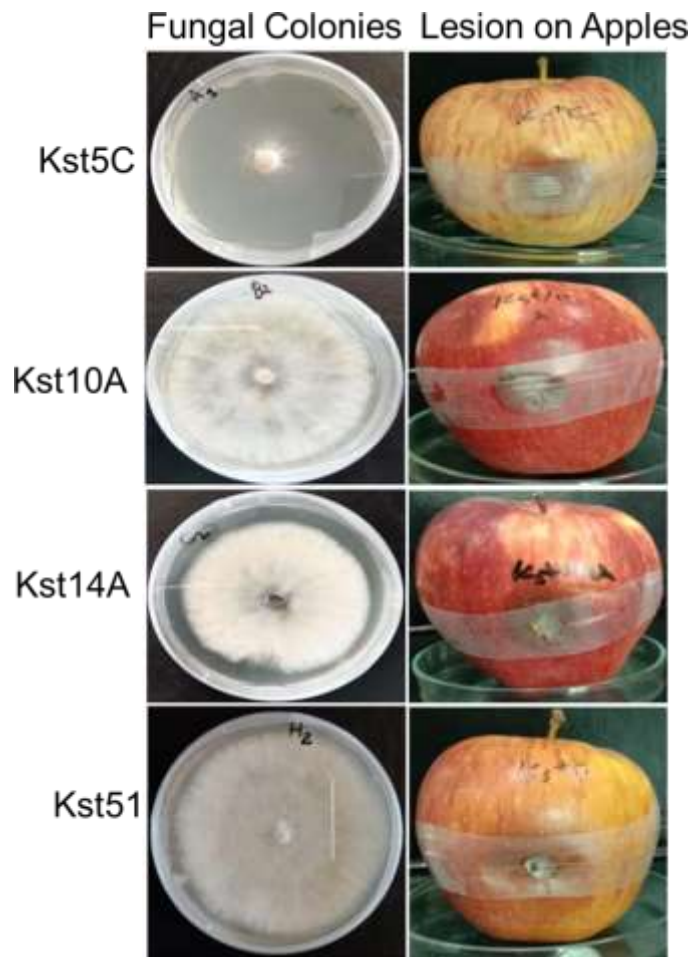


**Figure 3.57** shows the pathogenicity test of 4 *Botrytis* isolates (Kst5C, Kst10A, Kst14A & Kst51) along with their fungal morphology at 4<sup>th</sup> day.

Similarly, second pathogenicity was performed by taking 4 *Botrytis* isolates (Kst31C, Kst32B, Kst33A & Kst58). Three isolates (Kst31C, Kst32B, Kst33A) were infected with mycoviruses and the 4<sup>th</sup> one (Kst58) was virus free and considered as positive control. Mycelial plugs of same size were placed in holes of surface sterilized apples. Data was taken for 4 days. As in the Growth Comparison Assay, we observed slow growth of Kst31C and Kst33A so same case was observed in lesion spread on apple (Both were slow). While lesion size in case of Kst32b was same as compared to lesion size caused by Kst58. So, it was also confirmed here that even the virulence capacity of Kst31C & Kst33A were also halted by its mycoviruses (Figure 3.58).

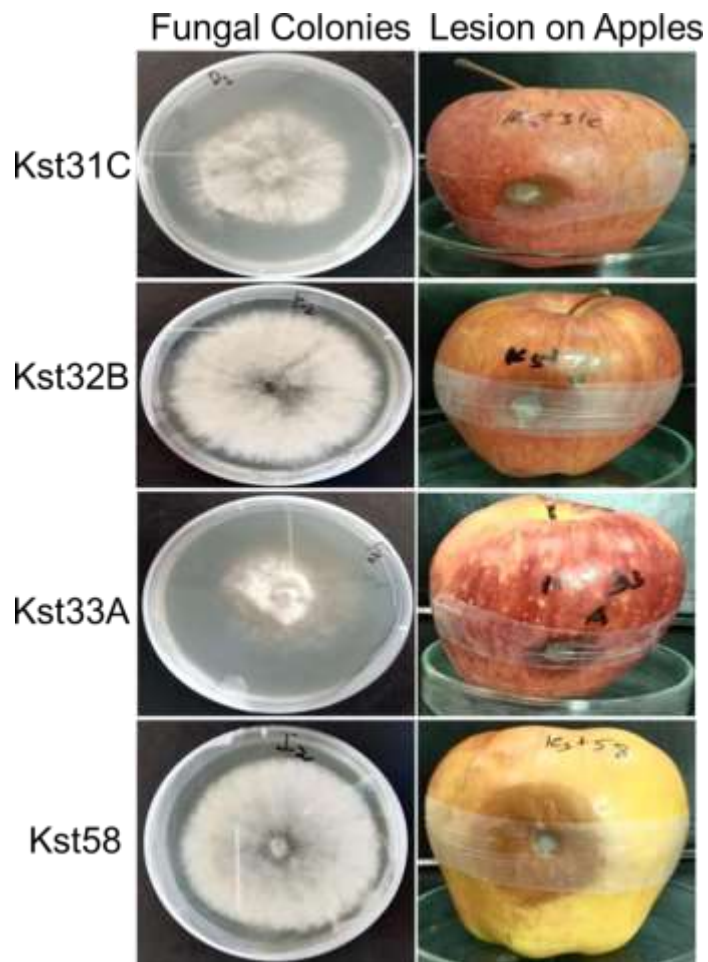


**Figure 3.58** Shows the pathogenicity test of 4 *Botrytis* isolates (Kst31C, Kst32B, Kst33A & Kst58) along with their fungal morphology at 4<sup>th</sup> day.

### 3.5.0 Choosing the compatible strains for generation of isogenic line for virus

## **transmission (Objective 5)**

### **3.5.1 Identification of compatible Botrytis strains for mycovirus transmission.**

#### **3.5.1.1 Bc-hch amplification for analysis of diversity and compatibility among fungal strains**

Bc-hch primers were used to for the amplification of 1171 bp sized fragment. The sequence of primers was 262 (5-AAGCCCTTCGATGTCTTGGA-3) and 520L (5-ACGGATTCCGAACTAAGTAA-3). Bc-hch is the homolog of the *het-c* vegetative incompatibility locus in *Neurospora crassa*. Digestion of the amplicon with Hha-I endonuclease usually results into two different size products corresponding to their respective groups. The larger band's size is determined by restriction profiles (650 bp in group I and 517 bp in group II). Current study suggested that all Botrytis strains collected here in Pakistan belong to group II (Figure 3. 59).

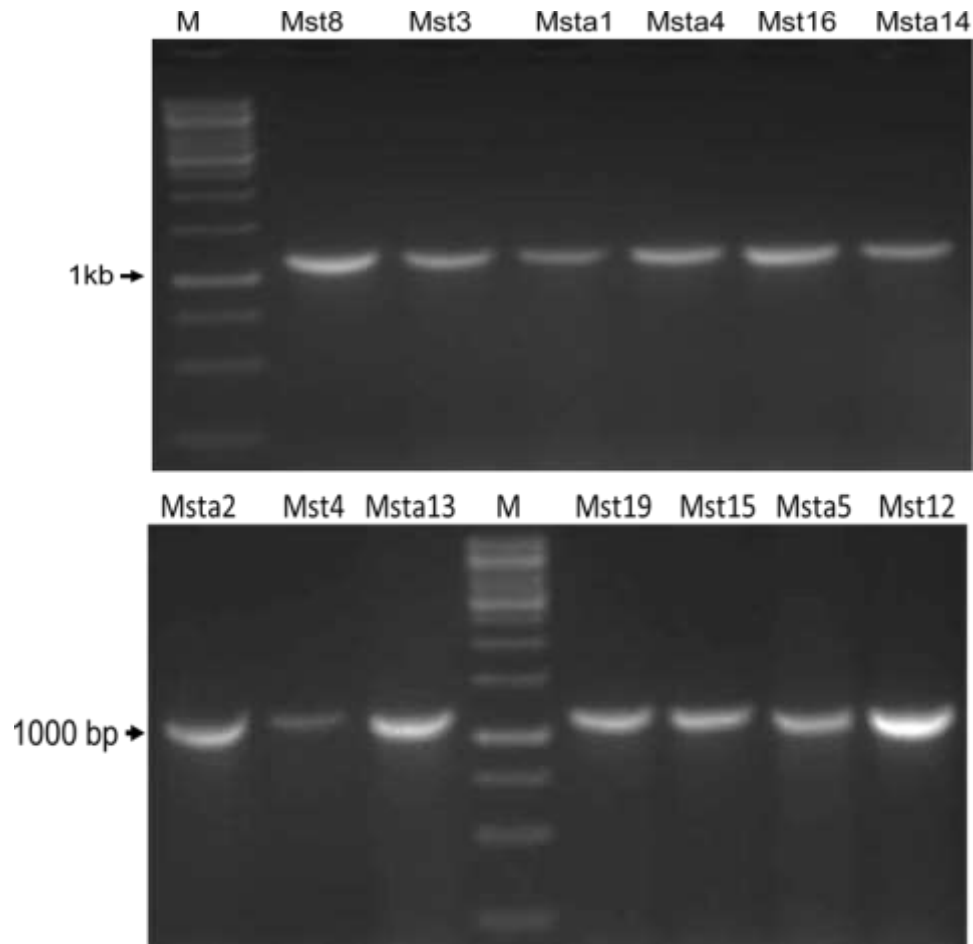


**Figure 3.59** PCR amplicon of Bc-hch gene using gene specific primers from different isolates.

The size of amplicon was almost 1.2 kb.

### **3.5.1.2 Enzymatic digestion of PCR amplicons for pattern analysis**

Single profile was observed after the digestion of amplicon by *Hha*-I restriction enzyme. Because our all strains belong to Group II (Figure 3.60). According to the literature members of Group II are more genetically diverse and successful pathogen as compared Group I. The *Botrytis* genus group II members were found compatible with each other and can easily exchange their cytoplasmic material.

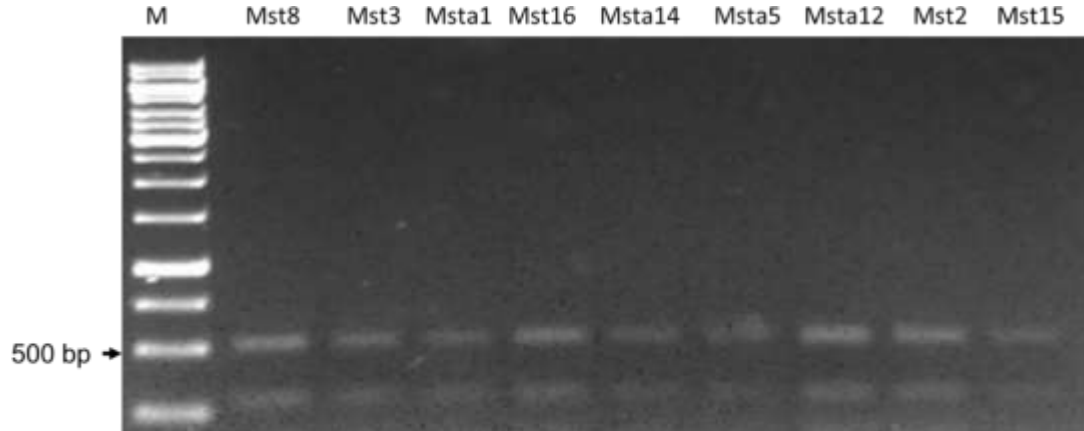


**Figure 3.60** Digestion Bc-hch amplicon with *Hha*-I endonuclease resulted into two different banding patterns corresponding to their respective groups.

### 3.6.1 Horizontal transmission of mycovirus (Objective 6)

#### 3.6.1.1 Hyphal Anastomosis for Test for evaluation of mycovirus impact on host

In order to assess the impact of mycovirus isogenic lines were created through hyphal anastomosis and since all the strain were from group II. Results of hyphal anastomosis suggested the viruses were transmitted successfully. One plug from Kst31 (donor) and one plug of Kst51 (recipient) were co-cultured (Figure. 3.61). After 3 days 4 plugs were taken from the mother plate of hyphal anastomosis. One plug was taken from donor to verify the presence of mycovirus whilst 3 plugs were taken (Near Middle and far regions of colony (Figure 3.61) from different locations on the recipient side to check the transfer of mycovirus.

#### 3.6.1.2 Confirmation of virus transmission though RT-PCR

For the confirmation of mycovirus transmission in recipient isolates, RT-PCR was performed. Gel analysis shows that mycovirus was transferred to near (N) and middle (M) region not to far (F) region. But the titer of mycovirus is less in M region as compared to N region and the titer of virus is highest in Donor region (Figure. 3.62)

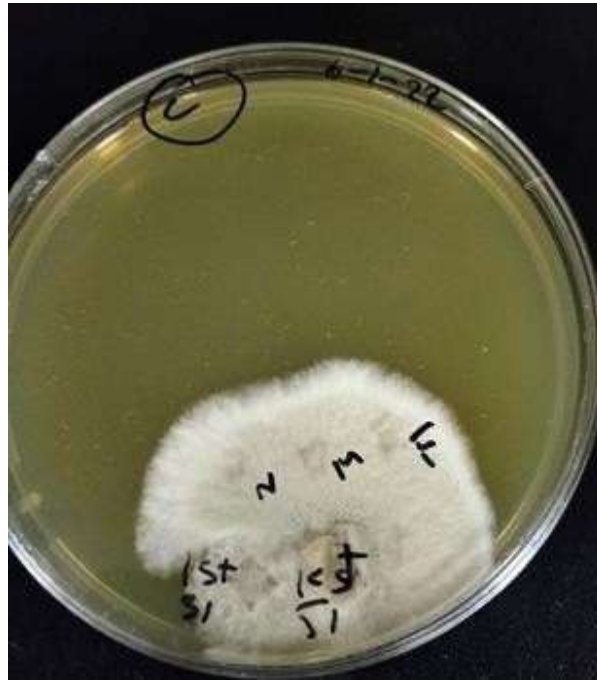


**Figure 3.61** shows picture of hyphal anastomosis, in which Kst31C is donor and Kst51 is potential recipient of mycovirus. Location of three plugs is also shown and these plugs were used for the determination of transfer of mycovirus.



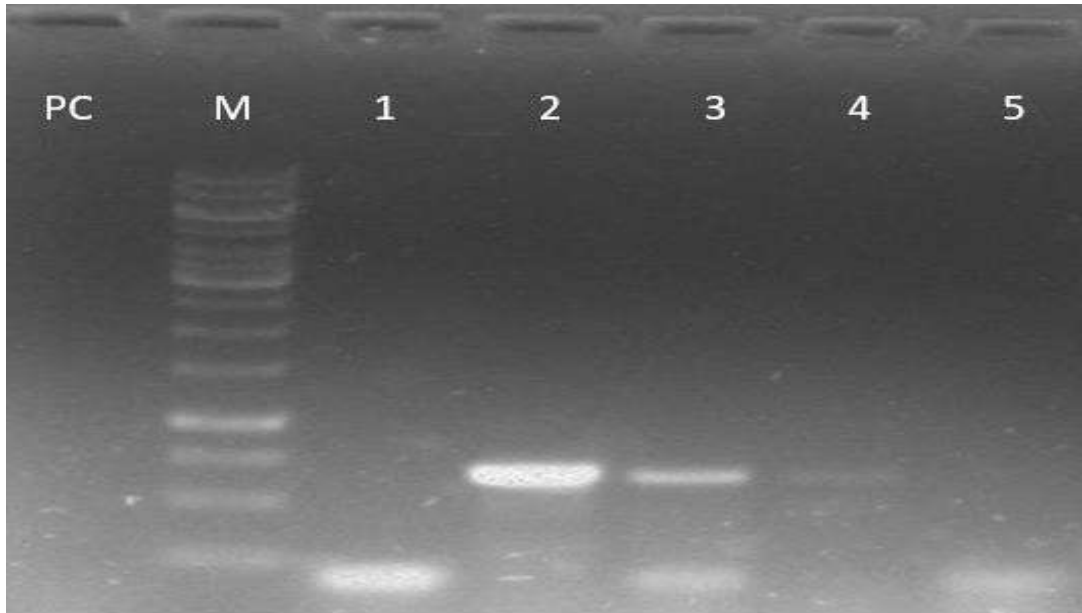


**Figure 3.62** shows RTPCR results of Endornavirus after hyphal anastomosis. Lane M as molecular marker, PC; PCR negative control, 1; Recipient strain, 2; positive control, 3; Near plug, 4; middle plug and 5; far plug of the recipient isolate.

### **3.7.1 Evaluation of potential hypovirulent strain for biocontrol**

**(Objective 7; Final objective)**

#### **3.7.1.1 Direct evaluation of hypovirulent mycovirus with (KST 51 Endornavirus infected and KST 51 Virus Free Isolate infected comparison on media and apple fruit**

Fungal isogenic lines were used for comparison of growth rates among virus infected and virus free strains. Virus-free (**KST 51 VF**) and Virus-infected (**KST 51 VI**) isolates were cultured on PDA plates. Experiment was performed by taking three replicates of each. Growth pattern and measurements of colonies were recorded for 4-7 days of post-inoculation. The colonies of VF isolate have much rapid rate of growth as compared to VI colonies (Figure. 3.48). The PDA plates of VF colonies were completely filled at 4<sup>th</sup> day of post-inoculation whilst VI colonies took 7 days to fill the PDA plates. Difference in growth pattern was also observed, the mycelial growth in VF plates was much dense as compared to VI plates which have much lighter growth pattern (Figure. 3.63 and Figure 3.64).

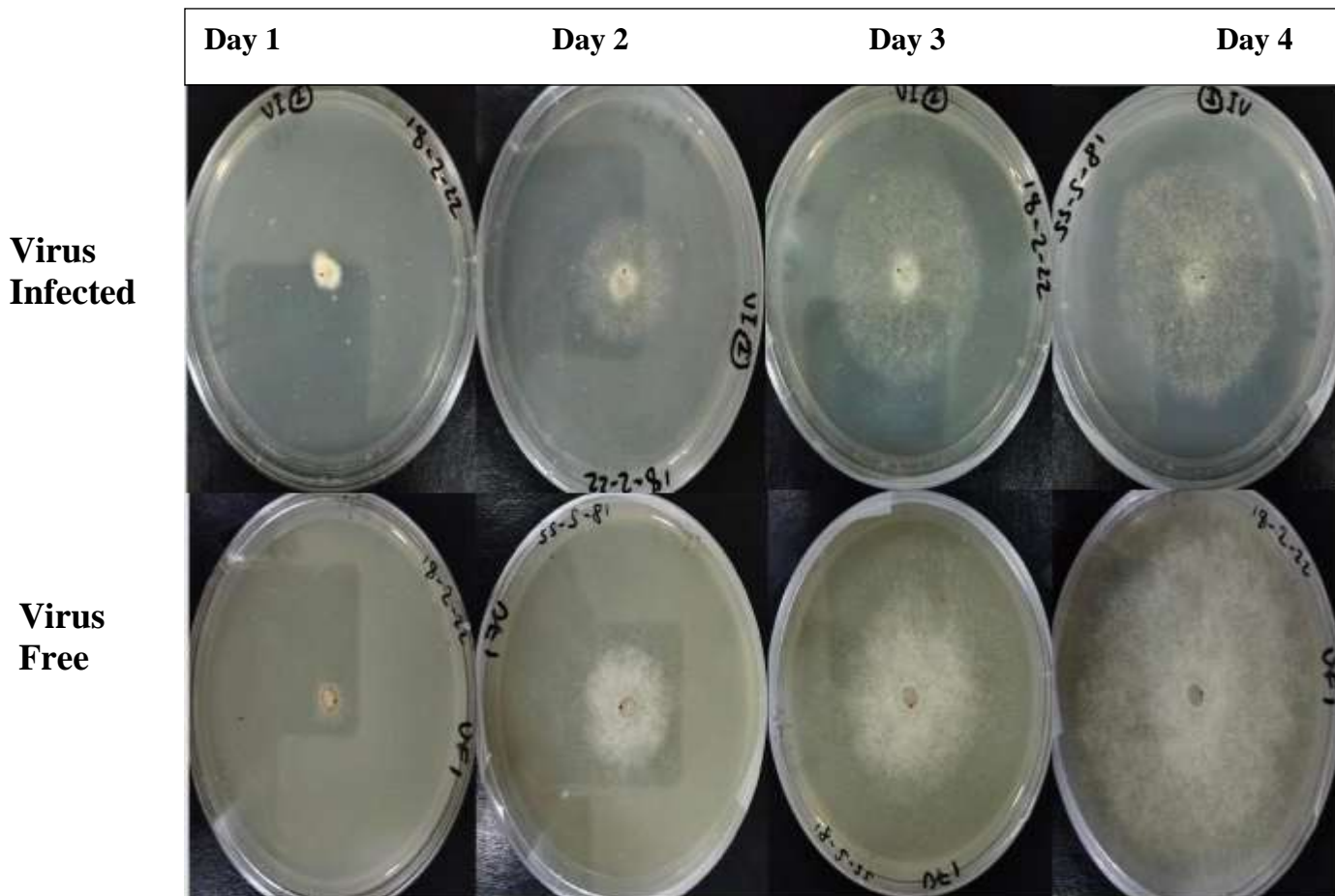


**Figure.3.63** Growth comparison test of virus free (VF) and virus infected isogenic lines to analyze the impact of virus on its host.



**Figure.3.64** shows the front views of growth pattern of KST 51 Virus infected (VI) and KST51-Virus free (VF) isogenic line at 7<sup>th</sup> day of post-inoculation.

### **Apple Assay of Hypovirulence inducing Endornavirus**

As the graph shows the impact of mycovirus (Endornavirus) on the virulence of its host fungus. According to observations, approximately for 72 hours (3 days) there was no prominent lesion on the apples. At 4<sup>th</sup> day infection starts, but the diameter of lesions on the apples having VF plugs increased rapidly as compared to apples having VI plugs. In case of control plugs (PDA plugs, no lesions were observed. (Figure 3.65)



**Figure 3.65 Pathogenicity** test of Endornavirus infected Kst51 with uninfected Kst51 showsthe diameter of lesions caused by KST51 virus infected (VI) and Virus Free (VF) isolates

### **3.7.2 Comparison of Growth Rate and fungal pathogenicity**

Growth rate of both VF and VI were compared statistically by making bar graphs which clearly shows the difference in speed of growth. Data of measurements was recorded for 7 days after the 24 hours of post-inoculation in case of media and VF plates were completely filled with mycelia at 4<sup>th</sup> day of inoculation but VI isolates took 7 days to fill the plates. But at 7<sup>th</sup> day there was prominent difference between the morphology of VF plates and VI plates (Figure 3.65). In VF plates growth of mycelia was uniform while in case of VI plates growth was scattered. For Pathogenicity assay at 4<sup>th</sup> day infection starts, but the diameter of lesions on the apples having VF plugs increased rapidly as compared to apples having VI plugs which showed less lesions. In case of control plugs (PDA plugs, no lesions were observed.

Pathogenicity Test

	R	Day 1	Day 2	Day 3	Day 4
	1	1.4	2.8	3	3.6
Virus Free	2	1.5	2.9	3.1	3.7
	3	1.6	3	3.2	3.8
Mean +SE		1.5+0.05	2.9+0.05	3.1+0.05	3.7+0.05
	R	Day 1	Day 2	Day 3	Day 4
		0.7	1.2	1.6	2.2
Virus Infected		0.8	1.3	1.7	2.1
		0.9	1.4	1.8	2.2
Mean +SE		0.8+0.05	1.3+0.05	1.7+0.05	2.1+0.05
P value		0.0005	0.00002	0.00003	0.00002

## Graphical Representation

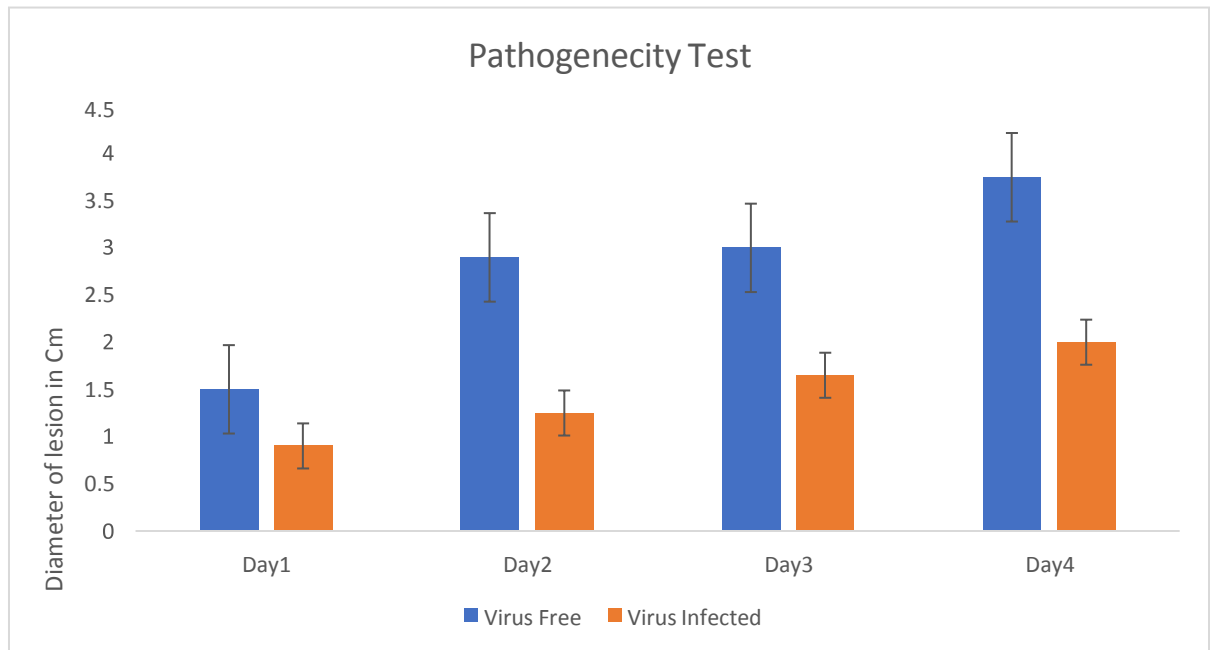


**Figure 3.67** shows the comparison of lesions caused by Virus-Free (VF) and Virus- Infected (VI) isolates on the host apple. As the P value (0.007) calculated was less than 0.05 so the difference observed were significant.

## 4. Discussion:



There are many different types of living things on earth, and because they are interdependent to survive, they create a variety of relationships that could be parasitic, mutualistic, or symbiotic. To maintain equilibrium, nature maintains a balance between all life forms (Trevors and Saier, 2011). Kingdom fungal members contribute to this. They are referred to as recyclers because they break down dead and decaying organic debris, which would otherwise build up and leave no room for other living things (Palaniveloo et al., 2020). They also return the nutrients to the soil. Fungi are important plant pathogens as well. Phytopathogenic fungi are responsible for over 70% of serious crop illnesses. Fungicides are frequently used to treat these illnesses, but in addition to harming both people and animals, some fungi are developing resistance to them (Palaniveloo et al., 2020). The grey mould fungus, *B. cinerea*, affects more than 200 crops globally (Williamson et al., 2007), and the majority of the products it affects are highly marketable fruits and vegetables, where any decline in aesthetic appeal has a significant negative influence on value. It is challenging to establish a control for the fungus since it can adapt to a variety of habitats worldwide and endure temperatures between 0 and 30 °C (Howitt et al., 2001). Like all other living things, fungi are susceptible to virus infection. Mycoviruses are used by nature to control how pathogenicity in fungi changes (Pearson et al., 2009; Chen et al., 1994; Milgroom, 1999; Nuss, 1992; Nuss, 2005). So, simply, we can consider mycoviruses as best alternatives against fungicides. Keeping in view the hypovirulent properties of these viruses have gained importance in past few decades and may be used as biological control of phytopathogenic fungus in the field Kyrychenko et al., 2018; McCabe et al., 1999; Milgroom and Cortesi, 2004; Oh et al., 2018; Pearson et al., 2009; Wang et al., 2014; Wang et al., 2018b). Anyhow the vegetative incompatibility (VIC) based on programmed cell death is still a hurdle for transmission of mycoviruses among different species species (Biella et al., 2002; Hyde et al., 2019; Wu et al., 2017). Multiple number of screening studies have been conducted to find out the potential of mycovirus as biological control (Abu-Mejdad et al., 2020; Arjona-López et al., 2020; Floudas et al., 2020). Earlier studies reported that incidence rates have been observed (ranging from a small number

upto 90%). So far, infection of *Botrytis cinerea* with mycoviruses have been reported in previous studies (Castro *et al.*, 1999; Castro *et al.*, 2003; Howitt *et al.*, 2001, 2006; Howitt *et al.*, 1995; Vilches & Castillo, 1997; Wu *et al.*, 2010; Wu *et al.*, 2007). According to literature, the reported effects on the phenotype of infected *Botrytis cinerea* isolates vary from minor to major, whilst some of these mycoviral infections have resulted in reduced virulence (Nuss, 2011; Pearson *et al.*, 2009). The first detailed study of mycoviruses infecting *Botrytis cinerea* was conducted by (Howitt *et al.* 1995) by observing virus-like particles (VLPs) and also on the detection of dsRNAs from mycelial extracts. VLPs observed in *Botrytis cinerea* exhibited various shapes (isometric, bacilliform and flexous) (Howitt *et al.* 1995). With the advancement of cDNA sequencing technology, huge number of specues of RNA mycoviruses, including BVF (B otrytis v irus F), BVX (Botrytis v irus X), BcMV1 (Botrytis cinerea mitovirus 1), BfTV1 (Botryotinia fuckeliana totivirus 1), BfPV1 (Botryotinia fuckeliana partitivirus1) and Bc378V1 (Botrytis cinerea CCg 378 virus 1) infecting *B. cinerea*, and BpRV1 (Botrytis porri RNA virus 1) infecting *B. porri* (Book reference). Horizontal transmission refers to transmission of mycoviruses between two individuals via hyphal anastomosis (hyphal fusion) (Nuss 2005). Wu *et al.* (2007, 2012) reported that BcMV1 and BpRV1 in the hypovirulent isolates of CanBc-1 (*B. cinerea*) and GarlicBc-72 (*B. porri*) were successfully transmitted to virulent SC isolates CanBc-1c-66 (derived from CanBc-1) and GP72SC35 (derived from GarlicBc-72), respectively, through hyphal contact (possibly through hyphal fusion). However, BcMV1 and BpRV1 failed to transfect the virulent isolates CanBc-2 (*B. cinerea* ) and OnionBc-95 ( *B. porri* ), respectively, through hyphal contact (Wu *et al.* 2007 , 2012 ). It is well recognized that horizontal transmission of RNA mycoviruses is usually restricted by the vegetative incompatibility or heterokaryon incompatibility, which behaves as a barrier (Anagnostakis 1982; Brasier 1983; Charlton and Cubeta 2007 ; Dalzoto *et al.* 2006 ). Fungal vegetative incompatibility is a complex system controlled by *vic* genes or *het* genes (Cortesi and Milgroom 1998; Saup 2000). If two fungal isolates have different alleles at one or more *vic* loci, they are incompatible and considered as different vegetative compatibility groups (VCGs) (Saup 2000; Chap. 3). Previously not much work has been done on the

characterization of mycoviruses from Pakistani fungal isolates. Only few studies are available which reported the characterization of mycoviruses from phytopathogenic and environmental fungal samples. But there are no studies on the mycovirome characterization from *Botrytis cinerea*. During the screening of *Botrytis* isolates, a total of 9 *Botrytis* isolates were detected as positive for mycoviral infection. Mycoviruses are omnipresent and have been reported in almost all major groups of fungi, including *Botrytis*. Approximately 14 different sorts of mycoviruses have been detected in *Botrytis* species so far throughout the world. These mycoviruses can be used as biological control of deleterious fungus, as already it was done in case of *Cryphonectria parasitica* using CHV1

mycovirus. As the spread of *Botrytis* is cosmopolitan, present in every continent like Asia, Africa, Australia, America and Europe, causing grey mold and many other diseases. Previously *Botrytis* has been reported in Pakistan (Lahore and Gilgit Baltistan) causing Botrytis Bunch rot disease in grapes ([Abbas, 2017](#)). Current study reports 102 isolates of *Botrytis* from infected fruits of strawberry. Molecular identification is being done by ITS region amplification and subsequent sequencing. As *Botrytis* genus contain 28 species while *B.cinerea* is the most prevalent phytopathogen among all other. In order to access genetic diversity and potential to use mycovirus infected strains as biological control evaluation assessment indicated the current strains found were related to *B. cinerea* species Group II. All *Botrytis cinerea* isolates belonged to same genetic group (Group II) and considered as vegetatively compatible. It also depends on the geographic distribution of the species and also varies accordingly ([Fournier et al., 2003](#)) According to the literature, Group II is genetically more diverse and successful pathogen as compared to members of Group I ([Fournier et al., 2003](#); [Karchani-Balma et al., 2008](#)). These genetic diversity test results show that all the collected isolates locally from Pakistan belongs to GroupII. In our current study we have detected 22 different profiles of mycoviruses in nine *Botrytis* isolates which are considered to be compatible with each other so reducing the chances of vegetative incompatibility and program cell death thus supporting the mycovirus transmission. Some of the collected isolates also showed multiple infection of

viruses. After the successful transmission of mycovirus from virus infected *Botrytis cinerea* isolate to virus free *Botrytis cinerea* isolate and production of isogenic lines. Growth patterns of virus infected and virus free isolates have also been studied. Results showed that certain *Botrytis* isolates (Kst5C, Kst31C & Kst33A) have slow growth pattern as compared to other virus infected and virus free isolates. So, we suggest these three isolates (Kst5C, Kst31C & Kst33A) have infection of hypovirulent mycoviruses. Further experimentation on these isolates is still going. Since our all *Botrytis* isolates belong to Group II and have same genetic background, we have transferred hypovirulent viruses to virus-free isolates for the production of isogenic lines. By producing isogenic lines, impact of virus (BcEV4) has been studied in detail. Isogenic lines have been sent RNA seq to analyze the transcriptional difference between Virus infected and Virus free strains. So, in this way we will be able to cure *Botrytis* infections. Later on, it can be proved as future biological control of *Botrytis* in Pakistan.

## 5. Conclusion:

In this study, a total of 102 *Botrytis* isolates collected from different areas of Pakistan were screened for mycoviral infection. Classical dsRNA extraction revealed the nine isolates were positive with mycoviral infection. The overall calculated infection frequency rate was 8.8%. Moreover, the identification of virus positive isolates was done through ITS based confirmation. Total RNA from these isolates were sequenced by Next generation Sequencing to get the genomic sequences of viruses present in these isolates. Contigs obtained after assembly showed the presence of 23 mycoviruses residing in these 6 *Botrytis* isolates. Some virus sequences were complete and few were partial sequences. The molecular characterization of viruses was performed completed which showed novel features and the complete sequences have been submitted in NCBI Genbank database. The characteristics of BcEV4 infection were different from majority of known endornavirus infection, which are mostly cryptic ([Roossinck, 2015](#)). We identified a new Endornavirus BcEV4 from *B. cinerea* isolate Kst31 in this work. ORF finder analysis confirmed a single big ORF in the genome of BcEV4. The lack of GT motif in other reported and BcEV4 genome suggest that it is not necessarily required for viral replication. Previous studies suggested that this motif was acquired from fungal hosts through the process of evolution, protect these viruses from host immune system ([Linder-Basso et al., 2005](#)). The RdRp domain is a member of the RNA-dependent RNA polymerase RdRp 2 family which function in replication and this observation suggests that endornaviruses are capable of independent replication. Furthermore, the BcEV4 RdRp domain comprises eight conserved motifs (A to D), which are identical to the RdRps of already reported endornavirus including HmEV1 and CbEVC. Based on this observation we suggest that BcEV4 is a novel mycovirus in family *endornaviridae*. BcEV4 infection is particularly stable in *B. cinerea* Kst31 mycelia. In our laboratory, we were unable

to establish a virus-free strain by hyphal tipping and hyphal fragmentation of virus-containing strain Kst31. But we were successful in transmitting this virus to virus-free strain through horizontal transfer as both strain falls in group II. The new strain was used for testing the pathogenicity with apple assay which confirmed the hypovirulent nature of endornavirus (BcEV4). Genomic characterization of mycoviruses infected isolates were followed by Biological characterization. Initially the comparison of virus infected isolates was made with uninfected Botrytis strain to see any obvious morphological changes. The isolates showing debilitating influence on the host were selected for further analysis. In order to assess the influence of Botrytis mycoviruses isogenic lines were generated. Before that the isolates were assessed for the compatibility through apparently associated with symptomless infections however few Botrytis strains showed obvious morphological changes or reduce the virulence in their fungal hosts which includes Kst 31 Kst 14 A and Kst Kst 10 A and Kst 5C.

A representative was followed Pathogenicity test was also performed and the impact of fungal viruses on their respective host was also determined, which showed that BcEV4, BcFV1 and BcFV2 showed hypovirulence. Thus, we conclude that the mycovirome identified from Pakistani isolates of Botrytis showed unique features from already reported viruses.

## **6. Future Prospects:**

### **6.1 Direct application of hypovirulent virus on the fungal infections in the field trials or application of transgenic cDNA clones (infectious clones) with an expectation of debilitating effects on the health of fungi (Biocontrol).**

It is indeed a matter of great interest to broaden the host range of mycoviruses infecting *Botrytis* species so as to utilize their potential as a biological control agent not only for controlling phytopathogenic infection like Grey Molds but also other phytopathogenic fungal infection. Hypovirulent mycoviruses identified in this study can be used to make infectious clones which can be very useful in bio-control of fungal infection in plants. The strategy can be seen in Figure 6,1 For that purpose the complete genome of these viruses will be amplified using primers designed from the 3' and 5' UTRs. The amplified complete genome will be ligated in a pUC-19 vector (Figures 6.2 and 6.3) by Gibson assembly ([Siridechadilok et al., 2013](#)). The ligated vector will be transformed into *E. coli* bacterial cells for increasing the copy number and the positive cells will be selected *via* RT-PCR. Which can be further transfected to fungal protoplasts to check how these viruses behave in experimental hosts. Furthermore, we can also check the function of viral hypothetical genes by inserting point mutations in the viral genome. The effect can be analyzed in both parental host strain and also in experimental hosts. Moreover, the mechanism of Mycovirus induced gene silencing is not well studied in *Botrytis* species infected with mycoviruses and also different other fungi. So, there is a need to compare the RNA expression of virus infected and virus free isolates to get wholesome image of reduced virulence in *Botrytis* species.

## 7. References:

Abbas, A., 2017. A Report of Grey Mold Disease on Grapes Caused By *Botrytis cinerea* in Gilgit-Baltistan, Pakistan. *Clinical Biotechnology and Microbiology* 1, 117-119.

Abro, M.A., 2013. Nitrogen fertilization of the host plant influences susceptibility, production and aggressiveness of *Botrytis cinerea* secondary inoculum and on the efficacy of biological control. Université d'Avignon.

Adams, I.P., Glover, R.H., Monger, W.A., Mumford, R., Jackeviciene, E., Navalinskiene, M., Samuitiene, M., Boonham, N., 2009a. Next-generation sequencing and metagenomic analysis: a universal diagnostic tool in plant virology. *Mol Plant Pathol* 10, 537-545.

Adams, I.P., Glover, R.H., Monger, W.A., Mumford, R., Jackeviciene, E., Navalinskiene, M., Samuitiene, M., Boonham, N.J.M.p.p., 2009b. Next-generation sequencing and metagenomic analysis: a universal diagnostic tool in plant virology. *Mol Plant Pathol* 10, 537-545.

Al Rwahnih, M., Daubert, S., Golino, D., Rowhani, A., 2009. Deep sequencing analysis of RNAs from a grapevine showing Syrah decline symptoms reveals a multiple virus infection that includes a novel virus. *Virology* 387, 395-401.

Baeza, M., Bravo, N., Sanhueza, M., Flores, O., Villarreal, P., Cifuentes, V.J.V.j., 2012. Molecular characterization of totiviruses in *Xanthophyllomyces dendrorhous*. 9, 1-11.

Beever, R., Weeds, P.J.B.b., pathology, control. Kluwer, D., 2004. *Botrytis* taxonomy and genetic variation.

Bellemain, E., Carlsen, T., Brochmann, C., Coissac, E., Taberlet, P., Kauserud, H., 2010. ITS as an environmental DNA barcode for fungi: an in silico approach reveals potential PCR biases. *BMC Microbiology* 10, 189.



Bhatti, M.F., Jamal, A., Bignell, E.M., Petrou, M.A., Coutts, R.H.J.M., 2012. Incidence of dsRNA mycoviruses in a collection of *Aspergillus fumigatus* isolates. *Mycopathologia* 174, 323-326.

Bhatti, M.F., Jamal, A., Petrou, M.A., Cairns, T.C., Bignell, E.M., Coutts, R.H.A., 2011. The effects of dsRNA mycoviruses on growth and murine virulence of *Aspergillus fumigatus*. *Fungal Genetics and Biology* 48, 1071-1075.

Billard, A., Fillinger, S., Leroux, P., Bach, J., Lanen, C., Lachaise, H., Beffa, R., Debieu, D., 2011. Fenhexamid Resistance in the *Botrytis* Species Complex, Responsible for Grey Mould Disease.

Calvo-Garrido, C., Roudet, J., Aveline, N., Davidou, L., Dupin, S., Fermaud, M., 2019. Microbial Antagonism Toward *Botrytis* Bunch Rot of Grapes in Multiple Field Tests Using One *Bacillus ginsengihumi* Strain and Formulated Biological Control Products. 10.

Carisse, O., Levasseur, A., Van der Heyden, H., 2012. A new risk indicator for botrytis leaf blight of onion caused by *Botrytis squamosa* based on infection efficiency of airborne inoculum. 61, 1154-1164.

Castro, M., Kramer, K., Valdivia, L., Ortiz, S., Castillo, A., 2003. A double-stranded RNA mycovirus confers hypovirulence-associated traits to *Botrytis cinerea*. *FEMS microbiology letters* 228, 87-91.

Cheung, N., Tian, L., Liu, X., Li, X., 2020. The Destructive Fungal Pathogen *Botrytis cinerea*-Insights from Genes Studied with Mutant Analysis. *Pathogens* 9, 923.

Chiba, S., Salaipeth, L., Lin, Y.H., Sasaki, A., Kanematsu, S., Suzuki, N., 2009. A novel bipartite double-stranded RNA Mycovirus from the white root rot Fungus *Rosellinia necatrix*: molecular and biological characterization, taxonomic considerations, and potential for biological control. *Journal of virology* 83, 12801-12812.

Ciliberti, N., Fermaud, M., Roudet, J., Rossi, V., 2015. Environmental Conditions Affect

Botrytis cinerea Infection of Mature Grape Berries More Than the Strain or Transposon Genotype. *Phytopathology* 105, PHYTO10140264R.

Coenen, A., Kevei, F., Hoekstra, R.F., 1997. Factors affecting the spread of double-stranded RNA viruses in *Aspergillus nidulans*. *Genetical research* 69, 1-10.

Coutts, R.H.A., Livieratos, I.C., 2003. A Rapid Method for Sequencing the 5'- and 3'-Termini of Double-Stranded RNA Viral Templates using RLM-RACE. 151, 525-527.

Dawe, A., Nuss, D., 2001. Hypoviruses and Chestnut Blight: Exploiting Viruses to Understand and Modulate Fungal Pathogenesis. *Annual review of genetics* 35, 1-29.

De Guido, M., De Miccolis Angelini, R., Pollastro, S., Santomauro, A., Faretra, F.J.J.o.P.P., 2007. Selection and genetic analysis of laboratory mutants of *Botryotinia fuckeliana* resistant to fenhexamid. 203-210.

Dean, R., Van Kan, J.A.L., Pretorius, Z.A., Hammond-Kosack, K.E., Di Pietro, A., Spanu, P.D., Rudd, J.J., Dickman, M., Kahmann, R., Ellis, J., Foster, G.D., 2012. The Top 10 fungal pathogens in molecular plant pathology. *Molecular plant pathology* 13, 414-430.

Dewey, F.M., Grant-Downton, R., 2016. Botrytis-biology, detection and quantification, Botrytis—the fungus, the pathogen and its management in agricultural systems. Springer, pp. 17-34.

Dobbs, E., Deakin, G., Bennett, J., Archibald, C., Jones, I., Grogan, H., Burton, K., 2021. Viral

Interactions and Pathogenesis during Multiple Viral Infections in *Agaricus bisporus*. *mBio* 12.

Dolja, V., Koonin, E., 2012. Capsid-Less RNA Viruses.

Donaire, L., Ayllón, M.A.J.M.p.p., 2017. Deep sequencing of mycovirus- derived small RNAs from *Botrytis* species. 18, 1127-1137.

El-Ramady, H., domokos-szabolcsy, E., Abdalla, N., Taha, H., Fári, M., 2015. Postharvest Management of Fruits and Vegetables Storage, pp. 65-152.

Fillinger, S., Elad, Y., 2016. *Botrytis*-the fungus, the pathogen and its management in agricultural systems. Springer.

Fournier, P.E., Dumler, J.S., Greub, G., Zhang, J., Wu, Y., Raoult, D., 2003. Gene sequence-based criteria for identification of new rickettsia isolates and description of *Rickettsia heilongjiangensis* sp. nov. *Journal of clinical microbiology* 41, 5456-5465.

Ghabrial, S.A., 1998. Origin, Adaptation and Evolutionary Pathways of Fungal Viruses. *Virus genes* 16, 119-131.

Ghabrial, S.A., 2008. Totiviruses, in: Mahy, B.W.J., Van Regenmortel, M.H.V. (Eds.), *Encyclopedia of Virology (Third Edition)*. Academic Press, Oxford, pp. 163-174.

Ghabrial, S.A., Castón, J.R., Jiang, D., Nibert, M.L., Suzuki, N., 2015. 50-plus years of fungal viruses. *Virology* 479-480, 356-368.

Ghabrial, S.A., Suzuki, N., 2009. Viruses of plant pathogenic fungi. *Annual review of phytopathology* 47, 353-384.

González-Fernández, E., Kennedy, R., Osborn, R., Fernández-González, M., Rodríguez-Rajo, F.J., 2021. *Botrytis cinerea* Airborne Conidia and Their Germination Ability Assessed by Immunological Methods in a NW Spain Vineyard. 11, 1441.

Hao, F., Ding, T., Wu, M., Zhang, J., Yang, L., Chen, W., Li, G., 2018. Two Novel Hypovirulence-Associated Mycoviruses in the Phytopathogenic Fungus *Botrytis cinerea*: Molecular Characterization and Suppression of Infection Cushion Formation. *Viruses* 10, 254.

- Hollings, M., 1962. Viruses Associated with A Die-Back Disease of Cultivated Mushroom. *Nature* 196, 962-965.
- Holz, G., Coertze, S., Williamson, B., 2007. The ecology of *Botrytis* on plant surfaces, *Botrytis: Biology, pathology and control*. Springer, pp. 9-27.
- Howitt, R.L., Beaver, R.E., Pearson, M.N., Forster, R.L.J.J.o.G.V., 2001. Genome characterization of *Botrytis* virus F, a flexuous rod-shaped mycovirus resembling plant 'potex-like' viruses. *82*, 67-78.
- Howitt, R.L.J., Beaver, R.E., Pearson, M.N., Forster, R.L.S., 2006. Genome characterization of a flexuous rod-shaped mycovirus, *Botrytis* virus X, reveals high amino acid identity to genes from plant 'potex-like' viruses. *Archives of Virology* 151, 563-579.
- Hrabáková, L., Grum-Grzhimaylo, A.A., Koloniuk, I., Debets, A.J.M., Sarkisova, T., Petrzik, K., 2017. The alkalophilic fungus *Sodiomyces alkalinus* hosts beta- and gammapartitiviruses together with a new fusarivirus. *PLOS ONE* 12, e0187799.
- Hua, L., Yong, C., Zhanquan, Z., Boqiang, L., Guozheng, Q., Shiping, T., 2018. Pathogenic mechanisms and control strategies of *Botrytis cinerea* causing post-harvest decay in fruits and vegetables. *Food Quality and Safety* 2, 111-119.
- Hugenholtz, P., Tyson, G.W.J.N., 2008. *Metagenomics*. 455, 481-483.
- Jaspers, M., Seyb, A., Trought, M., Balasubramaniam, R.J.P.p., 2013. Overwintering grapevine debris as an important source of *Botrytis cinerea* inoculum. *62*, 130-138.
- Kanematsu, S., Shimizu, T., Salaipeth, L., Yaegashi, H., Sasaki, A., Ito, T., Suzuki, N., 2014.

Genome rearrangement of a mycovirus *Rosellinia necatrix* megabirnavirus 1 affecting its ability to attenuate virulence of the host fungus. *Virology* 450-451, 308-315.

Karchani-Balma, S., Gautier, A., Raies, A., Fournier, E., 2008. Geography, plants, and growing systems shape the genetic structure of Tunisian *Botrytis cinerea* populations. *Phytopathology* 98, 1271-1279.

Köhl, J., Kolnaar, R., Ravensberg, W.J., 2019. Mode of Action of Microbial Biological Control Agents Against Plant Diseases: Relevance Beyond Efficacy. 10.

Linder-Basso, D., Dynek, J.N., Hillman, B.I., 2005. Genome analysis of *Cryphonectria hypovirus 4*, the most common hypovirus species in North America. *Virology* 337, 192-203.

Magliani, W., Conti, S., Gerloni, M., Bertolotti, D., Polonelli, L.J.C.m.r., 1997. Yeast killer systems. 10, 369-400.

Marzano, S.-Y.L., Nelson, B.D., Ajayi-Oyetunde, O., Bradley, C.A., Hughes, T.J., Hartman, G.L., Eastburn, D.M., Domier, L.L.J.J.o.v., 2016a. Identification of diverse mycoviruses through metatranscriptomics characterization of the viromes of five major fungal plant pathogens. 90, 6846-6863.

Marzano, S.Y., Nelson, B., Ajayi, O., Bradley, C., Hughes, T., Hartman, G.L., Eastburn, D., Domier, L., 2016b. Identification of Diverse Mycoviruses through Metatranscriptomics Characterization of the Viromes of Five Major Fungal Plant Pathogens. *Journal of virology* 90, JVI.00357-00316.

Mertely, J., Chandler, C., Xiao, C., Legard, D.J.P.d., 2000. Comparison of sanitation and fungicides for management of *Botrytis* fruit rot of strawberry. 84, 1197-1202.

Milgroom, M.G., Cortesi, P., 2004. Biological control of chestnut blight with hypovirulence: a critical analysis. *Annual review of phytopathology* 42, 311-338.

Nibert, M.L., Ghabrial, S.A., Maiss, E., Lesker, T., Vainio, E.J., Jiang, D., Suzuki, N., 2014. Taxonomic reorganization of family Partitiviridae and other recent progress in partitivirus

research. *Virus research* 188, 128-141.

Nuss, D.L., 2005a. Hypovirulence: mycoviruses at the fungal-plant interface. *Nature reviews. Microbiology* 3, 632-642.

Nuss, D.L., Koltin, Y.J.A.r.o.p., 1990. Significance of dsRNA genetic elements in plant pathogenic fungi. *Annual review of phytopathology* 28, 37-58.

Nuss, D.L.J.N.R.M., 2005b. Hypovirulence: mycoviruses at the fungal-plant interface. 3, 632-642.

Osaki, H., Sasaki, A., Nomiya, K., Tomioka, K., 2016. Multiple virus infection in a single strain of *Fusarium poae* shown by deep sequencing. *Virus genes* 52, 835-847.

Panno, S., Davino, S., Caruso, A.G., Bertacca, S., Crnogorac, A., Mandić, A., Noris, E., Matic, S., 2021. A Review of the Most Common and Economically Important Diseases That Undermine the Cultivation of Tomato Crop in the Mediterranean Basin. 11, 2188.

Pearson, M.N., Beever, R.E., Boine, B., Arthur, K., 2009. Mycoviruses of filamentous fungi and their relevance to plant pathology. *Molecular plant pathology* 10, 115-128.

Poveda, J., Barquero, M., González-Andrés, F., 2020. Insight into the Microbiological Control Strategies against *Botrytis cinerea* Using Systemic Plant Resistance Activation. 10, 1822.

Roossinck, M.J., 2015. Metagenomics of plant and fungal viruses reveals an abundance of persistent lifestyles. 5.

Rupp, S., Weber, R.W.S., Rieger, D., Detzel, P., Hahn, M., 2017. Spread of *Botrytis cinerea* Strains with Multiple Fungicide Resistance in German Horticulture. 7.

Salaipeth, L., Chiba, S., Eusebio-Cope, A., Kanematsu, S., Suzuki, N.J.J.o.G.V., 2014. Biological properties and expression strategy of *rosellinia necatrix* megabirnavirus 1 analysed in an experimental host, *Cryphonectria parasitica*. *J Gen Virol* 95, 740-750.

Schaad, N.W., Frederick, R.D.J.C.j.o.p.p., 2002. Real-time PCR and its application for rapid plant disease diagnostics. 24, 250-258.

Siridechadilok, B., Gomutsukhavadee, M., Sawaengpol, T., Sangiambut, S., Puttikhunt, C., Chin-inmanu, K., Suriyaphol, P., Malasit, P., Sreaton, G., Mongkolsapaya, J., 2013. A simplified positive-sense-RNA virus construction approach that enhances analysis throughput. *Journal of virology* 87, 12667-12674.

Sotirovski, K., Rigling, D., Heiniger, U., Milgroom, M.G., 2011. Variation in virulence of *Cryphonectria hypovirus 1* in Macedonia. *Forest Pathology* 41, 59-65.

Tanaka, T., Eusebio-Cope, A., Sun, L., SUZUKI, N., 2012. Mycoreovirus Genome Alterations: Similarities to and Differences from Rearrangements Reported for Other Reoviruses. 3.

Van der Heyden, H., Dutilleul, P., Charron, J.-B., Bilodeau, G.J., Carisse, O., 2021. Monitoring airborne inoculum for improved plant disease management. A review. *Agronomy for Sustainable Development* 41, 40.

van Kan, J.A.L., Shaw, M.W., Grant-Downton, R.T., 2014. Botrytis species: relentless necrotrophic thugs or endophytes gone rogue? *Molecular plant pathology* 15, 957-961.

Vilches, S., Castillo, A., 1997. A double-stranded RNA mycovirus in *Botrytis cinerea*. *FEMS microbiology letters* 155, 125-130.

Wang, S., Kondo, H., Liu, L., Guo, L., Qiu, D., 2013. A novel virus in the family Hypoviridae from the plant pathogenic fungus *Fusarium graminearum*. *Virus research* 174, 69-77.

Ward, Y., Young, R., Shatwell, R.J.J.o.M.S., 2004. Application of Raman microscopy to the analysis of silicon carbide monofilaments. 39, 6781-6790.

Ware, J.S., Roberts, A.M., Cook, S.A.J.H., 2012. Next generation sequencing for clinical diagnostics and personalised medicine: implications for the next generation cardiologist. 98, 276-281.

Wickner, R.B., Fujimura, T., Esteban, R., 2013. Viruses and prions of *Saccharomyces cerevisiae*. *Advances in virus research* 86, 1-36.

Williamson, B., Tudzynski, P., Kan, J., 2007. *Botrytis cinerea*: The cause of grey mould disease. *Molecular plant pathology* 8, 561-580.

Wu, M., Jin, F., Zhang, J., Yang, L., Jiang, D., Li, G., 2012. Characterization of a novel bipartite double-stranded RNA mycovirus conferring hypovirulence in the phytopathogenic fungus *Botrytis porri*. *Journal of virology* 86, 6605-6619.

Wu, M., Zhang, L., Li, G., Jiang, D., Ghabrial, S.A., 2010a. Genome characterization of a debilitation-associated mitovirus infecting the phytopathogenic fungus *Botrytis cinerea*. *Virology* 406, 117-126.

Wu, M., Zhang, L., Li, G., Jiang, D., Ghabrial, S.A.J.V., 2010b. Genome characterization of a debilitation-associated mitovirus infecting the phytopathogenic fungus *Botrytis cinerea*. *J Virology* 406, 117-126.

Wu, M.D., Zhang, L., Li, G.Q., Jiang, D.H., Hou, M.S., Huang, H.C., 2007. Hypovirulence and Double-Stranded RNA in *Botrytis cinerea*. *Phytopathology*<sup>TM</sup> 97, 1590-1599.

Xie, J., Jiang, D., 2014. New Insights into Mycoviruses and Exploration for the Biological Control of Crop Fungal Diseases. *Annual review of phytopathology* 52, 45-68.

Yaegashi, H., Nakamura, H., Sawahata, T., Sasaki, A., Iwanami, Y., Ito, T., Kanematsu, S., 2013. Appearance of mycovirus-like double-stranded RNAs in the white root rot fungus, *Rosellinia necatrix*, in an apple orchard. *FEMS Microbiology Ecology* 83, 49-62.

Yaegashi, H., Sawahata, T., Ito, T., Kanematsu, S., 2011. A novel colony-print immunoassay reveals differential patterns of distribution and horizontal transmission of four unrelated mycoviruses in *Rosellinia necatrix*. *Virology* 409, 280-289.